

ANALYSIS OF WNT5A FUNCTION IN DEVELOPMENT AND DISEASE USING THE CHICKEN MODEL

by

Sara Hosseini-Farahabadi

M.D., MASHHAD UNIVERSITY OF MEDICAL SCIENCES, 2004

A THESIS SUBMITTED IN PARTIAL FULFILLMENT OF
THE REQUIREMENTS FOR THE DEGREE OF

DOCTOR OF PHILOSOPHY

in

The Faculty of Graduate and Postdoctoral Studies

(Cell and Developmental Biology)

THE UNIVERSITY OF BRITISH COLUMBIA

(Vancouver)

April 2014

© Sara Hosseini-Farahabadi, 2014

Abstract

Mouse and human genetic data suggests that *Wnt5a* is required for jaw development but the specific role in facial skeletogenesis and morphogenesis is unknown. The aim of this thesis is to study functions of *WNT5A* during mandibular development in chicken embryos.

We initially determined that *WNT5A* is expressed in developing Meckel's cartilage but in mature cartilage expression was decreased to background. This pattern suggested that *WNT5A* is regulating chondrogenesis so to determine whether initiation, differentiation or maintenance of matrix was affected I used primary cultures of mandibular mesenchyme. I found that *Wnt5a* conditioned media allowed normal initiation and differentiation of cartilage but the matrix was subsequently lost. Collagen II and aggrecan, two matrix markers, were decreased in treated cultures. Degradation of matrix was due to the induction of metalloproteinases, *MMP1*, *MMP13*, and *ADAMTS5* and was rescued by an MMP antagonist. The effects of *Wnt5a* on cartilage were mainly due to stimulation of the non-canonical JNK/PCP pathway as opposed to antagonism of the canonical Wnt pathway.

To increase the clinical relevance of my work I studied the functional consequences of two human *WNT5A* mutations (C182R and C83S) causing human Robinow syndrome. Retroviruses containing mutant and wild-type versions of *WNT5A* caused shortening of beaks and limbs; however, the phenotypes were more frequent and severe with mutations. Mechanisms responsible for micrognathia were assessed. Decreased cell proliferation and impaired chondrocyte organization and intercalation were seen with all constructs. The effects of mutant proteins on the migration of mesenchymal cells were tested in organ cultures of the mandible. The C83S and to a lesser extent C182R forms of *WNT5A* inhibited the normal migration of dye-

labeled mesenchymal cells. The lack of cell migration was similar to that reported in *Wnt5a* null mice and therefore suggested that the *WNT5A* mutations are causing a loss-of-function.

We conclude that WNT5A is required during early chondrogenesis to block canonical signaling thereby allowing cartilage to form. In addition, WNT5A is required for cells to migrate within the mandible and perhaps to form the elongated shape of the lower jaw. Finally WNT5A in conditions of excess has detrimental effects on cartilage integrity.

Preface

Chapter 2 has been published in:

Sara Hosseini-Farahabadi, Poongodi Geetha-Loganathan, Katherine Fu, Suresh Nimmagadda, Hoe Joong Yang, Joy M. Richman: Dual functions for WNT5A during cartilage development and in disease. *Matrix Biology* 2013 June, 32(5):252-64.

I conducted the majority of the experiments and wrote most of the manuscript.

Authors' Roles:

Sara Hosseini-Farahabadi: study design, data collection (micromass culture, qPCR, luciferase assay, cell migration assay, most viral injections), data analysis, data interpretation, drafting manuscript, revising manuscript content

Dr. Poongodi Geetha-Loganathan: data collection (viral injection of *WNT5A* into embryos for late analysis of skeleton)

Katherine Fu: data collection (radioactive in situ hybridization, immunofluorescence staining with CSPG antibody, cloning)

Dr. Suresh Nimmagadda: data collection (viral injection of *WNT5A* into embryos for early analysis of skeleton)

Hoe Joong Yang: data collection (4-12-day micromass culture treated with Wnt5a-CM)

Dr. Joy M. Richman: study design, data analysis, data interpretation, drafting manuscript, revising manuscript content

I performed the majority of experiments for chapter 3. Cell proliferation and apoptosis assays were done by Katherine Fu but I took all the images and did the analysis. I also performed all data analysis for this chapter.

This project was conducted with the approval of the UBC Animal Ethics board (#A11-0351). This ethics proposal is renewed annually. The embryos used in this study were from White Leghorn eggs from the University of Alberta. The flock is regularly tested for pathogens and is currently disease-free. Consequently, these animals are suitable for RCAS studies.

Table of contents

Abstract.....	ii
Preface.....	iv
Table of contents	vi
List of tables.....	xi
List of figures.....	xii
List of abbreviations	xiv
Acknowledgements	xviii
1. Introduction.....	1
1.1 Overview.....	1
1.2 Facial development in the chicken embryo	2
1.3 Osteo/chondrogenesis in the face.....	5
1.4 Signaling pathways that operate during facial development	8
1.4.1 BMPs.....	9
1.4.2 FGFs.....	10
1.4.3 SHH.....	10
1.4.4 Endothelins	11
1.4.5 WNTs.....	11
1.4.5.1 Canonical WNT signaling.....	13
1.4.5.2 Non-canonical WNT signaling.....	16
1.4.5.2.1 Wnt5a.....	18
1.4.5.3 WNT antagonists.....	20

1.4.5.4	<i>WNT</i> gene expression patterns	21
1.5	Rationale	23
1.6	Approach.....	24
1.7	Hypotheses	25
1.8	Objectives	25
2.	Dual functions for WNT5A during cartilage development and in disease	26
2.1	Introduction.....	26
2.2	Materials and methods	28
2.2.1	Chicken embryos	28
2.2.2	In situ hybridization	29
2.2.3	Retrovirus construction and injection into the face	29
2.2.4	Skeletal staining.....	29
2.2.5	Micromass culture.....	30
2.2.6	Staining and quantification of matrix	31
2.2.7	Immunohistochemistry and TUNEL.....	31
2.2.8	Quantitative RT-PCR.....	32
2.2.9	Luciferase reporter assay	32
2.2.10	Statistical analysis	33
2.3	Results.....	33
2.3.1	Stage-specific expression of <i>WNT5A</i> during cartilage formation and differentiation in mandible.....	33
2.3.2	Temporally-restricted effects of <i>Wnt5a</i> on Alcian Blue stained matrix in micromass culture	38

2.3.3	MMP1, MMP13 and ADAMTS5 mediate the Wnt5a-induced loss of Alcian Blue staining of cartilage matrix in mandibular primary cultures	44
2.3.4	Exogenous Wnt5a antagonizes canonical Wnt signalling and activates the JNK/PCP pathway in mandibular mesenchyme	49
2.3.5	Wnt5a treatment causes degradation of limb cartilage in the same manner as cartilage derived from facial mesenchyme	52
2.4	Discussion	54
2.4.1	The normal role of Wnt5a during development of cartilage.....	55
2.4.2	Wnt5a negatively affect matrix stability in conditions of excess	57
2.4.3	The Wnt5a micromass phenotype is not due to precocious chondrocyte hypertrophy.....	58
2.4.4	The signaling pathway used by Wnt5a to degrade matrix involves JNK.....	59
3.	Role of WNT5A in mandibular morphogenesis.....	62
3.1	Introduction.....	62
3.2	Materials and methods	66
3.2.1	Virus preparation and injection.....	66
3.2.2	Immunofluorescence antibody staining of virus protein	67
3.2.3	BrdU, TUNEL staining and analysis	67
3.2.4	Cell tracking.....	68
3.2.5	Chondrocyte intercalation analysis	68
3.3	Results.....	69
3.3.1	Human <i>WNT5A</i> mutations cause shortening of limb and mandible in chicken.....	69

3.3.2	Wt <i>WNT5A</i> and <i>WNT5A</i> mutations reduce cell proliferation	74
3.3.3	Oriented cell movement is impaired in the embryos injected with RCAS:: <i>WNT5A</i> ^{C83S}	76
3.3.4	Chondrocyte elongation and organization is lost in the embryos infected with RCAS:: <i>wtWNT5A</i> , RCAS:: <i>WNT5A</i> ^{C182R} and RCAS:: <i>WNT5A</i> ^{C83S}	80
3.4	Discussion	83
3.4.1	Human <i>wtWNT5A</i> and <i>WNT5A</i> mutations causing DRS negatively affect length of the limb which may result from a convergent extension defect	84
3.4.2	Chondrocyte shape and organization in the mandible is affected by <i>WNT5A</i> imbalance.....	85
3.4.3	The role of <i>WNT5A</i> signaling is to regulate cell proliferation.....	86
3.4.4	<i>WNT5A</i> mutations disrupt normal oriented cell movements in mandible	87
3.4.5	The point mutations in <i>WNT5A</i> may act in a dominant-negative manner to reduce signaling	90
4.	Discussion.....	94
4.1	Concluding remarks	94
4.1.1	In vivo versus in vitro differences in the phenotypes caused by <i>WNT5A</i> suggest context dependent signaling is taking place.....	94
4.1.2	Spatially and temporally-controlled WNT antagonists may participate in mandibular patterning and cartilage differentiation.....	95
4.1.3	PCP signaling pathway regulated by <i>WNT5A</i> mediates cartilage development and mandibular morphogenesis.....	96
4.1.4	MMPs and cell migration: a mechanism at play?.....	97

4.1.5	Face and limb with unique embryonic origins and functions share developmental mechanisms	98
4.2	Overall significance	101
4.3	Future directions	101
	Bibliography	104

List of tables

Table 1.1 Mouse knock-outs of the canonical pathway components with craniofacial defects.	16
Table 1.2 Mouse knock-outs of the non-canonical Wnt pathway components.	20
Table 1.3 Mouse knock-outs of the Wnt antagonists with craniofacial defects.....	21
Table 2.1 Quantitative-PCR primers used for <i>MMP13</i> , <i>ADAMTS5</i> , <i>SOX9</i> and <i>COL2A1</i> amplification.	32
Table 2.2 Apoptosis and proliferation of cells in 8 day micromass cultures of mandibular mesenchyme.....	44
Table 2.3 QPCR for <i>SOX9</i> and <i>COL2A1</i> genes.	48
Table 3.1 Primers used to incorporate mutations into human <i>WNT5A</i>	66
Table 3.2 Primer sets used to check human <i>WNT5A</i> inserts in DF1 cells.....	70
Table 3.3 Biological replicates and detailed phenotype analysis of embryos injected with viruses into mandibular prominences.	71
Table 3.4 Biological replicates and detailed phenotype analysis of embryos injected with viruses into prospective limb region.	71
Table 3.5 Biological replicates of cell tracking experiment.....	80
Table 3.6 Arguments discussing whether <i>WNT5A</i> mutations work as loss or gain of function.	90

List of figures

Figure 1.1 Steps of facial development.....	4
Figure 1.2 Different types of bone and cartilage	8
Figure 1.3 Canonical Wnt signaling pathway.....	15
Figure 1.4 Non-canonical Wnt signaling pathways.	19
Figure 2.1 Expression of <i>WNT5A</i> in the avian craniofacial skeleton.....	35
Figure 2.2 Early analysis of RCAS:: <i>GFP</i> and RCAS:: <i>WNT5A</i> injection into mandibular region.	36
Figure 2.3 Late analysis of in vivo injection of RCAS:: <i>GFP</i> and RCAS:: <i>WNT5A</i> retroviruses into lower beak.....	37
Figure 2.4 Delayed effects of excess Wnt5a-CM on cartilage matrix in mandibular micromass cultures.....	40
Figure 2.5 Wnt5a does not affect total cell numbers in cultures.....	41
Figure 2.6 Wnt5a has a cumulative effect on cartilage matrix.	42
Figure 2.7 Expression of chondroitin sulfate at different stages in the head.	42
Figure 2.8 Expression of chondroitin sulfate glycosaminoglycan is decreased in Wnt5a-treated cultures.	43
Figure 2.9 Matrix metalloproteinases and Aggrecanases mediate loss of cartilage matrix.	47
Figure 2.10 Wnt5a represses canonical and activates non-canonical JNK mediated signaling pathways in mandibular mesenchyme.....	51
Figure 2.11 Wnt3a-CM inhibits early chondrogenesis in micromass cultures of mandibular mesenchyme.	52

Figure 2.12 Wnt5a treatment causes degradation of limb cartilage in the same manner as cartilage in the face.	54
Figure 2.13 Summary of Wnt5a functions during cartilage development and disease....	61
Figure 3.1 PCR analysis to confirm presence of hWNT5A in DF1 cells.	71
Figure 3.2 In vivo injection of RCAS:: <i>GFP</i> , RCAS:: <i>wtWNT5A</i> , RCAS:: <i>WNT5A^{C182R}</i> and RCAS:: <i>WNT5A^{C83S}</i> retroviruses into mandible.	72
Figure 3.3 In vivo injection of RCAS:: <i>GFP</i> , RCAS:: <i>wtWNT5A</i> , RCAS:: <i>WNT5A^{C182R}</i> and RCAS:: <i>WNT5A^{C83S}</i> retroviruses into limb.	73
Figure 3.4 Effects of <i>WNT5A</i> and its mutations on cell proliferation and cell death.....	75
Figure 3.5 Procedures used for cell migration assay	77
Figure 3.6 Cell movement studies in the embryos injected with RCAS:: <i>GFP</i> , RCAS:: <i>wtWNT5A</i> , RCAS:: <i>WNT5A^{C182R}</i> and RCAS:: <i>WNT5A^{C182R}</i>	78
Figure 3.7 Cell movement studies in the embryos injected with RCAS:: <i>GFP</i> , RCAS:: <i>wtWNT5A</i> , RCAS:: <i>WNT5A^{C182R}</i> and RCAS:: <i>WNT5A^{C182R}</i>	79
Figure 3.8 Chondrocyte intercalation and shape is affected in the embryos infected with RCAS:: <i>wtWNT5A</i> , RCAS:: <i>WNT5A^{C182R}</i> and RCAS:: <i>WNT5A^{C83S}</i>	82
Figure 3.9 Summary of effects of <i>WNT5A</i> mutations on mandibular morphogenesis. ...	93
Figure 4.1 Summary of WNT5A functions during facial normal and defective development.	100

List of abbreviations

Abbreviation	Definition
ADAMTS	A Disintegrin and Metalloproteinase with Thrombospondin motifs
ANOVA	One-way analysis of variance
AP2a	Activating Protein 2a
APC	Adenomatous Polyposis Coli
ATF2	Activating transcription factor 2
BMP	Bone morphogenetic protein
BrdU	5-bromo-2'-deoxyuridine
C	cysteine
Ca	Calcium
CamKII	Calmodulin kinase II
CE	Convergent extension
CM	Conditioned Media
Col	Collagen
CS	Chondroitin sulfate
CSPG	Chondroitin sulfate proteoglycan
Ct	Cycle threshold
DAPI	4',6-diamidino-2-phenylindole
DF1	Chicken embryo fibroblast cell line
DiI	Dioctadecyl-tetramethylindocarbocyanine
DiO	Dioctadecyloxacarbocyanine
DKK	Dickkopf

DLX	Distal-less homeobox
DMEM	Dulbecco's modified eagle's medium
DODAC	N,N-dioleoyl-N,N-dimethylammonium chloride
DOPE	1,2 dioleoyl glycerol-3-phosphorylethanolamine
DRS	Dominant form of Robinow syndrome
Dvl	Dishevelled
EtOH	Ethanol
FGF	Fibroblast growth factor
Fzd	Frizzled
g	gallus
GFP	Green fluorescent protein
GSK3	Glycogen Synthase Kinase 3
GTPase	Guanosine triphosphate
h	human
HBSS	Hank's Balanced Salt Solution
HH	Hamburger Hamilton
Hox	Homeotic complex
IF	Immunofluorescence
Ihh	Indian hedgehog
JNK	Jun nuclear kinase
KOH	Potassium hydroxide
LiCl	Lithium Chloride
LRP	Low Density Lipoprotein Receptor-Related Protein

MMP	Matrix Metalloproteinase
NFAT	Nuclear factor of activated T-cells
OTX	Orthodenticle homeobox
PBS	Phosphate buffered saline
PCNA	Proliferating Cell Nuclear Antigen
PCP	Planar Cell Polarity
PFA	Paraformaldehyde
PITX	Pituitary homeobox
Pk	Prickle
PKC	Protein kinase C
PNA	Peanut agglutinin
PTHrP	Parathyroid hormone-related protein
qPCR	Quantitative polymerase chain reaction
R	Arginine
RCAS	Replication-competent avian sarcoma-leukosis virus long terminal repeat with Splice acceptor
Ror	Receptor tyrosine kinase-like orphan receptor
Runx2	Runt-related transcription factor 2
S	Serine
sFRP	secreted Frizzled related protein
SHH	Sonic hedgehog
SOX	Sex determining region Y homeobox
TCF/LEF	T-cell factor/Lymphoid enhancing factor

TUNEL	Terminal deoxynucleotidyl transferase dUTP nick end labeling
WNT	Wingless-related MMTV integration site, related to the Drosophila gene Wingless
wt	wild type

Acknowledgements

I would like to express my special appreciation and gratitude to my supervisor, Dr. Joy Richman, from whom I learned thoughtful thinking in science. I am so grateful for her guidance, support and valuable suggestions throughout my graduate training over the past 6 years.

I am also grateful to my supervisory committee members, Dr. Charles Shuler, Dr. Michael Underhill and Dr. Virginia Diewert for their invaluable advice and support and the Underhill lab for helping with luciferase assays.

I would like to thank the Canadian Institute of Health Research for supporting this project via grants to Dr. Joy Richman and myself.

I would also like to thank all current and previous Richman lab members Dr. Poongodi Geetha-Loganathan and Dr. Suresh Nimmagadda for their friendship and helpful discussions, Dr. John Abramyan, Dr. Stephen Drain, Dr. Adrian Danescu, Dr. Layne Myhre, Kelvin Leung, Cheryl Whiting, Dr. Gregory Handrigan and Dr. Norihisa Higashihori for their help and inspiration. I would particularly like to express my sincere gratitude to Katherine Fu for her genuine friendship, encouragement and endless help. Thank you Kathy!

Special thanks to my family. I am so grateful to my parents and in-laws for their constant support.

Words cannot express my most sincere appreciation to my beloved husband, Alireza, who spent sleepless nights with and was always my support in the moments when there was no one to answer my queries. Thank you for being so patient and devoted, Alireza!

At the end, I would like to express my love and appreciation to my little daughter, Eileen, who always kept my spirits up throughout writing this dissertation by keeping me playing and laughing!

1. Introduction

1.1 Overview

The three most frequent congenital defects involve abnormal embryonic development of the heart, neural tube and the face. All occur either as isolated anomalies or as part of a syndrome and all have a complex etiology consisting of environmental and genetic risk factors. Of these, neural tube defects are in decline due to folic acid supplementation but the frequency of craniofacial defects has remained the same for decades. The burden of care for individuals with craniofacial abnormalities such as clefts or mandibular hypoplasia is very high and can exceed congenital heart defects in terms of the number of interventions needed to restore function. It is therefore critical to find ways to prevent or reduce the severity of these defects. Human genetic studies are helping to identify genes that contribute to increased risk of clefting (Dixon et al., 2011) but less is known about the causes of other more rare craniofacial defects such as those affecting the mandible. Mandibular hypoplasia/micrognathia is a clinical feature of the syndromes Treacher Collins (Dixon, 1996), Pierre Robin Anomalad (Segreti and Maumane, 1977) and hemifacial microsomia (Kosaki et al., 2007). Syndromes such as these affect many structures in addition to the head. Understanding the pathophysiology of the craniofacial defects can provide insights into normal development of the head as well as other regions of the body that use the same molecular signaling pathways.

Signaling pathways are composed of interacting proteins. We and others have been working on the secreted proteins that are present in the face and have made significant advances in identifying critical roles for FGF (Fibroblast Growth Factor), BMP (Bone Morphogenetic Protein) and most recently WNT signalling (Wingless-related MMTV integration site, related to the *Drosophila* gene wingless) (Abzhanov et al., 2004; Marcucio et al., 2005; Szabo-Rogers et al., 2008; Szabo-Rogers et al., 2010). However, although we know that these growth factors are able to affect facial

development, how, and at which levels these pathways intersect to control morphogenesis, is unknown. Starting with the human syndrome and then using animal models to answer in detail how the signaling protein functions is the way forward.

There are few human syndromes caused by *WNT* mutations (Niemann et al., 2004). Among those, is Robinow syndrome which is caused by mutations in *WNT5A* or *WNT5A* receptor, *ROR2* (Person et al., 2010). Patients with Robinow syndrome have facial abnormalities including micrognathia (Person et al., 2010). Also, gain- and loss-of-function of *Wnt5a* in mouse has devastating effects on mandibular morphogenesis and skeletogenesis (Yamaguchi et al., 1999; Yang et al., 2003). However, the precise roles of *WNT5A* during mandibular development need to be studied in detail.

Our animal model is chicken and we have shown that most *WNT* genes are strongly expressed in the chicken face (Geetha-Loganathan et al., 2009). In this dissertation, I have acknowledged the questions of how *WNT5A* functions during mandibular development and how disruption in *WNT5A* signaling causes facial defects.

1.2 Facial development in the chicken embryo

Vertebrate facial development begins with the generation of neural crest cells, a group of epithelial cells that derive from the dorsal edges of the neural tube and transform into mesenchyme (Le Douarin et al., 2004). In the avian embryo, neural crest cell migration occurs between stage 7-15 (Kontges and Lumsden, 1996). In avian embryos, all facial bones are formed by Hox-negative neural crest-derived mesenchyme originating from rhombomere 1, 2 and anterior regions (Fig. 1.1A)(Couly et al., 1993; Gross and Hanken, 2008; Kontges and Lumsden, 1996; Le Douarin et al., 2004; Noden and Trainor, 2005). These cells are designated as facial skeletogenic neural crest and when removed no facial skeleton will be formed (Creuzet et al., 2005). The remaining Hox-positive neural crest cells originating from rhombomere 2 and the rest

of the neural tube cannot form intramembranous facial bones (Creuzet et al., 2005). There is still controversy about the embryonic origin of frontal bones in chicken as some groups say they originate from neural crest cells (Couly et al., 1993; Gross and Hanken, 2008), whereas others showed them to be mesodermal (Gross and Hanken, 2008; Noden, 1982). Migrating neural crest cells in the prospective facial region populate the pharyngeal arches (Fig. 1.1A), surround the mesodermal core and are externally covered by the ectoderm (Graham, 2003; Noden and Trainor, 2005). The mesoderm and neural crest are tightly coordinated so that muscles insert into the relevant skeletal elements (Grenier et al., 2009; Noden and Trainor, 2005).

The rostral jaw is derived from midbrain neural crest cells whereas the most caudal structures are formed by cells originating from rhombomere 1 and 2 (Kontges and Lumsden, 1996; Mina, 2001).

At stage 18 in the chicken (3 days of incubation), the facial prominences (frontonasal mass, maxillary, lateral nasal, and mandibular) begin their outgrowth phase which lasts until stage 28 (5.5 days of incubation; Fig. 1.1B). The frontonasal mass makes contact and fuses with the maxillary prominences to form the continuous upper lip at stage 29 (Will and Meller, 1981). Failure of facial prominences to meet and fuse at the appropriate time causes cleft lip (Ashique et al., 2002). Epithelial-mesenchymal interactions are involved in outgrowth and morphogenesis of facial structures. Epithelium is required for the outgrowth of prominences whereas the mesenchyme determines the form of each prominence (Richman and Tickle, 1989). Epithelia are interchangeable between facial prominences and to some extent between face and limb (Richman and Tickle, 1989, 1992). The skeletal derivatives of avian facial prominences have been determined (Fig. 1.1C)(Lee et al., 2004; Richman et al., 2006; Richman and Tickle, 1989, 1992; Wedden, 1987).

Species-specific timing of skeletal differentiation is dictated by neural crest-derived mesenchyme (Merrill et al., 2008; Schneider and Helms, 2003; Yu et al., 2013). The length of the upper beak is established by the prenasal cartilage. The premaxillary bones are largely responsible for species-specific form of the upper beak e.g. the wide bill of the duck (Wu et al., 2006; Wu et al., 2004). The sides of the beak are formed by the maxillary prominences. Maxillary, palatine, jugal and quadratojugal bones support the roof of the mouth. In the lower beak, mesenchyme determines the size and shape of Meckel's cartilage shown by quail-duck chimeras. In these experiments, cartilage was developed at the faster pace of the quail donor mesenchyme in the host (Eames and Schneider, 2008). In the lower beak, it is Meckel's cartilage that drives growth and provides the initial skeletal support (Bhaskar et al., 1953). As mentioned above, we can predict which skeletal elements will be affected in our targeted manipulations of the early head.

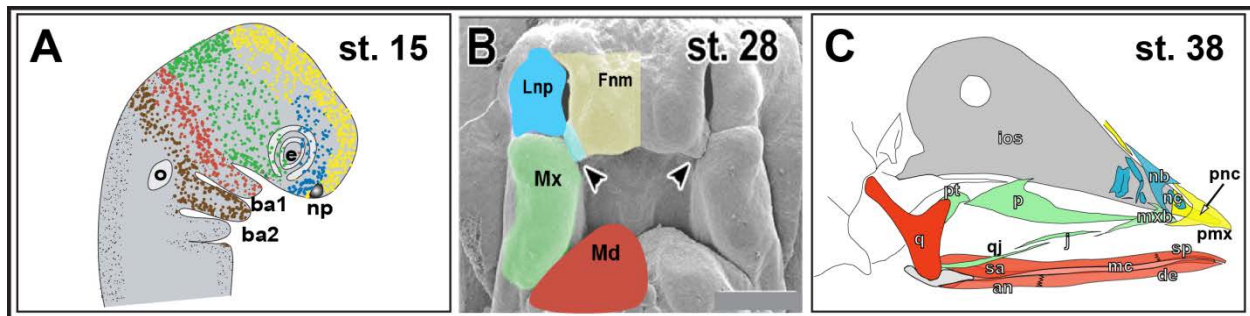


Figure 1.1 Steps of facial development

Facial development starts with migration of neural crest cells from dorsal margins of neural tube to ventral regions of the head (A) where they form facial prominences including frontonasal mass, lateral nasal, maxillary and mandibular prominences (B). Fnm, Lnp and Mx make contact (arrowheads in B) and fuse together to form upper beak and mandibular prominences form lower beak. Each prominence forms several skeletal elements (C). KEY: an — angular, ba — branchial arch, de — dentary, Fnm — frontonasal mass, IOS — Interorbital septum, j — jugal, Lnp — lateral nasal prominence, mc — meckel's cartilage, Md — mandible, Mx — maxillary, mxb — maxillary bone, nb — nasal bone, nc — nasal conchae, np — nasal pit, o — otic vesicle, p — palatine, pmx — premaxilla, pnc — prenasal cartilage, pt — pterygoid, q — quadrate, qj — quadratojugal, sa — surangular, sp — splenial.

1.3 Osteo/chondrogenesis in the face

There are two types of bone formation (Fig. 1.2). The first type is endochondral ossification during which mesenchymal condensations differentiate into cartilage which is later replaced by bone. Endochondral ossification takes place in the long bones and vertebral column and the growth plates are where bone longitudinal growth occurs. There are also sites of endochondral ossification in the skull, although these are primarily in the cranial base and occipital region (McBratney-Owen et al., 2008).

Intramembranous bone is formed by direct differentiation of osteoblasts from mesenchyme. The origins of the mesenchyme may be neural crest or mesoderm. Most craniofacial bones are formed by intramembranous ossification (Gross and Hanken, 2008).

The avian face is perhaps more complicated than that of the mammal since in addition to endochondral and intramembranous bone formation there are persistent cartilages such as Meckel's and ear cartilages (Eames et al., 2003). Meckel's cartilage remains cartilaginous up until hatching and possibly beyond while replacement cartilages such in the quadrate, undergo hypertrophy and eventually form bones beginning prenatally. In mammals Meckel's cartilage disappears as they mature (Wang et al., 2013b). Chondrogenesis and osteogenesis in the chicken begin at stages 29 and 34, respectively (Murray, 1963). The intramembranous bones are completed by stage 41 (Abzhanov et al., 2007).

In the lower jaw, the rostral part is supported by the splenial and dentary bones whereas in the posterior Meckel's cartilage is surrounded laterally by the surangular and medially by the angular bones. The angular articulates with the quadrate. Angular, surangular, splenial and dentary bones are formed through intramembranous ossification and quadrate is formed by endochondral ossification (Gross and Hanken, 2008).

The key transcription factors for intramembranous and endochondral bone formation are *Runx2* and *SP7/Osterix* (Eames et al., 2003). *Runx2* is the earliest osteogenic marker which acts upstream of *Osterix* (Ducy et al., 1997). In mice in which *Runx2* was deleted in the germline, there was a complete absence of all bones although cartilage still forms (Ducy et al., 1997; Otto et al., 1997). The osteogenic matrix markers in the order of their appearance include *Col1a2*, Osteopontin, and bone sialoprotein or integrin binding sialoprotein and Osteocalcin (James et al., 2005; Kern et al., 2001).

The master chondrogenic program in persistent and replacement cartilage is under the control of *Sox* genes including *Sox5*, *Sox6* and *Sox9* (Eames et al., 2003). Deletion of *Sox9* in the neural crest cells prevents all craniofacial cartilages from forming and in their place, ectopic bone is found (Mori-Akiyama et al., 2003). Collagens 2, 9 and 11 are markers of newly deposited chondrogenic matrix. *Col2a1* is a specific isoform of *Col2* and is activated by *Sox9* directly binding to *Col2a1* minimal enhancer which has an activity in chondrocyte differentiation (Eames et al., 2003; Lefebvre et al., 1997; Lefebvre et al., 1998). *Sox* genes also activate *Aggrecan*, the other marker of chondrogenic matrix (Lefebvre et al., 1998). Cartilage matrix deficient mice which lack a small sequence of *Aggrecan* gene are characterized by a short stature and short snout (Watanabe et al., 1994). Important markers of prehypertrophic and hypertrophic chondrocytes during endochondral ossification include secreted signals *Ihh*, PTHrP, and the matrix protein, *Col10a1* (James et al., 2005; Yang et al., 2003). In *Col10a1* null mice the hypertrophic zone was reduced (Gress and Jacenko, 2000). Targeted deletion of *Ihh* in mice delays chondrocyte maturation and osteoblast differentiation leading to defects in the formation of endochondral bones (St-Jacques et al., 1999). The receptor of Hh signaling, *Patched* is another cartilage marker (Eames and Helms, 2004).

Surprisingly, the majority of histological and molecular skeletogenic markers are conserved among different types of bones in the chicken (Eames and Helms, 2004) with a few exceptions. *Patched* was detected in the limb persistent articular cartilage but not in Meckel's cartilage. Both face and limb persistent cartilages were similarly lacking COL10A, a protein that is strongly expressed in the hypertrophic zone of replacement cartilage. In regards to intramembranous bone, the only subtle molecular difference is *BMP6* which is expressed in the facial intramembranous bone and not in the limb endochondral bones. The other conserved bone markers between face and limb include *COL1A1*, *BMP4* and *RUNX2*. All other histological markers and collagens are identical (Eames and Helms, 2004).

In functional experiments in which *SOX9* was overexpressed in the replacement cartilage of the second pharyngeal arch, the ceratobranchial cartilage lost *COL10* and *RUNX2* expression resembling a persistent cartilage. The opposite effect was seen by injection of virus expressing *RUNX2* into a persistent cartilage in the neck. Markers of replacement cartilages i.e. expression of *COL10* and *RUNX2* in addition to *SOX9* and *COL2* were induced (Eames et al., 2004). Thus *SOX9* is necessary and sufficient to create persistent cartilages and *RUNX2* is sufficient to trigger a replacement cartilage program.

By the time skeletal differentiation has begun there has been extensive signaling to set up the pattern which includes the shape, size and arrangement of the individual skeletal elements to make up the whole skull.

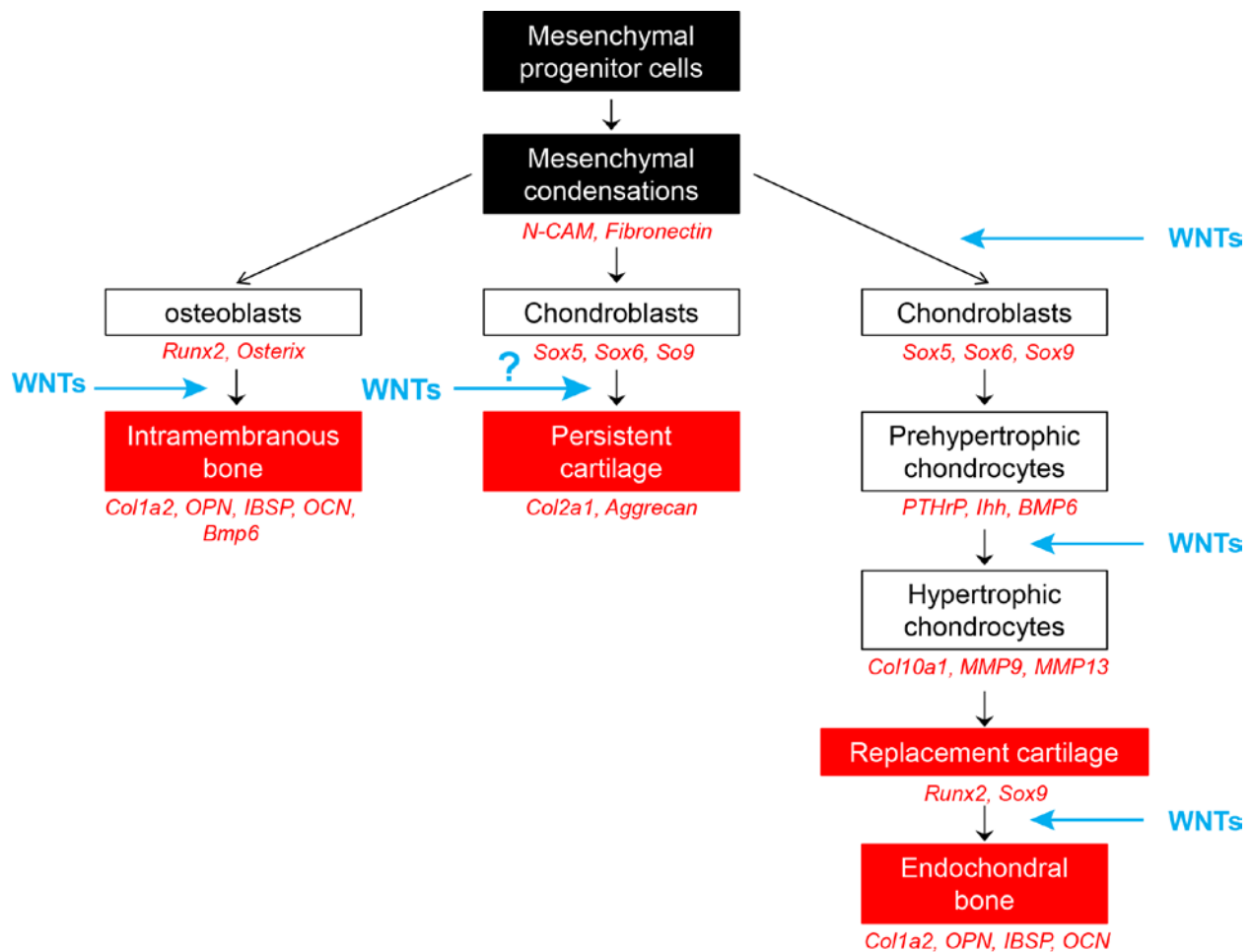


Figure 1.2 Different types of bone and cartilage

Skeletogenesis starts with mesenchymal progenitor cells forming mesenchymal condensations. Mesenchymal condensations are then differentiated into either osteoblasts to form intramembranous bones as in the face or chondroblasts in which case they form persistent cartilages of the face or replacement cartilages being replaced by endochondral bones as in the limbs. The chondrogenic and osteogenic markers are shown in red italic font. WNTs are among several inputs involved in skeletogenesis whose roles have been shown in different steps of bone and cartilage development; however, the specific roles of WNT signaling in the development of persistent cartilages are still unknown.

1.4 Signaling pathways that operate during facial development

Signalling interactions are required in the face to establish the identity of each facial prominence and its derivatives (Helms et al., 2005). Some of these signals include BMPs, FGFs, SHH, WNTs and Endothelins.

1.4.1 BMPs

The maxillary processes and their skeletal derivatives are patterned by Bone morphogenetic proteins (BMPs) and Retinoic acid (RA). In the presence of Noggin (BMP antagonist) and Retinoid acid, maxilla is transformed into frontonasal mass leading to duplication of the upper beak (Lee et al., 2001). Abzhanov et al. found that expression of *BMP4* in chicken upper face correlates with the depth and width of the beak among Darwin's finches as overexpression of *BMP4* leads to broader beaks whereas antagonizing BMPs by *Noggin* leads to formation of a narrower beak (Abzhanov et al., 2004). Wu et al. showed an increase in length, depth and width of the beak by overexpressing *BMP4* in all beak-forming prominences (Wu et al., 2004). Viruses expressing constitutively active BMP receptors in maxillary prominences also led to outgrowth of cartilage elements (Ashique et al., 2002). Overexpression of BMP signaling using replication competent virus (RCAS) expressing *BMP2* or *BMP4* leads to truncated lower jaw and ectopic cartilage formation at the expense of bone whereas inhibiting BMP signaling by using RCAS::*Noggin* causes a shortened lower beak with reduced bone and cartilage (Hu et al., 2008). Mandibular outgrowth was also affected by BMP signaling manipulation as shown by implanting BMP beads into mandible. Application of BMP7 beads to the medial regions of mandibular prominences induced formation of a cartilage rod extending from Meckel's cartilage whereas in the lateral edge, it ended up with absent or reduced Meckel's cartilage at early stages of development (Mina et al., 2002). Others obtained the same branching of Meckel's cartilage by applying BMP2 or BMP4 to the medial of mandibular prominences (Barlow and Francis-West, 1997). Therefore, BMP signaling has multiple fundamental roles in craniofacial development.

1.4.2 FGFs

FGFs are other signals regulating facial morphology. Overexpression of FGF8 in the chicken frontonasal mass epithelium using RCAS::*FGF8* lead to shortening of upper beak as well as reduced or missing of maxillary and frontonasal outgrowth (Abzhanov and Tabin, 2004). FGF signaling from nasal slit is important during normal lip formation by regulating cell proliferation since implanting beads soaked in FGF antagonist into lateral frontonasal mass adjacent to nasal slit caused cleft beak in chicken (Szabo-Rogers et al., 2008). Application of either FGF2 or FGF4 beads to the medial regions of mandibular prominences, promoted both mandibular outgrowth and Meckel's cartilage elongation in the lower jaw whereas implanting these beads to the lateral edges did not affect the growth or chondrogenesis of the mandible (Mina et al., 2002).

1.4.3 SHH

Frontonasal ectodermal zone which is featured by adjacent expression of *SHH* and *FGF8* directs morphogenesis of the middle and upper face (Cordero et al., 2004; Hu et al., 2003; Marcucio et al., 2005). Transplantation of this epithelium into either frontonasal or mandibular prominences of a host chicken induced ectopic upper and lower beak, respectively (Hu et al., 2003). Preventing the upregulation of *SHH* in facial epithelium by removing frontonasal crest or injecting hybridoma cells expressing an antibody to *SHH* caused a malformed face with lack of mediolateral expansion of the frontonasal region and truncation of distal upper beak (Marcucio et al., 2005). Sonic hedgehog is also an important signal expressed by the pharyngeal endoderm. There are instructive patterning cues from foregut endoderm to the skeletogenic Hox-negative neural crest cells that are required for lower jaw development (Couly et al., 2002; Richman and Lee, 2003; Schneider and Helms, 2003; Tucker and Lumsden, 2004). Grafting quail foregut

endoderm to the chicken embryonic head induces supernumerary skeletal elements (Couly et al., 2002). Removal of the rostral source of *SHH*, foregut endoderm, in the chicken leads to stage-dependent loss of bones and cartilages of lower jaw. Replacing foregut endoderm by SHH beads rescues the skeletal phenotype (Brito et al., 2006). Surgical ablation of the most anterior part of the endoderm in chicken embryo leads to a complete absence of the lower part of the nasal capsule, mesethmoid, and this phenotype was rescued by either a graft from an equivalent region of a stage-matched quail or SHH bead (Benouaiche et al., 2008). Therefore, SHH derived from the endoderm is required for proper upper and lower jaw development.

1.4.4 Endothelins

Mandibular identity is specified by endothelins, the proteins that constrict the blood vessels and raise blood pressure (Schiffrin, 2005). The loss of endothelins leads to a complete loss of Meckel's cartilage (Kurihara et al., 1994) and gain of vibrissae (Sato et al., 2008). Loss and gain of endothelin receptor function in the mandible in mice leads to duplicated maxillary or mandibular structures, respectively (Ruest et al., 2004; Sato et al., 2008).

1.4.5 WNTs

WNTs (wingless-related MMTV integration site, related to the *Drosophila* gene Wingless) are secreted glycoproteins that act as short-range intercellular signals (Nusse et al., 1991). The first Wingless gene was originally discovered in *Drosophila* embryos as a gene controlling segment polarity. There are 7 Wnt genes in *Drosophila* but this has expanded to 19 members in mammals (Logan and Nusse, 2004; Seidensticker and Behrens, 2000). The mammalian Wnts include Wnt1, Wnt2, Wnt2b, Wnt3, Wnt3a, Wnt4, Wnt5a, Wnt5b, Wnt6, Wnt7a, Wnt7b, Wnt8a, Wnt8b, Wnt9a, Wnt9b, Wnt10a, Wnt10b, Wnt11, and Wnt16. Most of these genes have confirmed orthologs in the chicken genome (Geetha-Loganathan et al., 2009).

Wnts have diverse roles in cancer and development. For example, dysregulation of the Wnt pathway leads to colorectal cancer and tooth agenesis (Lammi et al., 2004; Liu et al., 2000). In addition, roles for Wnts have been defined for axis formation (Sokol et al., 1991), somite patterning (Geetha-Loganathan et al., 2006), kidney morphogenesis (Carroll et al., 2005), limb bud initiation (Kawakami et al., 2001) and dorso-ventral limb patterning (Kawakami et al., 2001). According to the type of signaling stimulated by each Wnt they are classified as canonical (Fig. 1.3) and non-canonical (Fig. 1.4). The canonical Wnts include: Wnt1, Wnt2, Wnt2b, Wnt3, Wnt3a, Wnt7a, Wnt8a, Wnt8b, Wnt9a, Wnt9b, Wnt10a, Wnt10b, Wnt16 (Davis et al., 2008; Geetha-Loganathan et al., 2009) and the non-canonical Wnts include Wnt4, Wnt5a, Wnt5b, Wnt6, Wnt7b, and Wnt11 (Geetha-Loganathan et al., 2009). Some Wnts such as Wnt4 (Geetha-Loganathan et al., 2009; Hartmann and Tabin, 2000; Lyons et al., 2004; Tanigawa et al., 2011), Wnt6 (Linker et al., 2005; Schmidt et al., 2007), Wnt7b (Wang et al., 2005; Zheng et al., 2013) and Wnt5a (Mikels and Nusse, 2006; van Amerongen et al., 2012) can function via both canonical and non-canonical pathways.

There are several findings supporting the idea that there is no sharp line between canonical and non-canonical Wnt pathways. Others have shown that an increase in intracellular Ca^{2+} by several recombinant Wnt peptides including 3a, 4, 5a, 7a, 9b, 10b via non-canonical pathway facilitates nuclear translocation of β -catenin (major component of canonical pathway) in vitro (Thrasivoulou et al., 2013). Also it has been shown that Wnt3a and Wnt7b use non-canonical Wnt pathway to regulate bone formation in vitro and in vivo (Tu et al., 2007). Moreover, Lrp5/6, the canonical pathway co-receptors physically interact with Wnt5a and loss of Lrp6 causes phenotypes similar to gain of non-canonical function in both *Xenopus* and mouse i.e. defective elongation in *Xenopus* and exencephaly (open neural tube in cephalic region) and

heart defects in mouse. These phenotypes could be rescued by deletion of Wnt5a function (Bryja et al., 2009). Another supporting study is that Rac1, a component of non-canonical pathway, is required for nuclear localization of β -catenin and Rac1 knock-out mice show truncation of limb similar to loss of β -catenin function (Wu et al., 2008). Therefore, an integrated model of canonical and non-canonical Wnts is now more acceptable in which multiple components are involved in both pathways (van Amerongen and Nusse, 2009).

1.4.5.1 Canonical WNT signaling

Canonical Wnt signaling is the best understood Wnt signaling pathway (Fig. 1.3). Canonical Wnts bind to Frizzled (Fzd) receptors and Lrp co-receptors (Low density lipoprotein receptor related protein). Frizzled receptors are transmembrane proteins and there are 10 Fzd receptors in mammals with variable capacities to bind to different Wnts. There has been no success in assigning individual Wnts to individual Fzds and vice versa (Logan and Nusse, 2004). There is functional redundancy among Fzd members (MacDonald et al., 2009; Yu et al., 2010; Yu et al., 2012). Lrp co-receptors are required for canonical signaling and include Lrp5 and Lrp6 (He et al., 2004). Lrp5 and Lrp6 are phosphorylated upon binding of canonical Wnts. Upon formation of a Wnt-Fzd-Lrp complex, Dishevelled (Dvl) and Axin are recruited to Fzd and Lrp, respectively which leads to inhibition of β -catenin degradation complex (Axin, Adenomatous Polyposis Coli and Glycogen Synthase Kinase 3). Dishevelled has three domains consisting of DIX, PDZ and DEP. DIX and PDZ domains are utilized in canonical signaling whereas DEP and PDZ domains are active during non-canonical signal transduction (Komiya and Habas, 2008; Perrimon and Mahowald, 1987). Upon inhibition of β -catenin destruction complex, the free cytoplasmic β -catenin is translocated into the nucleus where it interacts with TCF/LEF transcription factors (T-cell factor/lymphoid enhancer factor) and activates transcription of Wnt

target genes such as c-myc, cyclinD and Axin2. In the absence of a canonical Wnt ligand, β -catenin degradation complex is activated leading to phosphorylation of β -catenin by glycogen synthase kinase 3 and casein kinase 1 and β -catenin degradation in proteasome (Angers and Moon, 2009; Gordon and Nusse, 2006; Komiya and Habas, 2008; MacDonald et al., 2009; Rao and Kuhl, 2010; Seidensticker and Behrens, 2000; Vlad et al., 2008). Changes in the function of any of these components can cause developmental defects. Table 1.1 shows craniofacial phenotype of mouse knock-outs of canonical pathway components.

Canonical Wnt pathway

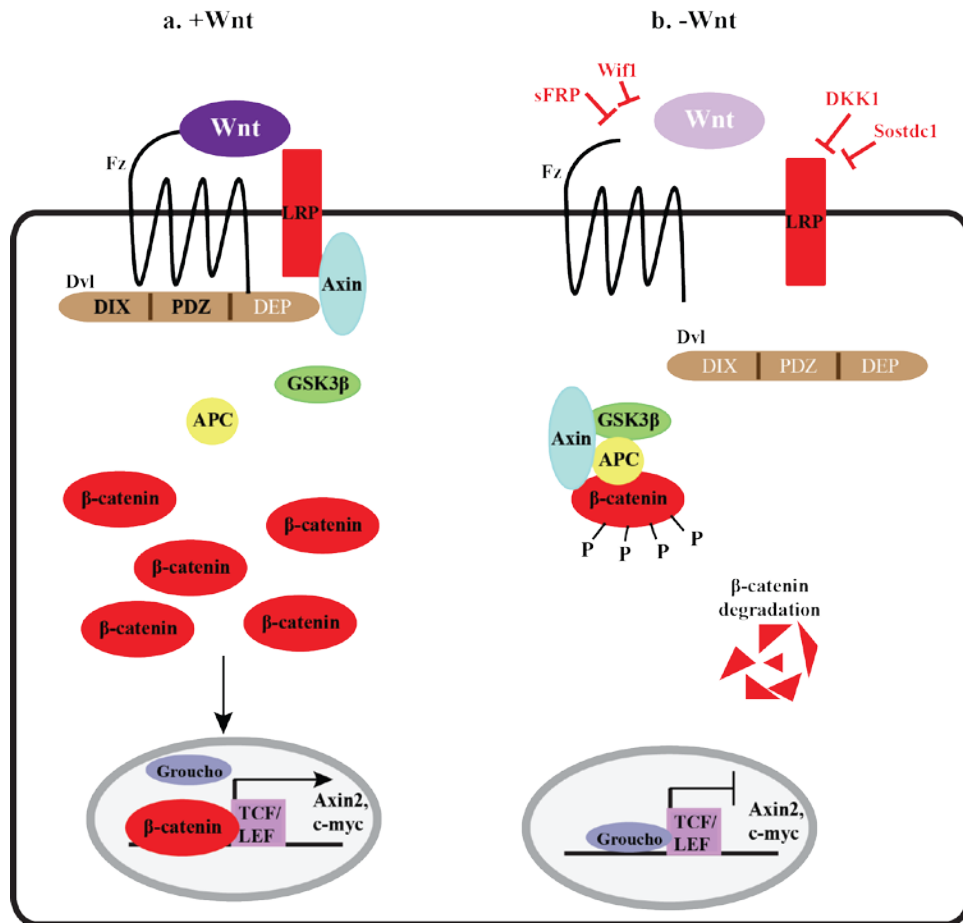


Figure 1.3 Canonical Wnt signaling pathway.

The canonical Wnt pathway involves β -catenin. The intracellular cascade is activated upon binding of a canonical Wnt to Fzd-Lrp receptor complex (a). Axin and Dvl are recruited to the receptor complex. Cytoplasmic β -catenin is then translocated into the nucleus, replaces the transcription repressor, Groucho and activates transcription of Wnt target genes via TCF/LEF transcription factor complex. In the absence of Wnt ligand or in the presence of canonical Wnt inhibitors (b), β -catenin degradation complex including Axin, Adenomatous Polyposis Coli (APC), and Glycogen Synthase Kinase-3 β (GSK3 β) is activated leading to destruction of β -catenin through a ubiquitin-proteasome pathway. Therefore, β -catenin does not enter the nucleus and transcription of target genes is repressed by Groucho and other transcription repressors.

Table 1.1 Mouse knock-outs of the canonical pathway components with craniofacial defects.

Gene knocked-out	Phenotype	Reference
<i>Wnt1</i>	Loss of midbrain and cerebellum	(Danielian and McMahon, 1996; McMahon and Bradley, 1990)
<i>Wnt3a</i>	Short lower jaw-abnormal cerebral cortex	(Yoshida et al., 2006)
<i>Wnt9a</i>	ectopic cartilage instead of bone in some cranial bones such as parietal	(Spatier et al., 2006)
<i>Wnt9b</i>	Cleft lip-cleft palate	(Carroll et al., 2005; Juriloff et al., 2004)
<i>Lrp5</i>	Decreased bone mass in calvaria	(Kato et al., 2002)
<i>Lrp6</i>	Cleft palate-small eye	(Pinson et al., 2000; Zhou et al., 2010)
<i>Lrp5;Lrp6</i>	Defective ossification in craniofacial skeleton	(Joeng et al., 2011)
<i>Gsk3</i>	Complete cleft of secondary palate	(He et al., 2010) (Liu et al., 2007)
<i>Axin2</i>	Short head and Premature fusion of cranial sutures-accelerated ossification	(Yu et al., 2005)
<i>Apc</i>	Absent forebrain and hindbrain and cranial structures-loss of mandible	(Buchert et al., 2010)
<i>β-catenin (Wnt1-cre)</i>	Loss of midbrain and part of hindbrain-loss of cranial bone and cartilage except a small part of Meckel's cartilage	(Brault et al., 2001)
<i>β-catenin (Dermo1-cre)</i>	Reduced ossification and ectopic cartilage formation	(Day et al., 2005; Rodda and McMahon, 2006)
<i>β-catenin (Ap2a-cre)</i>	Hypoplasia of all facial prominences-loss of all facial bones except parts of palatal shelves and zygomatic processes of maxilla	(Reid et al., 2011)
<i>β-catenin (Col2-cre)</i>	Short snout-cleft palate	(Akiyama et al., 2004)
<i>Tcf4;Lef1</i>	Underdeveloped maxilla-short nasal septum-wide set eyes (hypertelorism)-open eyelids	(Brugmann et al., 2007)

1.4.5.2 Non-canonical WNT signaling

Non-canonical Wnts (Fig. 1.4) also bind to Frizzled receptors (Veeman et al., 2003) but instead, activate either JNK/planar cell polarity (PCP) (Fanto and McNeill, 2004; Karner et al., 2006) or calcium signalling pathways (Kuhl et al., 2000). Major components of PCP pathway in vertebrates include Frizzled receptor (Fzd), cytoplasmic protein Dishevelled (Dvl), Prickle1/2

(Pk), transmembrane proteins, Vangl1/2 (homolog of Strabismus in *Drosophila*), Celsr1-3 cadherins (homolog of Flamingo in *Drosophila*) and the PCP effectors, Fuzzy, Inturned and Fritz (Gray et al., 2009a; Heydeck and Liu, 2011; Szabo-Rogers et al., 2010). Changes in the function of any of these components can cause defects in cell and tissue polarization resulting in phenotypic changes. Table 1.2 shows phenotypes of mouse knock-outs of non-canonical pathway components. Non-canonical Wnts such as Wnt5a, 5b, 11 bind to Fzd receptors and recruit Dvl to the membrane. Then small GTPases, Rac and Rho are activated through DEP and PDZ domains of Dvl leading to JNK activation. Vangl2 recruits Prickle which then in accompany with Dvl provides the cells asymmetry/polarity (Gao, 2012). Phenotypic analysis is a good readout for the PCP pathway (Gao, 2012). Other reliable readouts of this pathway include ATF2 luciferase reporter or c-jun/JNK phosphorylation assays (Gao, 2012; Ohkawara and Niehrs, 2011). The PCP pathway has crucial roles during convergent extension (CE) in *Xenopus* and zebrafish, neural tube closure, orientation of sensory hair cells in the inner ear in mammals and palate formation (Gao, 2012; Gao et al., 2011; He et al., 2008).

A few Wnts such as Wnt5a can increase intracellular calcium which then activates the Protein Kinase C (PKC), Calmodulin Kinase II (CamKII) and Calcineurin. This leads to activation of calcium pathway transcription factors such as NFAT and then appropriate cell responses (Kohn and Moon, 2005). This pathway is active during body plan specification in *Xenopus* and zebrafish and also has a role in the development of slow fiber muscles in chicken wing (Kohn and Moon, 2005).

The third non-canonical pathway is Fzd independent and includes the receptor tyrosine kinases, Ror1/2. Ror2 forms a complex with vangl2. Wnt5a can activate this complex and by

phosphorylating Dvl antagonizes canonical signaling (Ho et al., 2012). Wnt5a also regulates Vangl2 phosphorylation in a gradient manner (Gao et al., 2011).

It is not always possible to predict which pathway, canonical or non-canonical, will be used just from gene expression pattern. Receptor availability and specificity determines the pathway being activated. For example, Wnt5a binds Fzd4 and when this receptor is available canonical signalling will take place. The alternative receptor for Wnt5a is Ror2 and when it is used, canonical signalling is inhibited (Mikels and Nusse, 2006).

1.4.5.2.1 Wnt5a

Deletion of Wnt5a in mice has serious consequences on early facial prominence outgrowth that secondarily affects skeletal differentiation so it is difficult to determine the direct role on skeletogenesis. The limbs of knockout mice exhibit defective chondrogenesis and osteogenesis (Yamaguchi et al., 1999; Yang et al., 2003). Overexpression of Wnt5a in chondrogenic cells (Col2a1 promoter) caused a similar truncation of the jaws, smaller rib cage and shorter limb long bones (Yang et al., 2003). Over expression of *Wnt5a* in a temporal and spatial restricted manner leads to loss of hair follicles and bone loss in mouse via Wnt5a-mediated repression and activation of canonical Wnt signaling, respectively (van Amerongen et al., 2012). A human connection between WNT5A signaling and craniofacial abnormalities has also been shown. Robinow syndrome which has a craniofacial phenotype is caused by loss-of-function mutations of *ROR2* (Schwabe et al., 2004), the receptor that mediates non-canonical signaling of WNT5A. Furthermore, another study has shown that the dominant form of the same syndrome is caused by mutations of *WNT5A* gene (Person et al., 2010). The only studies on WNT5A function in chicken were done in the limb bud using overexpression strategies. Injection of a chicken retrovirus containing *WNT5A* delayed cartilage hypertrophy (Kawakami et al., 1999). The same virus has

unclear effects on chondrogenesis in primary limb mesenchyme cultures (Yang et al., 2003). Thus the precise roles for Wnt5a during facial skeletogenesis and the mechanism through which it works remain to be determined.

Non-canonical Wnt pathways

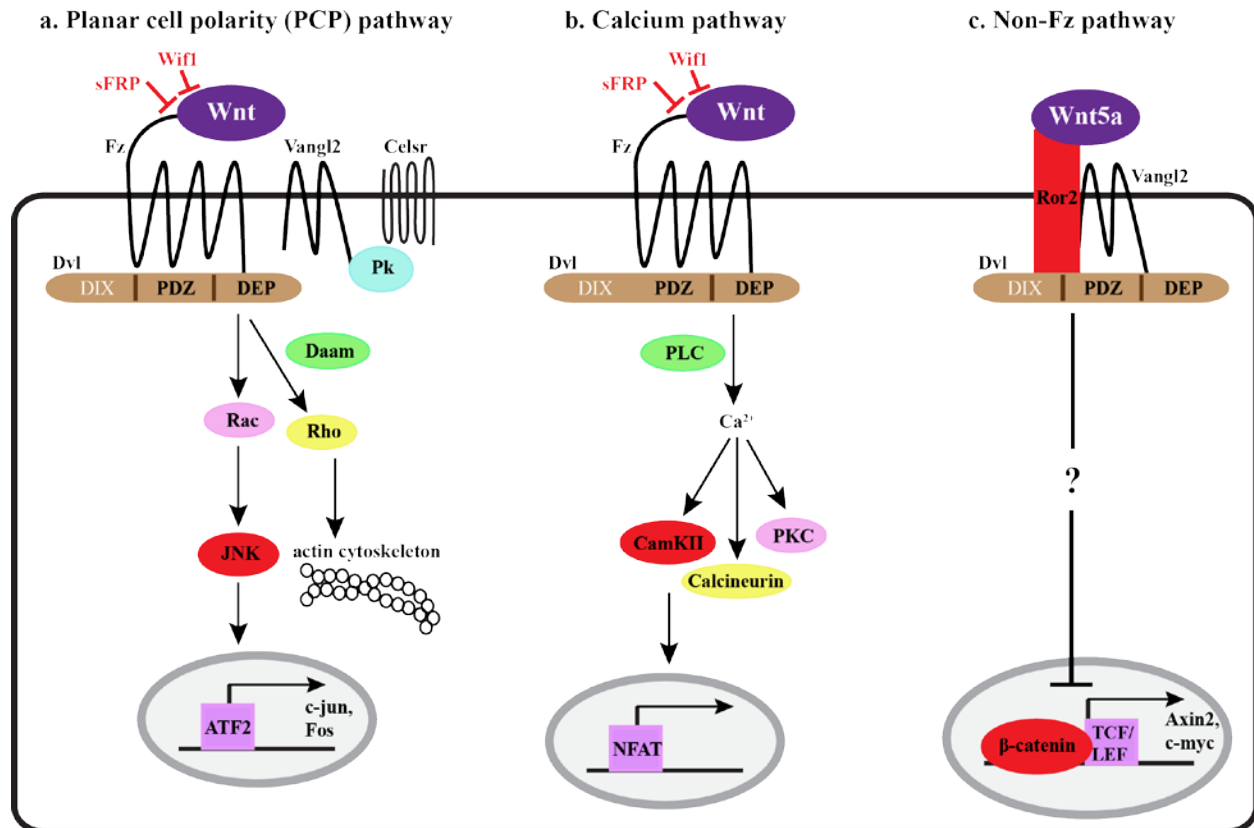


Figure 1.4 Non-canonical Wnt signaling pathways.

The non-canonical Wnt pathways do not involve LRP co-receptors and β -catenin. sFRP is an inhibitor of both canonical and non-canonical pathways. a) Planar cell polarity (PCP) pathway is characterized by an asymmetric distribution of Fzd, Dvl, Vangl2, Prickle (Pk) and Celsr, resulting in cell polarization. Signalling is activated by interaction of non-canonical Wnts with Fzd receptors. Signal is transmitted intracellularly through DEP and PDZ domains of Dvl which then activates Rac. Rho activation needs the participation of Daam downstream of Dvl. Rac then activates JNK, resulting in appropriate gene expression. Rho is a key player in cytoskeletal rearrangement. The transmembrane protein Vangl2 forms a complex with Pk which along with Celsr is involved in cell polarity. b) Calcium pathway is activated by the non-canonical Wnt binding to Fzd receptor and an increase in intracellular Ca^{2+} mediated by phospholipase C (PLC). This pathway also engages DEP and PDZ domains of Dvl. Increased Ca^{2+} leads to activation of protein kinase C (PKC), calcium-calmodulin kinase II (CamKII) and calcineurin leading to appropriate cell responses. c) Wnt5a can signal through any of the mentioned pathways above. It can also use the receptor tyrosine kinase, Ror2, in a complex with vangl2 and antagonizes canonical signaling. The mediating components in this pathway are still unknown.

Table 1.2 Mouse knock-outs of the non-canonical Wnt pathway components.

Gene knocked-out	Phenotype	Reference
<i>Wnt5a</i>	Small tongue, ears and snout-cleft palate-short limbs	(He et al., 2008; Yamaguchi et al., 1999; Zhu et al., 2012)
<i>Wnt5a;Ror2</i>	Cleft palate	(He et al., 2008)
<i>Fzd1;Fzd2</i>	Cleft palate-micrognathia	(Yu et al., 2010)
<i>Fzd3</i>	Curly tail-open neural tube-abnormal brain morphology (missing parts)-abnormal hindlimb morphology (flexed limbs)	(Wang et al., 2002)
<i>Fzd6</i>	Curly tail-defective orientation of ear hair cells-open neural tube	(Guo et al., 2004)
<i>Ror1;Ror2</i>	Short snout and limbs-defective embryonic elongation	(Ho et al., 2012)
<i>Ror2</i>	Cleft palate-short limbs and snout	(DeChiara et al., 2000; Schwabe et al., 2004)
<i>Vangl1;Vangl2</i>	Randomized left-right asymmetry-open neural tube-open eyelid	(Song et al., 2010)
<i>Vangl2^{LP/LP}</i>	Defective proximo-distal elongation of the limb-loss of middle phalange in all digits-whorled hair (<i>Looptail</i> mutants)	(Gao et al., 2011; Wang et al., 2011; Yin et al., 2012)
<i>Dvl1;Dvl2</i>	Open neural tube	(Hamblet et al., 2002)
<i>Prickle1</i>	Short snout-short and wide limbs-brachydactyly-loss of a phalangeal segment in digits 2-5	(Yang et al., 2013)
<i>Celsr1</i>	Kinked tail-whorled body hair-open neural tube-defective orientation of sensory hair cells in inner ear-open eyelid	(Curtin et al., 2003; Ravni et al., 2009)
<i>Inversin</i>	Complete inversion of the left-right body axis-reversal of embryo turning	(Morishima et al., 1998)
<i>Fuzzy</i>	Short mandible-cleft palate-open neural tube	(Gray et al., 2009a)

1.4.5.3 WNT antagonists

There are naturally occurring Wnt antagonists of Fzd receptors and Lrp co-receptors (Fig. 1.3 and 1.4). Fzd antagonists include sFRP (secreted Frizzled related proteins) and Wnt inhibitory factor 1. sFRP group of antagonists consists of sFRP1-5 where sFRP1-3 actively inhibit Wnt signaling by binding to either Fzd receptors or Wnts. Wnt inhibitory factor 1 binds to Fzd receptors and prevents direct interaction of Wnt with the receptor (Hsieh et al., 1999;

Kawano and Kypta, 2003; MacDonald et al., 2009). Lrp antagonists include Dickkopf (DKK1-4) and Sostdc1. Dkk1 is the most effective canonical Wnt antagonist among all Dkk proteins. Sostdc1 is another antagonist of the canonical pathway and disrupts the Wnt-Fzd-Lrp complex by directly binding to Lrp (He et al., 2004; Kawano and Kypta, 2003; MacDonald et al., 2009; Semenov et al., 2005). Therefore, sFRPs are antagonists of both canonical and non-canonical pathways whereas Dkks specifically inhibit canonical signaling. The other group of Wnt antagonists, Shisa proteins, trap Fzd receptors in the endoplasmic reticulum and prevent their trafficking on cell membrane and therefore antagonize Wnt signaling cell autonomously (MacDonald et al., 2009). Chibby and ICAT (inhibitor of β -catenin and TCF4) are canonical Wnt inhibitors which directly bind to β -catenin and prevent β -catenin interaction with TCF/LEF in the nucleus (Tago et al., 2000; Takemaru et al., 2003). Groucho is a transcription repressor which binds to TCF/LEF. Upon nuclear translocation of β -catenin, this molecule replaces Groucho and activates transcription of target genes (MacDonald et al., 2009). There are few mouse mutations of Wnt antagonists causing craniofacial defects. Table 1.3 shows the craniofacial phenotypes of mouse knock-outs of Wnt antagonists.

Table 1.3 Mouse knock-outs of the Wnt antagonists with craniofacial defects.

Gene knocked-out	Phenotype	Reference
<i>Dkk1</i>	Loss of entire face, frontal and most of parietal bones	(Mukhopadhyay et al., 2001)
<i>Sfrp1;Sfrp2</i>	Short snout	(Satoh et al., 2006)

1.4.5.4 WNT gene expression patterns

Expression pattern analysis of a gene is the first step to study gene function and helps to find out the mechanism of its action. Our lab has carried out a comprehensive expression study

on Wnts in the chicken face (Geetha-Loganathan et al., 2009). Of all the surveyed genes, these genes had facial expression: *gWNT2B*, *gWNT4*, *gWNT5A*, *gWNT5B*, *gWNT6*, *gWNT9B*, *gWNT11* and *gWNT16*. Others have reported *gWNT7A* is also present in the chicken facial epithelium (Dealy et al., 1993). *DKK1* as well as other genes in the Wnt pathway (*gLEF1*, *gCTNNB1*, *gFRZB*) are also expressed in the face in discrete patterns. Among these, the non-canonical WNTs (*5A*, *5B*, *11*) are entirely mesenchymal (Geetha-Loganathan et al., 2009). These genes are also expressed in the mesenchyme of mouse face and limb (Summerhurst et al., 2008). Previous studies have shown a similar pattern of *Wnt5a* expression in mouse (Gavin et al., 1990; Parr et al., 1993) and chicken embryos (Dealy et al., 1993; Geetha-Loganathan et al., 2009). The expression in the face is restricted to the medial mesenchyme of the mandibular prominences, caudal half of the maxillary prominences and lateral mesenchyme of the frontonasal mass at stages 24-28 (Geetha-Loganathan et al., 2009). In limb, a proximo-distal gradient expression of *WNT5A* is seen in the mesenchyme and ectoderm which will later be exclusive to distal mesenchyme surrounding digits (Dealy et al., 1993; Parr et al., 1993). The expression pattern of *WNT5A* relative to cartilaginous elements is suggestive of a role of *WNT5A* in cartilage development. The frizzled receptors are expressed more broadly than the Wnt ligands in the face (Geetha-Loganathan et al., 2009). *DVL1* and *DVL3* are also expressed in the face (Gray et al., 2009b) but chicken does not have a *DVL2* homologue.

The reporter mice engineered to express LacZ in response to activation of the TCF/LEF response elements (e.g. TOPGAL, BATgal) have been used to examine expression of the canonical WNTs in the face (Brugmann et al., 2007; Lan et al., 2006). These reporter mice show strong β -gal staining in the ectoderm and superficial layers of mesenchyme of the maxillary, lateral nasal, and mandibular prominences. Later, once osteogenesis begins, β -gal staining is

present in osteoblasts of the developing frontal bone (Day et al., 2005). β -gal staining in the BATgal mouse face was done in whole mount and may not have penetrated fully into differentiating skeletal tissues. Therefore, quantitative methods to measure canonical signalling that we have developed in chicken may be more informative than reporter gene expression in mice. There is still more baseline information needed for the chicken model. Our expression studies ended at stage 28 so it is still unknown whether particular Wnts are expressed around differentiating intramembranous bones or endochondral bones at older stages. It appears from gene expression at early stages that primarily non-canonical Wnt signalling is important in craniofacial development but this needs to be tested more rigorously.

1.5 Rationale

The importance of endogenous *Wnt5a* in development is highlighted by 100% perinatal mortality in *Wnt5a* deficient mice (Yamaguchi et al., 1999). Moreover, both gain and loss of *Wnt5a* function cause severe mandibular and limb phenotypes (Yamaguchi et al., 1999; Yang et al., 2003). High levels of endogenous *WNT5A* during early development in the face show critical roles for this signal in facial morphogenesis (Geetha-Loganathan et al., 2009). Also, *WNT5A* mutations in human cause shortening of the lower jaw (micrognathia) and limb in patients with dominant form of Robinow syndrome (Person et al., 2010). Here they studied the effects in zebrafish or frog embryos. In both cases they found there was an inhibition in function but the significance was not investigated in a relevant model system (Person et al., 2010). Also mouse studies did not look at craniofacial development (Yamaguchi et al., 1999; Yang et al., 2003). Therefore, it is necessary to study the functions of *WNT5A* during facial skeletogenesis and morphogenesis in detail.

1.6 Approach

To study the functions of WNT5A during facial development, my approach will be a combination of in vitro and in vivo studies. I will begin with in vitro studies because the process of skeletogenesis can be studied more directly. To expose mandibular primary mesenchymal cells to exogenous Wnt5a protein I will use Wnt5a-conditioned media collected from a *Wnt5a*-expressing cell line which is more biologically active than Wnt5a recombinant protein. The formation of cartilage matrix will be studied over time. I chose the micromass culture system since cartilage differentiation occurs spontaneously and quantification of cartilage matrix is relatively easy. In addition, the time of matrix exposure to exogenous Wnt5a is controllable.

My second strategy to determine the functions of WNT5A during mandibular morphogenesis is to use retroviral misexpression to locally change expression of *WNT5A* in the developing mandible in vivo. Using a replication-competent virus, RCASBP, we make sure that the whole area would be infected. I will ectopically express human *wtWNT5A* and the two human mutations (C182R and C83S) which cause human Robinow syndrome and then look at the effects on mandibular morphogenesis and cellular changes. Reproducibility of phenotypes will make it possible to analyze the earlier defects in cell behaviour that lead to skeletal changes. For the in vivo studies I will compare my face results to those obtained on the limb. There is existing data on the effects of *WNT5A* virus on limb morphogenesis in the chicken and it is important to show whether my viral constructs are equivalent to those published by others. Furthermore, to understand the biology of the *WNT5A* mutations it will be important to study their effect on the limbs which are also impacted in Robinow syndrome.

1.7 Hypotheses

1. *WNT5A* is sufficient to regulate Meckel's cartilage initiation and differentiation in vivo and in vitro.
2. Mesenchymal *WNT5A* functions through non-canonical Wnt pathways to affect differentiation of facial cartilage in vitro.
3. Human *WNT5A* mutations expressed in the chicken will phenocopy aspects of Robinow syndrome including micrognathia and limb shortening in vivo.
4. Human *WNT5A* mutations impact oriented cell activities in the mesenchyme which interferes with convergent extension of mandibular mesenchyme.

1.8 Objectives

1. To characterize the effect of exogenous Wnt5a on initiation, differentiation, maturation of Meckel's cartilage in vitro.
2. To determine the Wnt pathways mediating Wnt5a effects on cartilage development in vitro.
3. To analyze the effects of human *wtWNT5A* and two *WNT5A* mutations found in dominant forms of Robinow Syndrome on avian mandibular morphogenesis.

2. Dual functions for WNT5A during cartilage development and in disease

2.1 Introduction

Wnt proteins are short-range secreted molecules (wingless-related MMTV integration site, related to the *Drosophila* gene *Wingless*) that control many aspects of skeletogenesis from development to post-natal bone homeostasis (Glass and Karsenty, 2007). Disruption of Wnt signalling mediates inflammatory diseases such as osteoarthritis (Yuasa et al., 2008) and mutations in human Wnt pathway genes affect the craniofacial and limb skeleton (Koay and Brown, 2005; Person et al., 2010). Of interest is Robinow syndrome which has a prominent craniofacial phenotype (micrognathia and clefting) and limb shortening and is caused by missense mutations in *WNT5A* (Person et al., 2010) or the alternative *WNT5A* receptor, *ROR2* (Minami et al., 2010).

In a comprehensive analysis of Wnt family members in the chicken face in pre-differentiation stages we found that *WNT5A*, *WNT5B* and *WNT11* were the only three genes with expression in skeletogenic facial mesenchyme (Geetha-Loganathan et al., 2009). Of the three, the expression of *WNT5A* is most abundant and is found in all of the facial prominences including the frontonasal mass which gives rise to midline skeleton of the upper beak, the maxillary prominences which form the palate and sides of the upper beak, the lateral nasal prominences which form the cartilaginous nasal turbinates and the mandibular prominences which form the lower beak. Furthermore, mouse knockouts of *Wnt5a* (He et al., 2008; Yamaguchi et al., 1999) and transgenic expression of *Wnt5a* with a type II collagen promoter (Yang et al., 2003) all have severe jaw defects. Thus the mouse data points to important roles for *Wnt5a* in skeletogenesis but it remains unclear as to what the precise functions are during initiation, differentiation and

maturation of the skeleton. Although some work has been carried out on the role of WNT5A in appendicular or axial skeletal development (Hartmann and Tabin, 2000; Yamaguchi et al., 1999; Yang et al., 2003), these data may not necessarily apply to the craniofacial skeleton. This is because the calvaria and facial skeleton are derived from cranial neural crest cells (Couly et al., 1993; Jiang et al., 2002) whereas in the trunk the skeletogenic tissue originates in the mesoderm. It is therefore necessary to carry out functional studies specifically on facial skeletogenic tissue and compare this to the limb.

The chicken is an excellent model in which to study embryonic skeletal patterning and differentiation both *in vivo* and *in vitro*. The embryo is directly accessible at various developmental stages and it is possible to alter gene expression or levels of signalling molecules to perturb skeletogenesis. Chondrogenesis begins at stage 29 and fully differentiates by stage 35 in chicken. Thus far, Wnt signalling has been studied in chicken limb skeletogenesis (Hartmann and Tabin, 2000; Kawakami et al., 1999). Avian-specific retroviruses expressing either *WNT4* or *WNT5A* were directed to developing limb buds *in vivo*. *WNT5A* delayed chondrocyte maturation whereas *WNT4* accelerated differentiation and hypertrophy (Hartmann and Tabin, 2000; Kawakami et al., 1999). It is not known whether WNT5A or for that matter any other Wnt ligand is sufficient to affect craniofacial skeletogenesis.

There are two main classes of Wnt signaling, the canonical and non-canonical pathways. For canonical Wnt signaling, the ligands bind to Frizzled and LRP co-receptors (LDL receptor related protein) which recruits Dishevelled (Dvl) and Axin away from the β -catenin destruction complex to the cell membrane. Cytoplasmic β -catenin accumulates and then translocates into the nucleus where it interacts with Tcf/Lef regulated transcription factors leading to activation of transcription. Wnt5a can activate canonical signaling but only if Frizzled 4 is present (Mikels

and Nusse, 2006; van Amerongen et al., 2012). Wnt5a can also stimulate non-canonical signaling which does not involve β -catenin. Wnt5a binds to Frizzled receptors (Frizzled 7) without LRP or can bind to Ror2 receptor (Kikuchi et al., 2012). When either of Fzd7 or Ror2 is bound by Wnt5a, the JNK/planar cell polarity (PCP) or calcium signalling pathways are activated leading to changes in actin cytoskeleton, cell polarity and cell movement (Kikuchi et al., 2012). Cross regulation between canonical and non-canonical signaling is also possible. Wnt5a can antagonize the canonical pathway via the Ror2 receptor (Mikels and Nusse, 2006). Since the mechanisms of Wnt5a action vary according to the system being studied (van Amerongen et al., 2012) functional tests in facial mesenchyme are essential to determine which pathway is being used.

Here, we have examined the role of WNT5A signalling during chondrocyte initiation, differentiation and maturation in chicken mandibular prominence using the RCAS retrovirus in vivo and by using murine Wnt5a protein added to micromass cultures in vitro. In this study, we discover dual roles for Wnt5a in development and disease. In development Wnt5a is expressed in the cartilage blastema, which may promote chondrogenesis. In conditions of excess, Wnt5a induces an unexpected, rapid loss of cartilage matrix and the degradation is due to the induction of metalloproteinase and aggrecanase enzymes.

2.2 Materials and methods

2.2.1 Chicken embryos

Fertilized white leghorn eggs were obtained from the University of Alberta and incubated to the appropriate embryonic stages (Hamburger and Hamilton, 1951). All experimental procedures were approved by the UBC Animal Care Committee.

2.2.2 In situ hybridization

Radioactive in situ hybridization was performed using ³⁵S-labelled-UTP *WNT5A* probe (Fokina and Frolova, 2006).

2.2.3 Retrovirus construction and injection into the face

Plasmid containing full length open reading frames for human *WNT5A* (Clone ID IOH39817) was obtained from Life Technologies. The *WNT5A* pENTRY plasmid was recombined with RCASBPY destination vectors using Gateway cloning (Loftus et al., 2001). Pathogen-free DF1 chicken fibroblasts (ATCC cat no. CRL-1590) were transfected with virus plasmid using the DODAC-DOPE method (Geetha-Loganathan et al., 2011). Transfections combined 1 µg of proviral DNA with 0.365 µl of DODAC-DOPE and the mixture was incubated at room temperature for 30 minutes. The lipoplexes were then added to a dish of 75% confluent DF1 cells. Virus was grown up and concentrated as described (Logan and Tabin, 1998). RCAS::*GFP* was obtained from S. Gaunt.

Cell pellets infected with either RCAS::*hWNT5A* or RCAS::*GFP* were injected into the mandibular region of stage 15 embryos. Embryos were incubated until stage 30 and 38 and then were fixed with 5% trichloroacetic acid and 4% PFA, respectively. Then they were stained for cartilage and bone as described (Plant et al., 2000).

2.2.4 Skeletal staining

Injected embryos were fixed in 100% ethanol for 4 days followed by Acetone for another 4 days. Acetone was washed off with dH₂O. Alcian Blue and Alizarin Red stains were made fresh (Stain: 1 vol. 0.3% Alcian blue 8GX in 70% EtOH, 1 vol 0.1% Alizarin red S in 95% EtOH, 1 vol Acetic acid, 17vol 70% EtOH). The samples were stained at room temperature on a shaker for 10 days. The stain was then rinsed off with dH₂O before clearing in 2% KOH+20% glycerol.

The clearing solution was changed every other day. When cleared, the samples were put into 50% glycerol then 100% glycerol and then were photographed.

2.2.5 Micromass culture

Stage 24 mandibular prominences or distal forelimb buds were used for micromass cultures as described (Richman and Crosby, 1990; Swalla et al., 1983). We determined in preliminary experiments that virtually all the chondrogenic potential resides in the lateral mandibular mesenchyme as reported by others (Langille, 1994) (data not shown). Since the full mandibular prominence gave the identical pattern of cartilage nodules as for the lateral mesenchyme and yielded a greater number of cells, all subsequent experiments were done using the whole mandibular prominence.

Trypsin (2%, crude) was used to remove the epithelium and then mesenchymal cells were mechanically dissociated and placed into high density culture (2×10^7 cells/ml). Wnt5a conditioned media (CM, Shimizu, 1997 #262) was freshly collected and diluted 1:1 with base media consisting of DMEM:F12, ascorbic acid, β -glycerol phosphate and antibiotics. Fetal bovine serum concentration was adjusted to be 10% of the total volume. Wnt3a conditioned media was collected and used in cultures the same way as Wnt5a (Hwang et al., 2005). LNCX control media was collected from the same parent Rat B1 fibroblast cell lines as used for Wnt5a and Wnt3a but in this case empty vector was used to transform the cells. Marimastat (10 μ M, Sigma Aldrich, cat no. M2699) was added to cultures beginning on day 3 of the culture period. JNK antagonist, TCS JNK 60 (TOCRIS, cat no. 3222) was applied at certain concentrations every other days (Kauskot et al., 2007). Human DKK1 recombinant protein (Peprotech Inc., cat no. 120-30) was added at the final concentration of 100 ng/ μ l every other days starting at the time of cell plating. Cell number was determined by digesting 4-day cultures with 0.01%

collagenase II (SigmaAldrich, cat no. C6885) at 37°C. Wnt5a-CM was added to cultures at the time of plating and cultures were grown for different days according to the experiment. A subset of Wnt5a-CM treated or control cultures were removed from the culture plate, fixed in 4% PFA, processed into 2% agarose and then embedded into paraffin. Cross sections through the nodules were either stained with Alcian Blue and Picrosirius Red or used for immunofluorescence or TUNEL assay.

2.2.6 Staining and quantification of matrix

Rhodamine-conjugated Peanut Agglutinin (PNA, Vector labs) was used to stain early condensations in 2 day cultures. Cultures were fixed, rinsed with 1X PBS and stained with PNA (10µg/ml in 1X PBS) overnight at 4°C. Four, 6, 8, 10 and 12 day cultures were stained using 0.5% Alcian Blue in 95% EtOH as described (Weston et al., 2000). The “Histogram” tool of Adobe Photoshop was used to determine the proportion of the culture occupied by cartilage. Between 5 to 8 cultures (biological replicates) were studied for each condition.

2.2.7 Immunohistochemistry and TUNEL

Adjacent sections were stained with monoclonal PCNA antibodies (VECTOR VP-P980; 1:250), used for fluorescence TUNEL reaction (ApopTag Apoptosis Kit, Chemicon, S7101) or used for immunofluorescence (IF) with collagen antibodies (Type II and X collagens, Developmental Studies Hybridoma bank; II-6B3-c and X-AC9-c, respectively; 1:250) or chondroitin sulfate (Developmental Studies Hybridoma bank; 9BA12; supernatant 28 ug/ml). A minimum of 3 cultures per condition were studied (biological replicates). Multiple sections (technical replicates) were averaged to give the mean value for the culture. For IF, antigen retrieval was carried out using 10mM Sodium Citrate, pH 6.0, followed by incubation in 0.5% hyaluronidase in HBSS for 30 min. Primary antibodies were applied overnight and signals were

detected with goat anti-mouse Alexa 488-conjugated secondary antibody (1:200). All IF and TUNEL slides were cover slipped using Prolong Gold with DAPI (Life Technologies, cat no. 36930). CS expression was examined under the confocal microscope. TO-PRO-3 iodide (Life technologies, cat no. T3605) was used as a nuclear marker.

2.2.8 Quantitative RT-PCR

Three to four micromass cultures were pooled to give one biological replicate. Two to 3 biological replicates were collected for each condition. Taqman based quantitative RT-PCR was carried out using avian primers for *MMP1*, *MMP13*, *ADAMTS5*, *SOX9*, *COL2A1* and human 18S for the housekeeping control gene. Relative expression was calculated using $\Delta\Delta C_t$ with the 4-day media control being the calibrator. Primer sequences are shown in Table 2.1. Quantitative-PCR cycling conditions were: 95°C for 10min, 40X (95°C for 15s, 60°C for 1min).

Table 2.1 Quantitative-PCR primers used for *MMP13*, *ADAMTS5*, *SOX9* and *COL2A1* amplification.

Gene	Forward primer	Reverse primer
<i>MMP13</i>	TGTTTCGCAGAACTCTGCTTTC	TCCGCATCCTGCATACTAACT
<i>ADAMTS5</i>	GCTGTGCAGTGATTGAAGATG	GAGGACATGAGGCGTTTACC
<i>SOX9</i>	AAGAGAACACCTTCCCCAAAG	GTCCAGTCGTAGCCCTTG
<i>COL2A1</i>	CCACCCTCAAATCCCTCAAC	GGTTCGGGTCAATCCAGTAATC

2.2.9 Luciferase reporter assay

Canonical Wnt activity was quantified using the SuperTopflash reporter (Ishitani et al., 2003) while non-canonical activity was measured with the ATF2-luciferase reporter (Ohkawara and Niehrs, 2011). Cells were transfected with 0.5ug Firefly reporter and 0.025ug Renilla luciferase at the time of plating as described (Geetha-Loganathan et al., 2011) and then were treated with control media, LNCX-CM, Wnt5a-CM (freshly collected from rat B1 fibroblasts),

Wnt3a-CM (freshly collected from NIH3T3 fibroblasts), LiCl (6mM), or combinations of these treatments. Luciferase activity was detected after 48 hours using the Dual Luciferase Assay kit (Promega). Three biological replicates were collected and each assay was repeated 4 times (technical replicates).

2.2.10 Statistical analysis

QPCR data were analyzed by the comparative $\Delta\Delta\text{Ct}$ method (Livak and Schmittgen, 2001). One-way analysis of variance (ANOVA) was carried out, followed by Fisher's post-hoc test for multiple comparisons using Statistica 6.0. TUNEL, PCNA and luciferase data were also analyzed by ANOVA followed by Fisher's post hoc testing.

2.3 Results

2.3.1 Stage-specific expression of *WNT5A* during cartilage formation and differentiation in mandible

Despite many studies on *WNT5A* during embryo development, there are no published expression data for *WNT5A* during skeletal differentiation stages of facial mesenchyme in either mouse or chicken. We addressed this gap by analyzing expression in stage 29-35 embryos (Hamburger and Hamilton, 1951) which covers the stages of cartilage differentiation and maturation as well as onset of intramembranous ossification. The highest levels of expression were localized to newly formed Meckel's cartilage at stage 29 (Fig. 2.1A-A'', B-B'') however by stage 35, the expression was markedly decreased (Fig. 2.1C-C''). There was also no expression in intramembranous bone at any stage. Therefore, there may be distinct temporal and tissue requirements for *WNT5A* signalling.

To determine the function of *WNT5A* in skeletogenesis we overexpressed human *WNT5A* in the mandibular prominence at stage 15, prior to cell specification using an avian-

specific retrovirus (RCASBPY). To see whether condensation formation and cartilage initiation were affected, we fixed a set of embryos at stage 30 or 6 days post injection. Whole mount Alcian blue staining of cartilage did not show any difference between RCAS::*WNT5A* (n = 19; 10 for sectioning and 9 for cartilage staining) and RCAS::*GFP* virus controls (n = 9; 5 for sectioning and 4 for cartilage staining, Fig. 2.2A-D) despite high levels of viral expression in the cartilage (Fig. 2.2E-F). Embryos injected with RCAS::*GFP* grown to stage 38 developed normally (Fig. 2.3A-C). However *WNT5A*-infected avian embryos (Fig. 2.3D-F; n = 16) had a pronounced mandibular phenotype consisting of deviated (81%) or shorter lower beaks (75%; Fig. 2.3D). The differentiation of mandibular bones was inhibited (87.5%; Fig. 2.3E,F) and Meckel's cartilage was shorter and was partially missing in most specimens (62.5%).

The early outgrowth of the mesenchyme might have been affected by RCAS::*WNT5A* as shown by the lower beak deviations at stage 38. However this seems unlikely based on the lack of an early mandibular phenotype. In addition, there appears to be no loss of cartilage progenitor cells, as judged by the normal cartilage at 30 (Fig. 2.2A-F). Later gaps appear in Meckel's cartilage so a different, post-differentiation mechanism may be at work. In addition indirect effects from interactions with virus infected tissues surrounding the skeleton is possible. We turned to micromass culture in which presumptive skeletogenic mesenchyme could be isolated from the surrounding ectoderm and exposed to Wnt5a protein in a temporally-controlled manner.

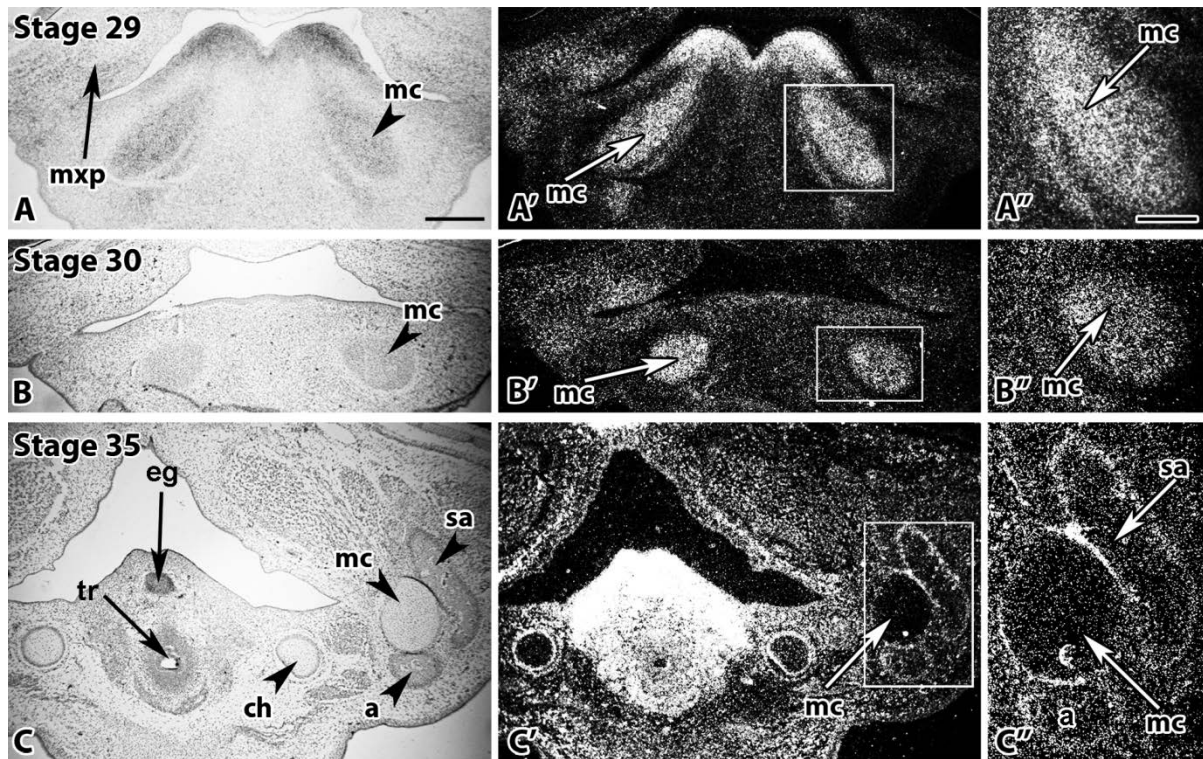


Figure 2.1 Expression of *WNT5A* in the avian craniofacial skeleton.

Radiolabeled in situ hybridization was carried out on transverse sections of chicken embryos. The left column images are photographed using bright field illumination, the right two columns are the same images photographed in darkfield. Signal (silver grains) appears white in darkfield images. **A-A''**) At stage 29, E6.5, expression of *WNT5A* is abundantly found in Meckel's cartilage. There is also signal in the maxillary mesenchyme and the midline of the mandible. **B-B''**) At stage 30, E7.5, Meckel's cartilage continues to express *WNT5A*. **C-C''**) at stage 35 or E9.5, there is abundant expression in the tongue mesenchyme (midline) and surrounding the trachea (arrow) but no expression of *WNT5A* within Meckel's cartilage. The ceratohyoid cartilage also does not express *WNT5A*. There is slightly stronger expression in the perichondrium and periosteum of the intramembranous mandibular bones (**C''**). KEY: a — angular bone, ch — ceratohyoid cartilage, eg — entoglossum, mc — Meckel's cartilage, mxp — maxillary prominence, sa — surangular bone, tr — trachea. Scale bar = 200 μ m for A-A', B-B', C-C', 100 μ m for A'', B'', C''.

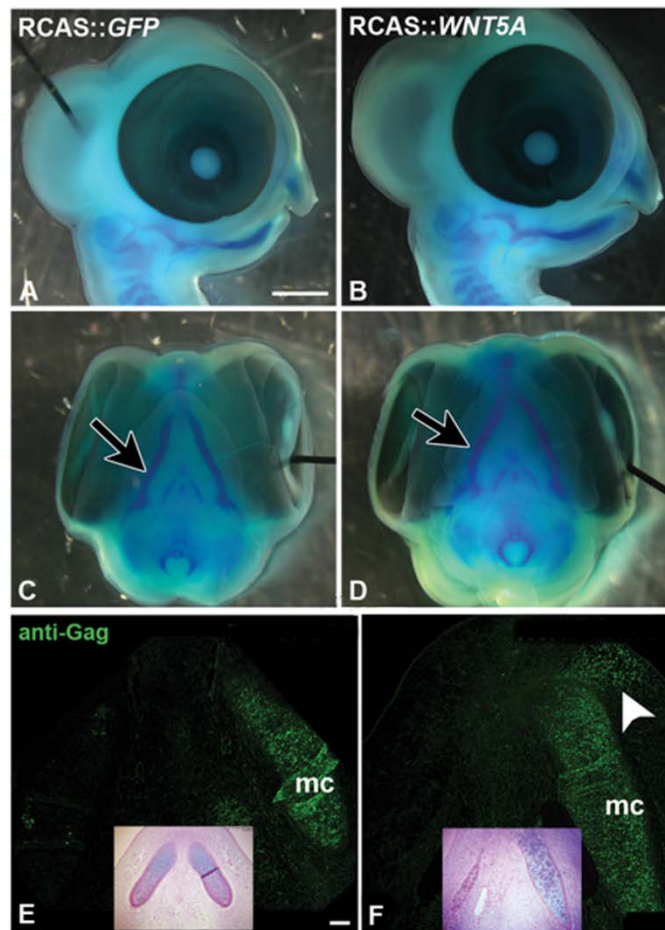


Figure 2.2 Early analysis of RCAS::*GFP* and RCAS::*WNT5A* injection into mandibular region. All embryos were injected at stage 15 and fixed at stage 30 (6 days post-injection). **A-D**) Embryos injected with RCAS::*GFP* and RCAS::*WNT5A* stained in whole mount with Alcian Blue and cleared in glycerol. The beak is not fully extended at stage 30 which is normal for this stage. The cartilage of the lower beak on the injected side has formed normally in RCAS::*GFP* (arrow in C) and RCAS::*WNT5A* (arrow in D). **E,F**) Immunofluorescence staining using the anti-Gag, viral protein monoclonal antibody, 3C2. The signal was detected with an Alexa 488 secondary antibody. Insets are near-adjacent sections from the same embryo stained with Picrosirius red and Alcian Blue. E) Control embryo was injected with RCAS::*GFP* on the right side showing virus localizing mainly to the cartilage. F) RCAS::*WNT5A* localized on the right side with virus within Meckel's cartilage and in adjacent tissue (white arrowhead). The embryo is tilted so that only the right side of Meckel's cartilage is included; however the size of the cartilage is similar on both sides. Key: mc – Meckel's cartilage Scale bar = 2 mm for A-D; 250 μ m for E, F.

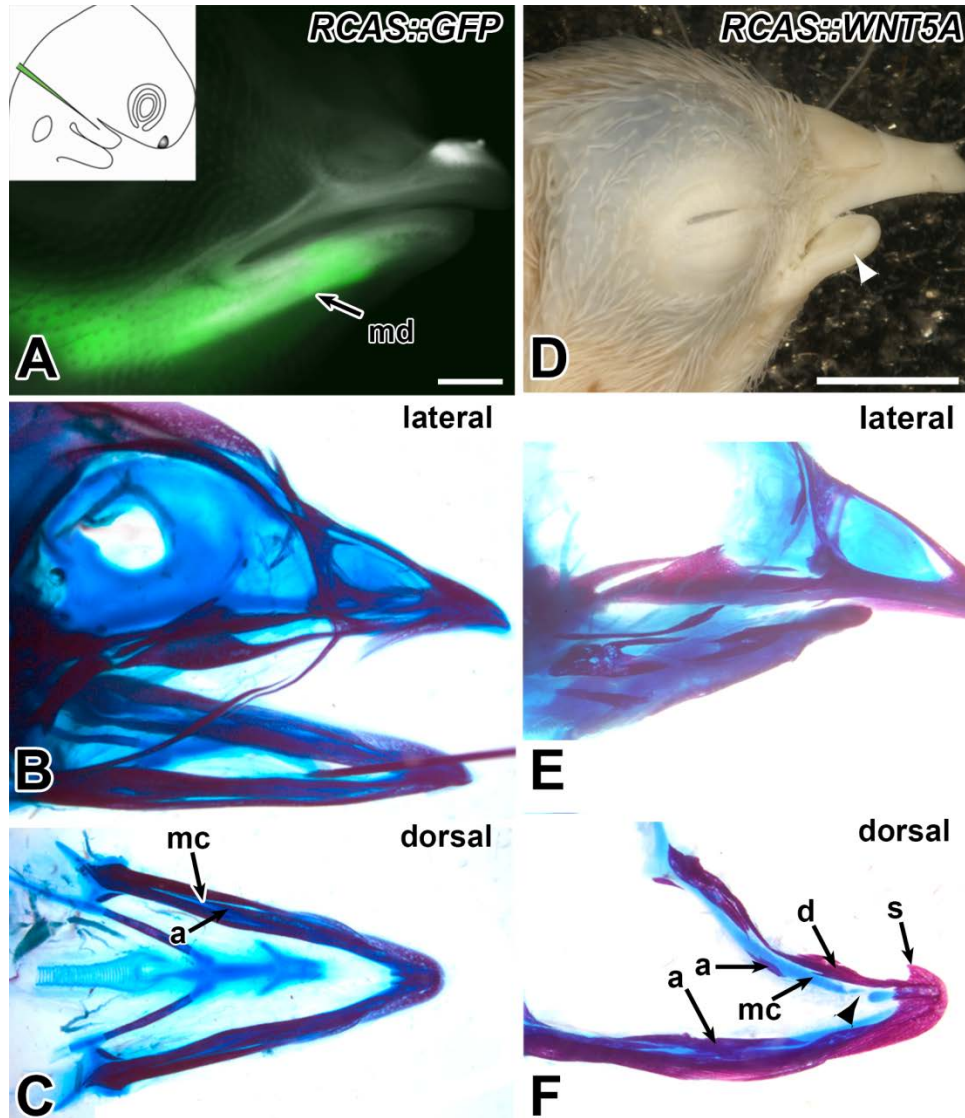


Figure 2.3 Late analysis of in vivo injection of RCAS::*GFP* and RCAS::*WNT5A* retroviruses into lower beak.

Embryos injected with either RCAS::*GFP* or RCAS::*hWNT5A* into the mandibular arch at stage 15 and fixed 10 days later at stage 38. **A)** Lateral view of fresh embryo showing native GFP fluorescence in the mandible. **B)** The whole mount stained skull from the same embryo as in **A** reveals that the upper and lower beaks have formed normally. **C)** Dorsal view of the beak shows the injected (arrows) and uninjected sides are normal. **D)** An embryo injected with RCAS::*hWNT5A* into the mandibular arch photographed externally and then after staining and clearing the skull (**E,F**). The lower beak is deviated towards the right and is shorter compared to the upper beak (white arrowhead). The upper beak has formed normally showing accurate injection technique. **E)** The whole mount stained skull reveals that many membranous bones in the lower beak either have not formed or are much smaller. **F)** The dorsal view shows that the injected side (uppermost) is lacking part of the splenial, surangular, dentary and angular bones. There is also a gap in Meckel's cartilage (arrowhead). Scale bar for **A** = 2 mm, bar in **D** applies to **B–F** = 5 mm. Key: a — angular bone, d — dentary bone, mc — Meckel's cartilage, s — splenial bone.

2.3.2 Temporally-restricted effects of Wnt5a on Alcian Blue stained matrix in micromass culture

Mandibular prominences contain ectomesenchymal cells derived from the Hox negative neural crest that will form cartilage, bone and non-mineralized connective tissue (Creuzet et al., 2005). There are also mesodermally-derived muscle cells (Ralphs, 1992). Culturing mesenchyme in high density culture promotes differentiation of all these cell types but here we are focusing on the cartilage since it is the tissue that initially expresses *WNT5A*. Conditioned media (CM) from a cell line that stably expresses murine Wnt5a (Shimizu et al., 1997) was used since the bioactivity is higher than recombinant protein. We examined time points from 2.12 days to determine the early and later effects of the protein. Two types of control media (parent cell line or base media) were tested and both promoted normal cartilage nodule formation (Fig. 2.4C, E, G were grown with LNCX parent cell line media, all other controls were grown with base media). Initially, there was no effect on the number or size of the earliest condensations as shown by PNA staining at 2 days (n = 6, Fig. 2.4A,B) and Alcian blue staining at 4 days (Fig. 2.4C,D). In support of these data, the total cell number in 4 day cultures was similar (Fig. 2.5). These data suggest that Wnt5a-CM does not impact cellular dynamics at these early stages of chondrocyte initiation.

Surprisingly in 6-day cultures there was almost a total loss of Alcian Blue stained nodules compared to controls (Fig. 2.4E,F,I). Remarkably, by 8 days, all of the blue matrix disappeared (Fig. 2.4G,H,I). Although the blue stain was gone there appeared to be ‘ghost’ nodules remaining in the culture. These unstained but fully formed nodules were pronounced when cartilage was allowed to fully develop to 4 days and then Wnt5a was added for up to 12 days (Fig. 2.6). We also determined the minimum length of exposure to Wnt5a was 3 days in order for the changes in matrix to be seen at 6 and 8 days (data not shown).

The removal of the matrix was not due to a selective loss of chondrogenic cells over time as there was no significant difference in the proportion of TUNEL positive cells or PCNA-positive proliferating cells in the nodules or adjacent mesenchyme in treated and control cultures (Table 2.2).

We suspected that the loss of Alcian Blue staining would be correlated with a reduction in the major collagens comprising cartilage and or a loss of sulfated proteoglycans which are stained by acid Alcian blue. Therefore we sectioned cultures and performed immunofluorescence antibody staining for type II collagen (COL2A1), type X collagen (COL10A1) and Chondroitin Sulfate glycosaminoglycan. At 4 and 6 days, there appeared to be equal staining of COL2A1 in control and Wnt5a-treated cultures (Fig. 2.4J-M) however, at 8 days COL2A1 intensity was greatly reduced compared to controls (Fig. 2.4N-O). The reduction could be due to decreased synthesis, increased breakdown of collagen or a combination of both mechanisms. In contrast COL10A1 appeared to be equivalent in treated and control cultures at 6 and 8 days (Fig. 2.4P-S). Chondrocyte lacunae seemed similar in controls and experimentals even though the staining of the matrix had changed colour and amount had decreased in treated cultures (Fig. 2.4 insets).

The absence of Alcian blue staining strongly suggested that proteoglycan degradation was taking place. Aggrecan (CSPG) is the most abundant structural proteoglycan in cartilage (Hardingham and Fosang, 1992). We obtained an antibody that recognizes the CS side chains rather than the core protein of CSPG since reduction in staining would indicate that degradation had taken place. During normal development, chondroitin sulfate is expressed starting at stage 30 in Meckel's cartilage (Fig. 2.7B) and increases in intensity at stage 35 (Fig. 2.7C-E). The control 6 and 8 day cultures resembled the mature stage 35 cartilage, CS was strongly expressed throughout the cartilage nodules (Fig. 2.8A-B'). In contrast, in Wnt5a-treated cultures expression

was lost within the nodules (Fig. 2.8C-D'). Therefore, Wnt5a is inducing clipping of the side chains of CSPG (Aggrecan) as well as reducing collagen II protein.

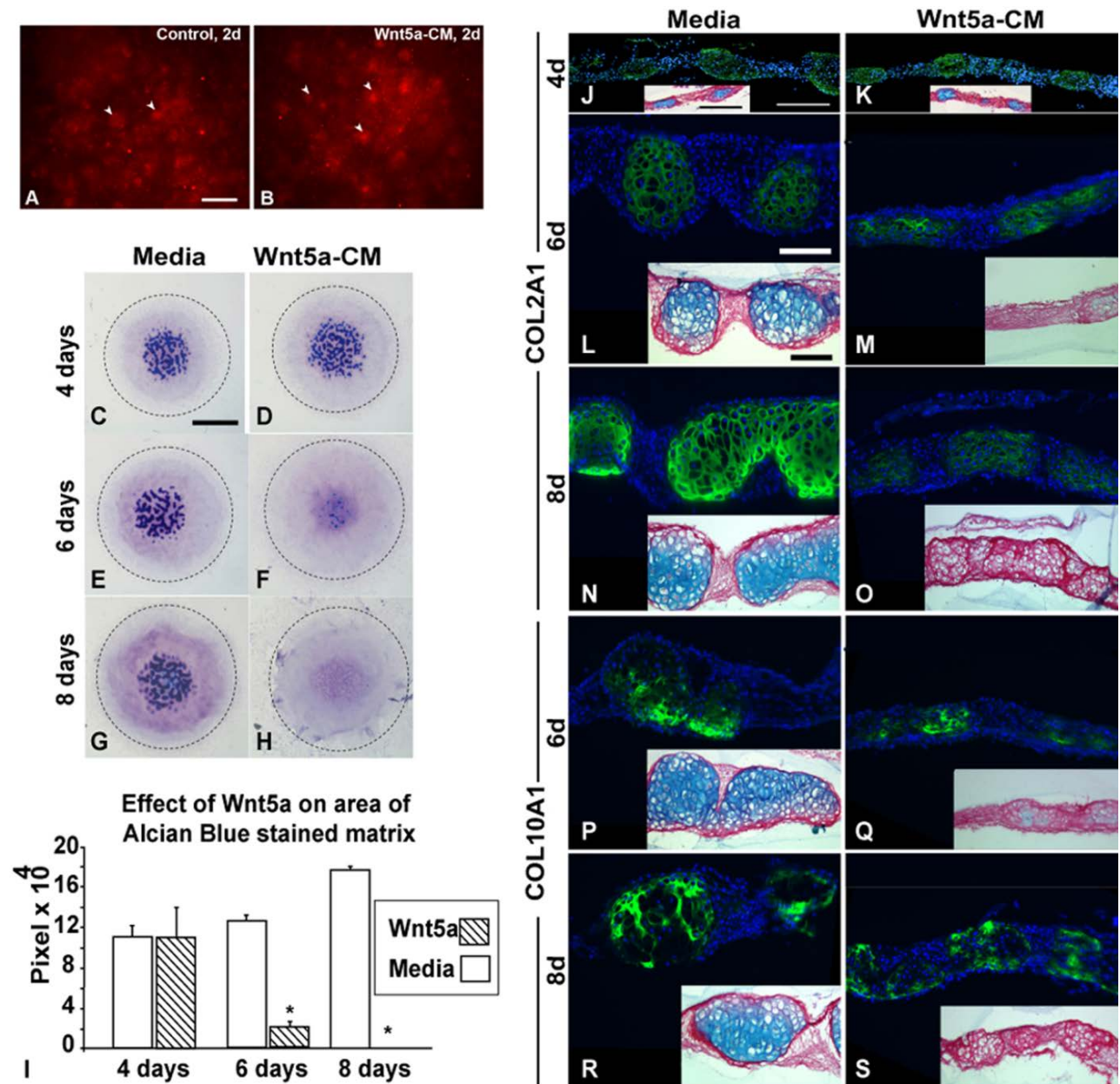


Figure 2.4 Delayed effects of excess Wnt5a-CM on cartilage matrix in mandibular micromass cultures.

A,B) Whole mount immunofluorescence staining of 2-day mandibular micromass cultures using rhodamine tagged PNA. There is no difference in the size or number of condensations in the control (A) versus the Wnt5a-CM treated cultures (B). **C-H)** Mandibular micromass cultures fixed, stained with Alcian Blue and counterstained with hematoxylin at various time points. C,E,G) Mandibular mesenchyme forms cartilage nodules. The dashed line indicates the edge of the culture. There is an increase in size of this fibroblastic fringe between 4 and 8 days. D,F,H) Cultures treated with Wnt5a-CM 1:1 diluted with base media form nodules at 4 days but these disappear by 6 and 8 days. **I)** Absolute area of culture stained with Alcian Blue measured using Adobe Photoshop select tool to quantify

the blue pixels. At 6 days there is a significant decrease in cartilage area ($P < 0.05$) and by 8 days there is no measurable Alcian Blue matrix. **J–S**) Paraffin sections of micromass cultures stained with antibodies to type II or X collagen. Photographs have been taken on the green (Alexa 488 secondary antibody) and blue channels (Dapi). Left column (J,L,N,P,R) are cultures treated with media only. Right column are cultures treated with 1:1 Wnt5a-CM:Base media (K,M,O,Q,S). J–M) Type II collagen has a similar expression strength in control and Wnt5a treated cultures at 4 and 6 days of culture. N,O) Type II collagen is strongly expressed in 8 days media control cultures, whereas staining is less intense in the Wnt5a-treated cultures (O). Intensity is similar to 4 and 6 days. P–S) Type X collagen is detectable in the cartilage nodules at 6 and 8 days at similar levels in the controls and Wnt5a-CM treated cultures. Expression is generally higher at the periphery of the nodules. Insets are near-adjacent sections from the same culture stained with Picrosirius red and Alcian Blue that show a loss of Alcian Blue staining and flattening of the nodules with Wnt5a treatment. Scale bar = 200 μm for A and B, 2 mm for C–H, 100 μm for J–S.

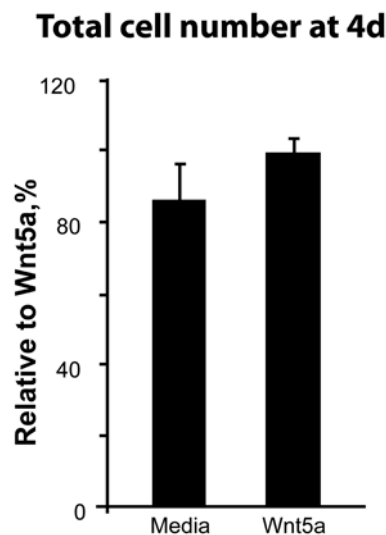


Figure 2.5 Wnt5a does not affect total cell numbers in cultures.

The cell number was estimated at 4 days after plating by removing cultures from dish using trypsin/EDTA solution (0.1% Trypsin and 0.001 M EDTA in Hank's calcium-magnesium-free buffer) for 5-10 minutes. Cultures were washed with medium and spun down. The medium was removed and cells were digested with 0.01% collagenase II (SigmaAldrich, cat no. C6885) at 37°C until the cells could be dissociated. The pellet was then resuspended in media and cells were counted in a hemocytometer.

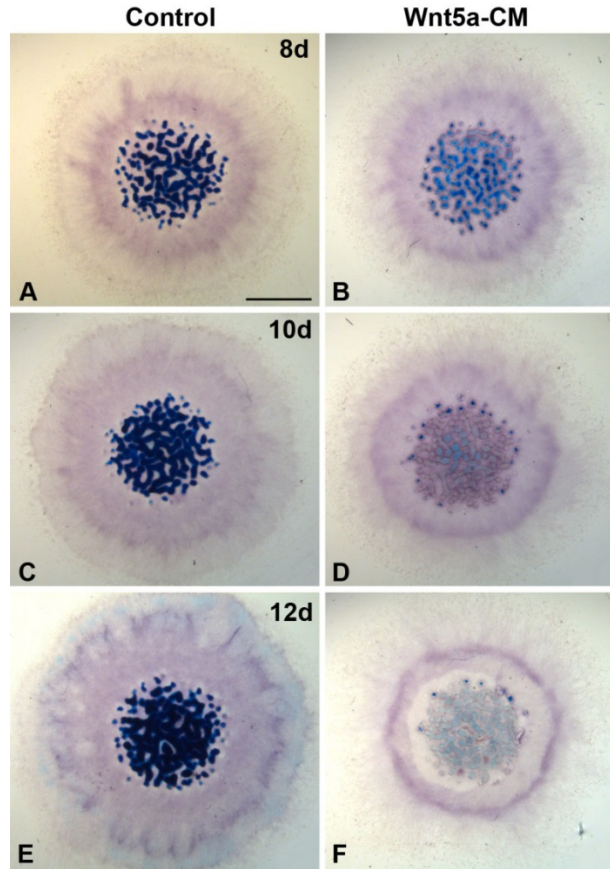


Figure 2.6 Wnt5a has a cumulative effect on cartilage matrix.

Mandibular micromass cultures stained with Alcian Blue and counterstained with hematoxylin at 12 days. **A, C, E**) Control cultures were grown for 12 days. Nodules begin to coalesce at 10 and 12 days but the area of the culture occupied by cartilage remains constant. All nodules retain intense blue staining. **B, D, F**) Micromass cultures started in control media and after cartilage had fully differentiated on day 4, base media was replaced with a 1:1 dilution of base media:Wnt5a-CM. Cultures were then grown for a further 8 days or for a total of 12 days. The majority of the Alcian blue stained matrix has been removed leaving 'ghost' nodules. Scale bar = 2mm for A-F.

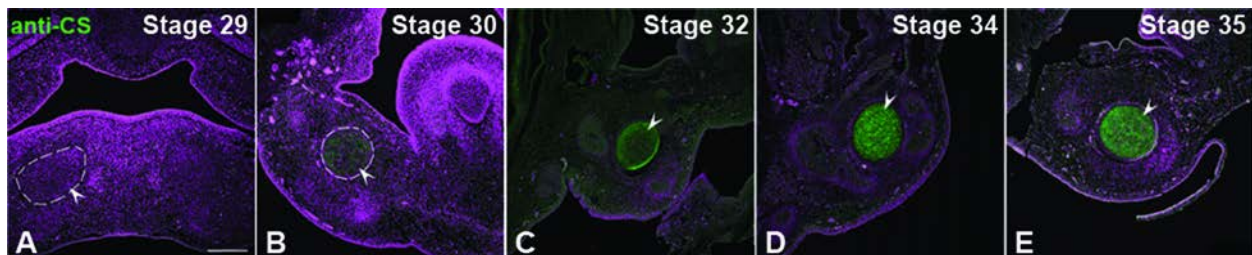


Figure 2.7 Expression of chondroitin sulfate at different stages in the head.

A-E) Paraffin sections of embryos at stages 29 (A), 30 (B), 32 (C), 34 (D) and 35 (E) stained with antibody against chondroitin sulfate glycosaminoglycans. Photographs have been taken on the green (Alexa 488 secondary antibody) and magenta channels (TO-PRO-3) with confocal microscopy. TO-PRO-3 Iodide was used as a nuclear marker. **A**) There is no expression of chondroitin sulfate in mc at stage 29. **B-E**) Expression of chondroitin sulfate is observed in mc starting stage 30 onwards (white arrowheads). The adjacent intramembranous bones are negative for CS staining. Scale bar = 250 μ m for A-E.

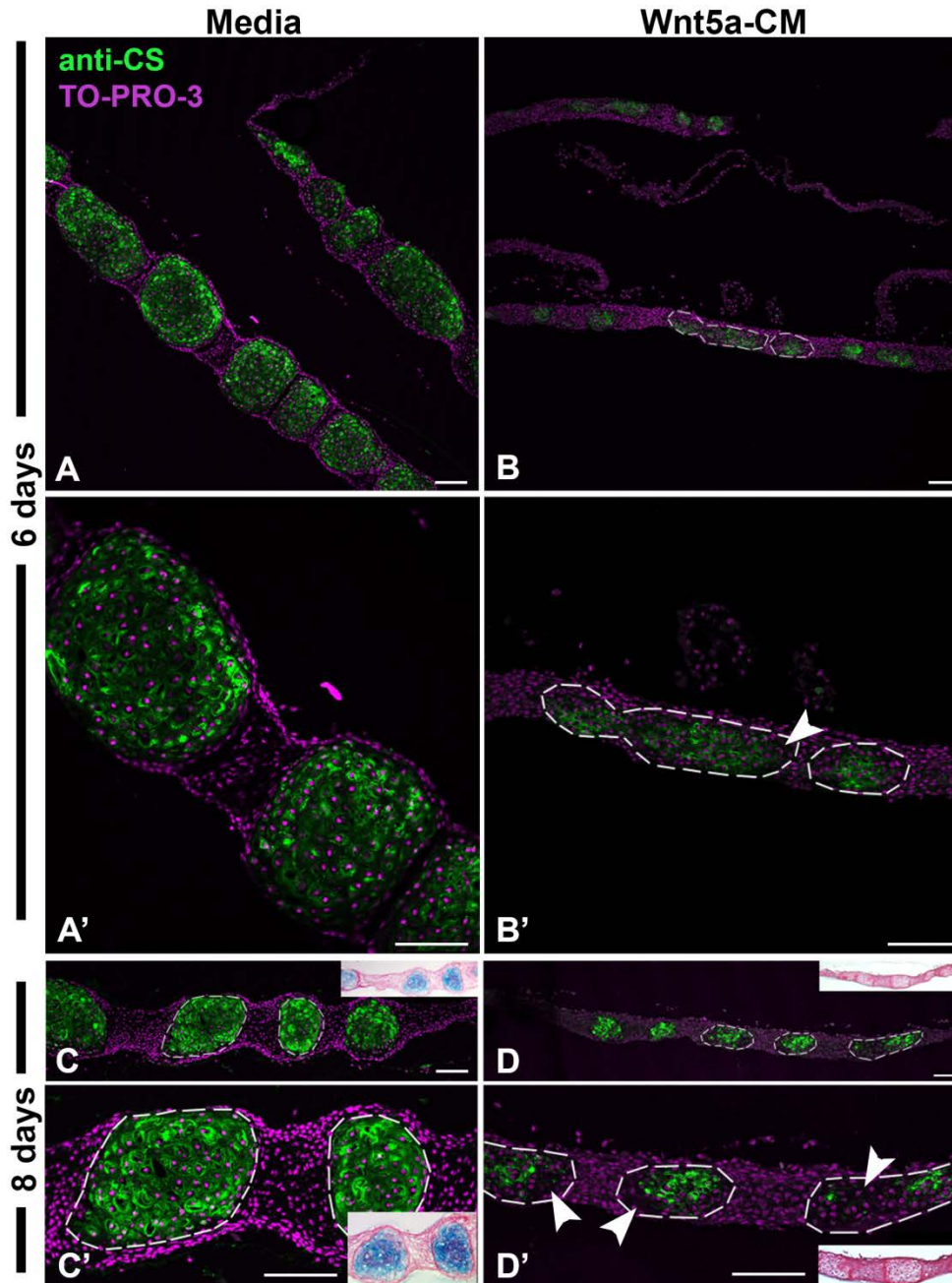


Figure 2.8 Expression of chondroitin sulfate glycosaminoglycan is decreased in Wnt5a-treated cultures.

A–D') Paraffin sections of micromass cultures stained with antibody against chondroitin sulfate. Primary antibody is detected with green Alexa 488 secondary antibody and the nuclei have been stained with TO-PRO-3 iodide. These are maximum intensity projections of a Z-stack (5–6 slices) taken with a confocal microscope. A, A', C, C') Cultures treated with media only. CS is expressed throughout the cartilage nodules at both 6 and 8 days with intensity increasing at 8 days. B, B', D, D') Cultures treated with Wnt5a-CM. Signal is absent in some parts of the nodules (white arrowheads in B', D') coinciding with the absence of Alcian Blue staining (insets). Scale bar = 100 μ m.

Table 2.2 Apoptosis and proliferation of cells in 8 day micromass cultures of mandibular mesenchyme.

Counts of total cell number as well as cells stained with either TUNEL or PCNA were made on two biological replicates for each of four conditions. One way ANOVA was carried out and no significant differences were found for TUNEL (P = 0.48). For PCNA, p = 0.02, so Tukey's Post-Hoc testing was done to identify groups with significant differences. The interstitial tissue had higher proliferation than the nodules but these values were unaffected by the type of media.

Proportion of TUNEL positive cells				
	Control nodules	Wnt5a nodules	Control interstitial	Wnt5a interstitial
Mean ± SD	3.1% ± 0.01	3.2% ± 0.01	8.8 % ± 0.07	6.8% ± 0.01

Proportion of proliferating cells stained with PCNA				
	Control nodules	Wnt5a nodules	Control interstitial	Wnt5a interstitial
Mean ± SD	3.7% ± 0.01	4.5% ± 0.02	24.8 % ± 0.09	26.4% ± 0.08

ANOVA plus Tukey's Post-hoc test P values (Bold are significant)				
	Control nodules	Wnt5a nodules	Control interstitial	Wnt5a interstitial
Control nodules		0.998	0.040	0.031
Wnt5a nodules	0.998		0.045	0.035
Control interstitial	0.040	0.045		0.985
Wnt5a interstitial	0.031	0.035	0.985	

2.3.3 MMP1, MMP13 and ADAMTS5 mediate the Wnt5a-induced loss of Alcian Blue staining of cartilage matrix in mandibular primary cultures

MMP1 and 13 (Matrix Metalloprotease 1 and 13) are involved in collagen catabolism and ADAMTS5 (A Disintegrin And Metalloproteinase with Thrombospondin motifs) degrades aggrecans (Caterson et al., 2000). Using qPCR we found that in control cultures there were initially low levels of *MMP1* and *MMP13* RNA. Interestingly in control cultures, *MMP1* and

MMP13 were differentially regulated; *MMP1* decreased whereas *MMP13* was upregulated by 6 days (Fig. 2.9A,B). *ADAMTS5* was not changed in control cultures between 4 and 6 days (Fig. 2.9C). In treated cultures, there was significant upregulation of all three genes by 6 days compared to control cultures (Fig. 2.9A,B,C). Thus the time course of induction of *MMP1* and *ADAMTS5* correlates closely with the degradation of the matrix. In addition, although *MMP13* normally increases during differentiation, addition of Wnt5a-CM bumps up expression to significantly higher levels. Thus all three enzymes are potentially involved.

The previous RNA expression experiments did not prove whether MMPs were directly involved in a functional sense. We therefore treated cultures first with Wnt5a for 3 days and then added a general MMP inhibitor, Marimastat (Whittaker et al., 1999), which binds to the zinc ion in the collagenase active site of MMPs, thereby inhibiting their action (Whittaker et al., 1999). Marimastat also inhibits Aggrecanase (Tortorella et al., 2009). After 6 days of culture, the controls were not visibly affected by Marimastat (compare Fig. 2.9D to F), however when Marimastat was added to Wnt5a-treated cultures on day 3, Alcian Blue staining was maintained for 6 days (compare Fig. 2.9E to G, n = 6). We next quantified the rescue by measure the levels of two chondrogenic RNAs, *SOX9* (Sry-box containing gene 9) and *COL2A1* (Fig. 2.9H,I). Unexpectedly, Marimastat on its own upregulated both genes. One day following Marimastat addition (4 days) a spike in expression of *SOX9* and *COL2A1* was seen however by 6 days, homeostasis had been restored and levels were comparable to base media without addition of Wnt5a-CM. These initial studies showed that the important time point to look for rescue was 6 days. Indeed, *SOX9* and *COL2A1* were increased almost 8- and 15-fold respectively in Marimastat+Wnt5a-CM treated cultures as compared to Wnt5a-CM treated cultures after 6 days (Fig. 2.9H,I).

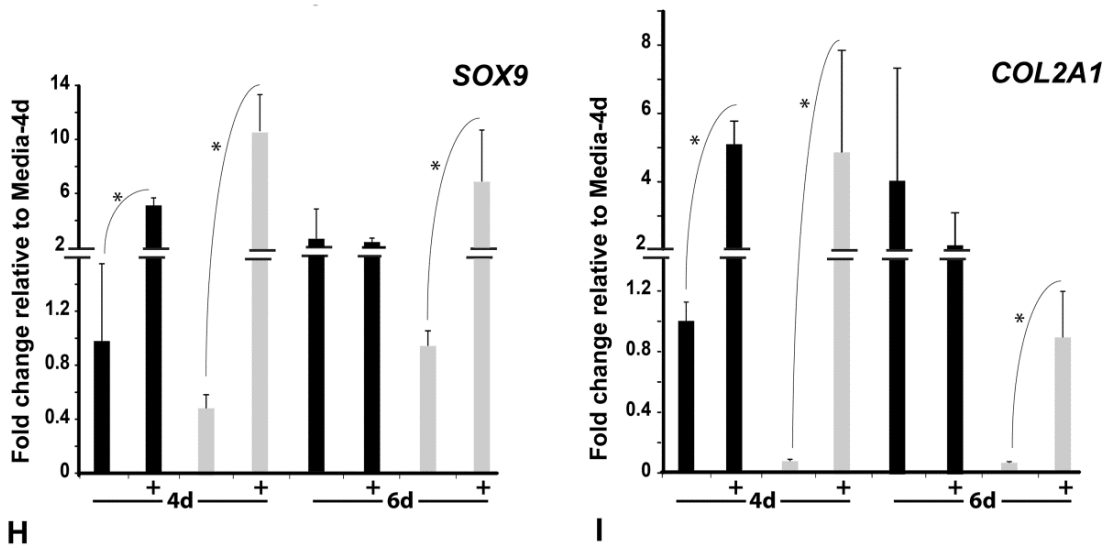
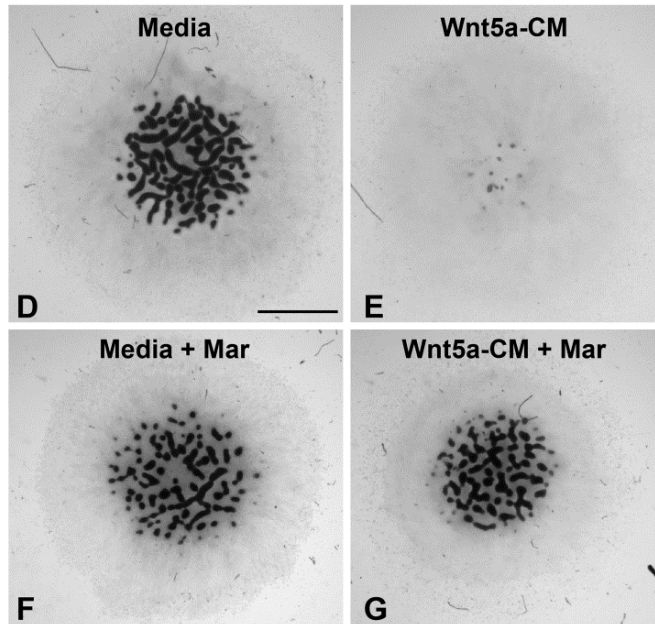
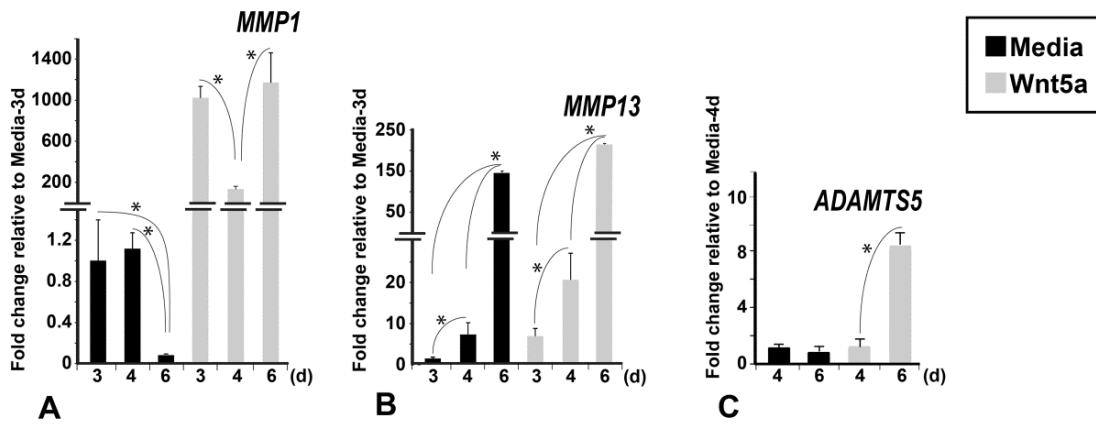


Figure 2.9 Matrix metalloproteinases and Aggrecanases mediate loss of cartilage matrix.

A,B,C) Fold-change induction of *MMP1*, *MMP13* and *ADAMTS5* in mandibular micromass cultures from stage 24 embryos. Expression is normalized to 18s RNA. Asterisks represent significant results. Breaks in the Y axis have been introduced to accommodate the range in values. A) There is a significant decrease in *MMP1* expression in control cultures by day 6. In contrast in treated cultures, *MMP1* expression is significantly higher than that in controls ($P < 0.0001$). In addition there is a dynamic pattern with high levels seen at day 3, a downregulation at day 4 and 9-fold upregulation at day 6. B) In media control cultures, *MMP13* is slightly induced at 3 and 4 days but is upregulated by 150-fold at 6 days. In treated cultures, there is significantly more *MMP13* present at all time points ($P = 0.04$ for 6 days). C) A significant increase in *ADAMTS5* expression is observed after 6 days following Wnt5a treatment ($P = 0.002$). **D–G)** Phenotypic rescue of chondrogenesis occurs following addition of Marimastat. D) Control cultures form numerous cartilage nodules. E) Very little cartilage is present in Wnt5a-treated cultures at 6 days. F) Marimastat on its own does not change nodule quantity or pattern. G) Marimastat added to Wnt5a-CM cultures at 3 days has rescued most of the matrix by 6 days of culture. **H,I)** Rescue of cartilage gene expression in Marimastat-treated cultures. Expression is normalized to 18s RNA. Marimastat (+ symbol on X axis indicates conditions where Marimastat was added) increases *SOX9* and *COL2A1* expression at 4 days but this equalizes to controls at 6 days. H) The decrease in *SOX9* expression was rescued by Marimastat in Wnt5a-treated cultures at days 4 and 6 and in controls on day 4 (P values in Table 2.3). I). Expression of *COL2A1* is significantly reduced on both 4th and 6th days following Wnt5a treatment and expression is rescued by Marimastat (P values in Table 2.3). KEY: M, Mar — Marimastat. Scale bar for D-G = 2 mm.

Table 2.3 QPCR for *SOX9* and *COL2A1* genes.

QPCR for *SOX9* and *COL2A1* genes in control and Wnt5a-treated cultures with or without Marimastat application after 4 and 6 days. Red values are considered significant.

SOX9

	Media-4d	Wnt5a-4d	Media+M-4d	Wnt5a+M-4d	Media-6d	Wnt5a-6d	Media+M-6d	Wnt5a+M-6d
	P values							
Media-4d		0.22554	0.005016	0.000802	0.360954	0.960634	0.074723	0.004722
Wnt5a-4d	0.22554		0.000471	0.00011	0.037831	0.243108	0.006197	0.000542
Media+M-4d	0.005016	0.000471		0.158502	0.016039	0.004552	0.115972	0.717476
Wnt5a+M-4d	0.000802	0.00011	0.158502		0.001901	0.000738	0.011264	0.319722
Media-6d	0.360954	0.037831	0.016039	0.001901		0.334867	0.280457	0.014118
Wnt5a-6d	0.960634	0.243108	0.004552	0.000738	0.334867		0.06797	0.004321
Media+M-6d	0.074723	0.006197	0.115972	0.011264	0.280457	0.06797		0.084301
Wnt5a+M-6d	0.004722	0.000542	0.717476	0.319722	0.014118	0.004321	0.084301	

COL2A1

	Media-4d	Wnt5a-4d	Media+M-4d	Wnt5a+M-4d	Media-6d	Wnt5a-6d	Media+M-6d	Wnt5a+M-6d
	P values							
Media-4d		0.004461	0.0332	0.118555	0.314249	0.002736	0.34918	0.815765
Wnt5a-4d	0.004461		0.000056	0.000271	0.000432	0.784062	0.000487	0.006797
Media+M-4d	0.0332	0.000056		0.574264	0.151388	0.000036	0.131897	0.020843
Wnt5a+M-4d	0.118555	0.000271	0.574264		0.440631	0.000177	0.399367	0.079566
Media-6d	0.314249	0.000432	0.151388	0.440631		0.000267	0.933186	0.21495
Wnt5a-6d	0.002736	0.784062	0.000036	0.000177	0.000267		0.000301	0.004143
Media+M-6d	0.34918	0.000487	0.131897	0.399367	0.933186	0.000301		0.241045
Wnt5a+M-6d	0.815765	0.006797	0.020843	0.079566	0.21495	0.004143	0.241045	

2.3.4 Exogenous Wnt5a antagonizes canonical Wnt signalling and activates the JNK/PCP pathway in mandibular mesenchyme

There is data to support Wnt5a acting via the JNK pathway in some contexts or via the alternative receptor, Ror2 to inhibit the canonical pathway (Mikels and Nusse, 2006). Wnt5a can also activate the canonical pathway depending on which receptor is present (Mikels and Nusse, 2006). To figure out which Wnt signalling pathway is being used in our experiments, we used luciferase assays since they are sensitive and quantitative readouts of pathway activity. This is the first time that such assays have been used on primary cultures of facial mesenchyme.

The positive controls, Wnt3a-CM or LiCl (GSK3 β antagonist) induced strong expression of the SuperTopflash reporter verifying that the canonical pathway components are present (Fig. 2.10A). Wnt5a failed to activate the reporter and instead blocked the increase in luciferase activity induced by canonical agonists LiCl and Wnt3a-CM (Fig. 2.10A). Using a different reporter for JNK/PCP pathways (ATF2-luciferase) we showed that Wnt5a-CM activated JNK/PCP signalling (Fig. 2.10B). Thus repression of canonical signalling and activation of JNK/PCP signaling by Wnt5a-CM are both correlated with the removal of cartilage matrix.

Further functional experiments were needed to determine the Wnt pathway that was mediating the cartilage matrix phenotype. First we wanted to characterize the effects of Wnt3a-CM on cartilage formation. The prediction is that since Wnt3a is a purely canonical Wnt in our system, it would have different effects on chondrogenesis than Wnt5a. Two days after adding Wnt3a-CM, there were no visible or quantitative differences in the nodules (n = 5; Fig. 2.11A-C). However, Wnt3a-CM inhibited the initial stages of cartilage differentiation at 4 days (n = 4; Fig. 2.11D,E). By 6-8 days there were still cartilage nodules in Wnt3a-treated cultures albeit far fewer than in control cultures (n = 5; Fig. 2.11F-I). Therefore, the micromass system revealed

distinct early functions of Wnt3a that are different from the later effects of Wnt5a on matrix stability.

As excess canonical signaling was inhibitory to cartilage formation, it seemed likely that antagonism of the pathway would derepress or accentuate chondrogenesis. In order to directly inhibit canonical signaling we added DKK1 recombinant protein to the media. First we confirmed that DKK1 antagonizes the canonical pathway in luciferase assays (Fig. 2.10C) and that DKK1 was able to rescue Wnt3a-induced cartilage phenotype in micromass cultures ($n = 5$; Fig. 2.10H,I). DKK1 on its own slightly enhanced chondrogenesis compared to controls (Fig. 2.10D, E). Furthermore, DKK1 protein had no effect on the loss of cartilage in Wnt5a-CM treated cultures ($n = 5$, Fig. 2.10F,G) allowing us to rule out the antagonism of canonical signaling as being the cause of the matrix degradation. Instead DKK1 and Wnt3a data show that the canonical pathway plays a repressive role in early chondrogenesis.

We next investigated whether JNK activation is required for Wnt5a effects on cartilage using a specific JNK antagonist, TCS JNK 6o (Kauskot et al., 2007). In dose-response experiments we showed that the antagonist did not change the pattern, number or intensity of staining in the nodules at 100 μM (Fig. 2.10J,L) but at 250 μM there was a slight decrease in the cartilage staining (Fig. 2.10N). Higher concentrations were toxic to the cells (data not shown). When TCS JNK 6o was added to Wnt5a-CM cultures, Alcian blue staining of the central nodules was maintained ($n = 9$, Fig. 2.10M,O). These partial rescues are striking when compared to the complete absence of Alcian blue staining in 100% of Wnt5a-CM treated cultures. The data are consistent with the involvement of the JNK pathway in the cartilage degradation phenotype.

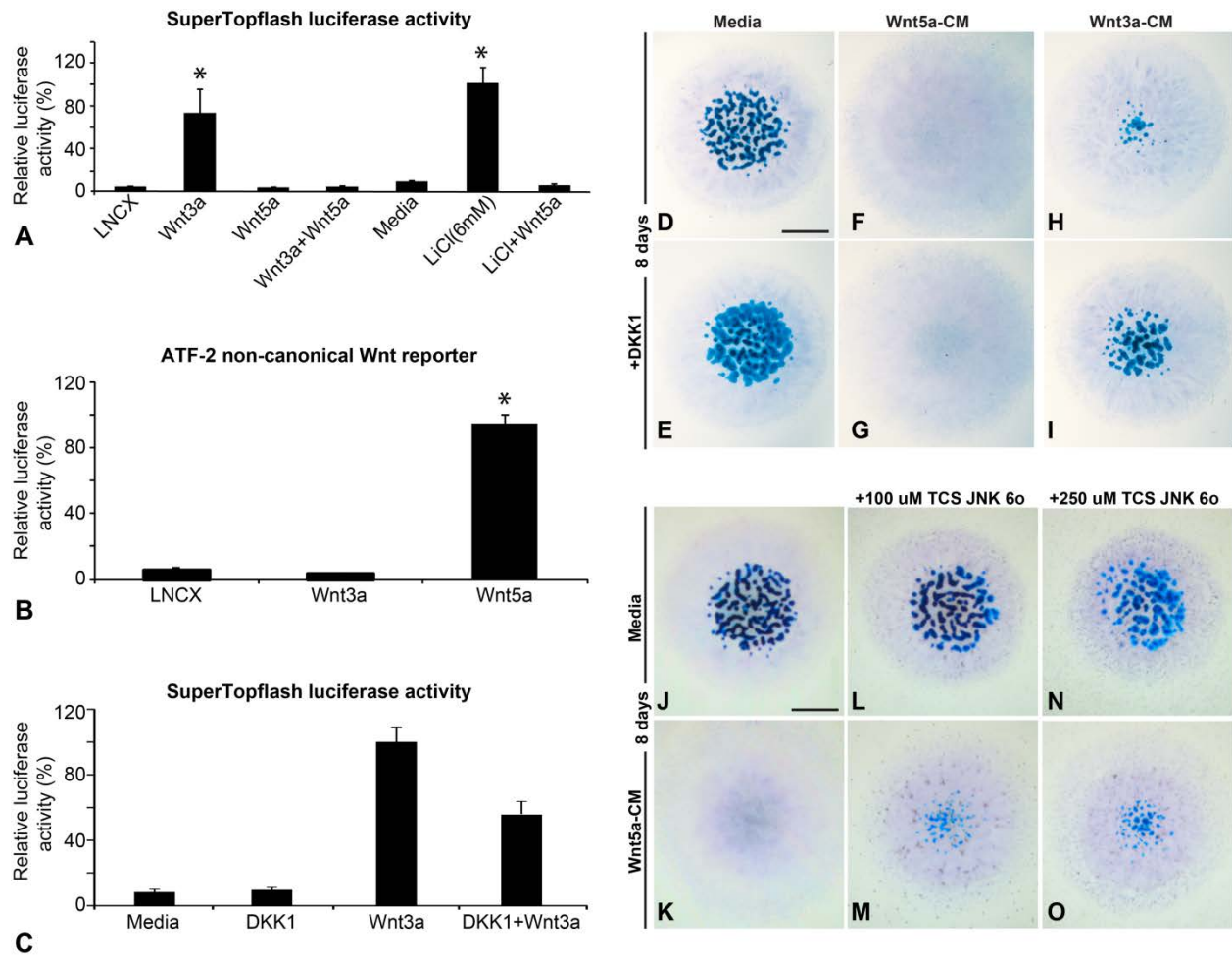


Figure 2.10 Wnt5a represses canonical and activates non-canonical JNK mediated signaling pathways in mandibular mesenchyme.

A–C) Relative luciferase reporter activity (Firefly/Renilla) in micromass cultures following 2 days of exposure to different conditions. Control cultures were treated with a 1:1 ratio of LNCX conditioned media: Base media. LNCX conditioned media was collected from the parent cell line used to express Wnt3a and Wnt5a. Media controls were grown in base media only. Wnt3a and Wnt5a treatments were 1:1 Wnt:base media. Wnt3a + Wnt5a consisted of 1:1:2 (Wnt3a:Wnt5a:Base media). LiCl salt was added at 6 mM. DKK1 was used at a concentration of 100 ng/ml. **A)** The SuperTopflash reporter contains Lef1 binding elements and therefore indicates activity of the canonical pathway mediated by β -catenin. Mandibular micromass cultures treated with Wnt3a-CM or LiCl (a GSK3 β antagonist) which are both canonical activators significantly stimulate the reporter. The addition of Wnt5a has no effect on the reporter supporting the idea that it is acting via non-canonical pathways. Wnt5a combined with either Wnt3a or LiCl can antagonize the activity of either agent. **B)** Activity of the ATF2-luciferase reporter indicates non-canonical, primarily JNK-mediated signaling. ATF2 activity is significantly increased following treatment with Wnt5a-CM. **C)** Adding DKK1 protein to Wnt3a-treated cultures significantly decreased SuperTopflash luciferase activity. **D–I)** DKK1 treatment of cultures. **D,E)** DKK1 caused the nodules to become confluent possibly by recruiting additional cells to the condensation or by derepressing chondrogenesis in adjacent fibroblastic cells. **F, G)** DKK1 does not alter the phenotype caused by Wnt5a alone. **H, I)** DKK1 rescued the Wnt3a-induced cartilage phenotype in micromass cultures. **J–O)** Micromass cultures were treated with a JNK antagonist, TCS JNK 60 at either 100 or 250 μ M. **J,K)** Cultures treated with Wnt5a-CM alone lose all blue staining in the nodules by 8 days. **L–O)** In the presence of the JNK antagonist a number of stained nodules persist. Scale bar = 2 mm for D–O.

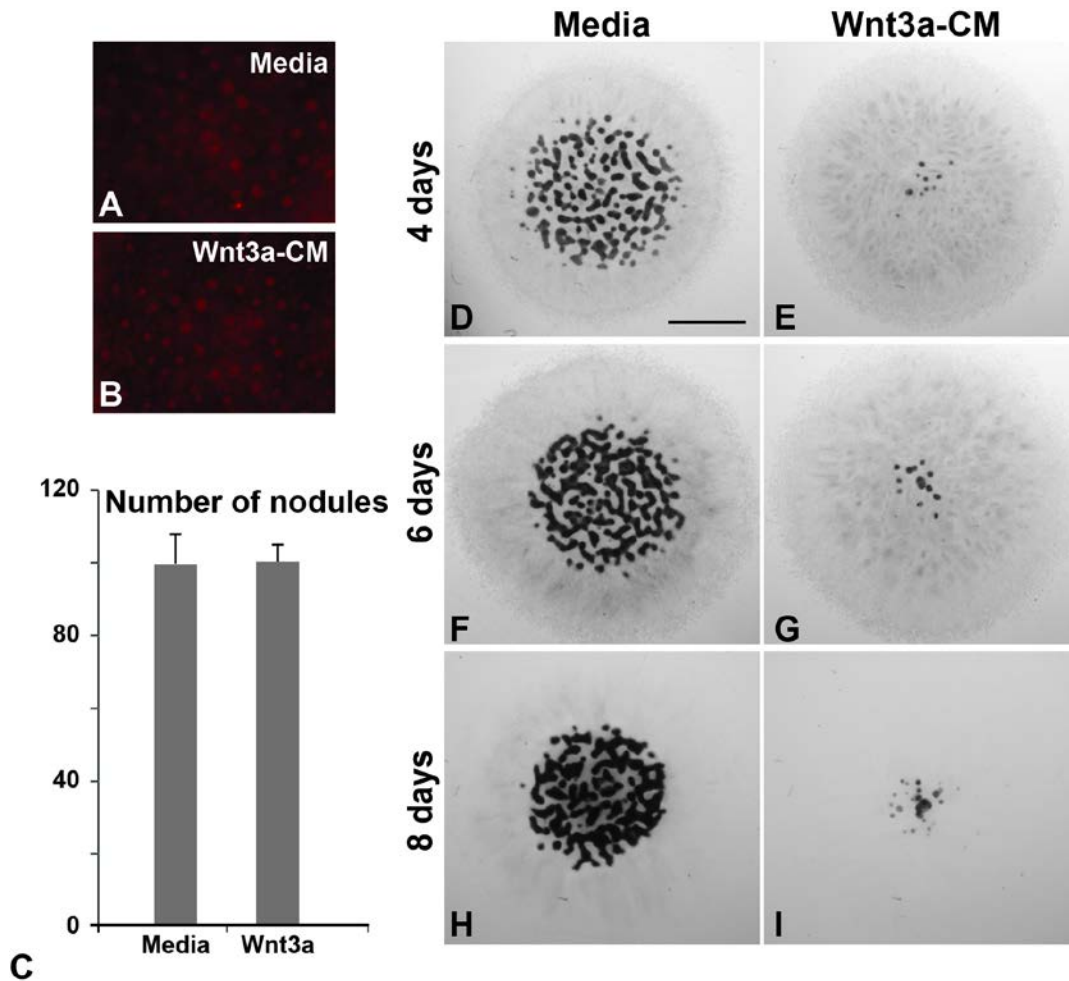


Figure 2.11 Wnt3a-CM inhibits early chondrogenesis in micromass cultures of mandibular mesenchyme.

A,B Two-day cultures stained with rhodamine-tagged peanut agglutinin (PNA). **C** There is no difference in the number of condensations in the control versus the Wnt3a-CM treated cultures. **D-I** Mandibular micromass cultures fixed, stained with Alcian Blue and counterstained with hematoxylin at various time points. **D,F,H** Mandibular mesenchyme in control media form numerous cartilage nodules. **E,G,I** Cultures treated with Wnt3a-CM 1:1 diluted with base media form few nodules at 4 days (E). These few nodules persist in the cultures even after 6 (G) and 8 days (I). Scale bar = 2 mm for D-I.

2.3.5 Wnt5a treatment causes degradation of limb cartilage in the same manner as cartilage derived from facial mesenchyme

The effects of Wnt5a on degradation of facial cartilage were very clear but we wanted to know whether these were universal effects that were independent of the embryonic origins of the cells. This is important since many diseases such as osteoarthritis affect not only the jaw joint but

other joints in the body derived from mesoderm. Several previous studies had added Wnt5a to limb micromass cultures from chicken (Church et al., 2002; Daumer et al., 2004; Tufan and Tuan, 2001) and mouse (Bradley and Drissi, 2010). However the chicken studies used RCAS retrovirus which has a long period of infection and thus a delay in cartilage phenotypes. The mouse study used recombinant Wnt5a but this was added intermittently. All these studies showed a slight reduction in cartilage matrix over time but some cartilage was always present at the end of the culture period. To be comparable to our facial results we used Wnt5a-CM and tested the effects on stage 24 forelimb mesenchyme. The time course of matrix loss in limb was similar to the mandible (Fig. 2.12A-F). *MMP13* was induced 15-fold at 4 days and 100-fold at 6 days compared to control media (Fig. 2.12G). Interestingly, in the control limb cultures, *MMP13* levels remains flat between 4 and 6 days whereas in the control mandibular cultures there is a steady increase of *MMP13* that is accentuated when Wnt5a is added. These data suggest there are some differences between facial and limb cultures in terms of *MMP13* expression in media controls but that the response to Wnt5a is identical.

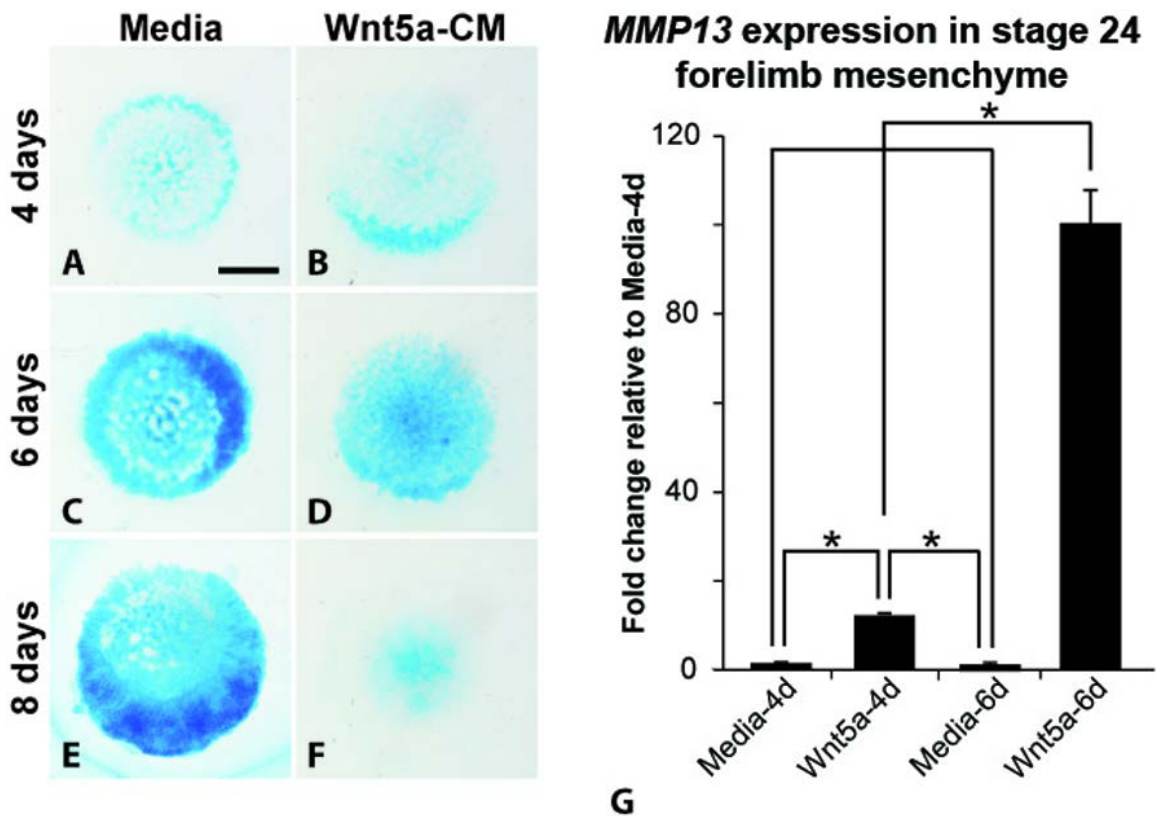


Figure 2.12 Wnt5a treatment causes degradation of limb cartilage in the same manner as cartilage in the face.

A-F) Micromass cultures from stage 24 distal limbs were fixed and stained with Alcian Blue at various time points. **A,C,E)** Distal limb mesenchyme forms cartilage sheets. There is an increase in size of the whole culture as well as the area of blue stained cartilage between 4 and 8 days. **B,D,F)** Cultures treated with Wnt5a-CM 1:1 diluted with base media form sheets at 4 days but these disappear gradually by 8 days. **G)** *MMP13* expression is normalized to 18s RNA. In Wnt5a treated cultures, there is significantly more *MMP13* present at both 4 and 6 days (ANOVA). The levels of *MMP13* do not change in the control cultures between day 4 and day 6. Scale bar for A-F=2 mm.

2.4 Discussion

In this study, we describe for the first time how Wnt5a functions in craniofacial chondrogenesis. The transient expression of *WNT5A* during development of Meckel's cartilage raised the question of whether Wnt5a has a role during normal initiation, differentiation or maturation of the facial skeleton. We showed that Wnt5a regulates matrix stability but not the initial steps of chondrogenesis. Instead during development, the main function of *WNT5A* is to keep canonical signaling low in the cartilage blastema, thereby promoting chondrogenesis.

Moreover we demonstrated that when provided to mature cartilage, Wnt5a is sufficient to induce matrix removal in neural crest and mesodermal-derived cartilage ligand and that the JNK pathway is mediating the matrix degradation.

2.4.1 The normal role of Wnt5a during development of cartilage

During normal development of the beak, there are relatively high levels of *WNT5A* during mandibular chondrogenesis. There are also antagonists expressed at early stages which might protect the cartilage from degrading effects of Wnts. Later, the cartilage ceases to express *WNT5A*, and we suggest based on our in vitro data that downregulation of *WNT5A* is necessary in order to preserve the matrix. The model we are proposing is that the main function of *WNT5A* during early chondrogenesis is to repress canonical signaling in order for cartilage to differentiate (Fig. 2.13A). Our gain and loss-of-function experiments with Wnt3a-CM and DKK1 showed canonical signaling must be suppressed in order for chondrogenesis to occur. Our data concurs with inhibitory effects of Wnt3a on chicken limb chondrogenesis although the effects were milder in the limb than the face (Hwang et al., 2005; Surmann-Schmitt et al., 2009). The luciferase assays showed that *WNT5A* is a strong antagonist of canonical signaling in mandibular mesenchyme. Taken together, the data suggest that high levels of *WNT5A* in early Meckel's cartilage in vivo may actually promote chondrogenesis. *WNT5A* may keep canonical signaling low in concert with other WNT antagonists such as *FRZB1* which is also expressed in Meckel's cartilage (Ladher et al., 2000). We do acknowledge that it is difficult to reconcile our in vitro data with the model. We would have predicted that by adding Wnt5a-CM canonical signaling would be repressed thereby promoting chondrogenesis. However there was neither an increase nor a decrease in Alcian blue staining in 4 day cultures. One possibility is that in micromass cultures the activation of the JNK pathway may have counterbalanced the effects of

repressing the canonical pathway. The increase in JNK signaling is likely to have caused the observed decrease in *COL2A1* and *SOX9* expression at 4 days which will subsequently lead to decreased type II collagen in the cultures. In vivo it is possible that the levels of endogenous WNT5A are not high enough to activate JNK signaling. The levels of activity of the ATF2-luciferase reporter were indeed very low in freshly isolated mandibular mesenchyme, which is consistent with this idea. To answer this question definitively we would need a reporter mouse for Wnt-activated JNK signaling but this has not yet been developed.

There are similarities in the expression pattern of *Wnt5a* in the limb and face. In mouse and chicken limb buds, *Wnt5a* is extensively expressed in undifferentiated limb mesenchyme but at later stages no expression is detected in differentiating cartilage (Gavin et al., 1990; Kawakami et al., 1999). Instead, *Wnt5a* is restricted to the perichondrial layer of differentiated cartilage similar to Meckel's cartilage. This suggests that WNT5A may play a general role in repressing canonical signaling in chondrogenic condensations in vivo, but later must be downregulated in order to preserve matrix. Perichondrial expression of WNT5A also suggests a role of WNT5A in appositional growth of Meckel's cartilage mediated by perichondrium.

The effects of excess *Wnt5a* on chicken limbs (Hartmann and Tabin, 2000; Kawakami et al., 1999) and in transgenic mice (Yang et al., 2003) have been described as shortening and failure to progress to hypertrophy. Proliferation was reduced and *Col2a1* expression was decreased. Both upper and lower jaws were shorter in the *Col2a1-Wnt5a* transgenic mice than in control embryos but detailed histological analysis has not been carried out (Yang et al., 2003). It is therefore not known whether excess WNT5A reduced the cartilage matrix. Our retroviral studies on the lower beak are different than those in the limb since hypertrophy does not occur in Meckel's cartilage (Eames and Helms, 2004).

Micromass culture experiments using *WNT5A* delivered as a retrovirus (Church et al., 2002; Daumer et al., 2004; Tufan and Tuan, 2001) or recombinant Wnt5a protein (Bradley and Drissi, 2010) are similar to our results. There was no inhibition of early chondrogenesis and in some cases there was even a slight increase (Bradley and Drissi, 2010; Church et al., 2002) in the presence of excess WNT5A. These in vitro data are consistent with the model that Wnt5a may promote early chondrogenesis. We extended the work of these other groups by culturing the limb mesenchyme longer, thus revealing the matrix degradation phenotype.

2.4.2 Wnt5a negatively affect matrix stability in conditions of excess

Our studies extended the in vitro experiments to the point where matrix was completely removed, thereby uncovering the enzymatic process induced by Wnt5a. Part of the mechanism is the induction of an enzymatic process affecting matrix maintenance (Fig. 2.13B). The addition of exogenous Wnt5a-CM simulates diseases in which expression is increased such as the human inflammatory disease, osteoarthritis. Amongst WNT ligands, a significant increase in *WNT5A* expression has been observed in osteoarthritic joints compared to joints of normal control subjects using microarray analysis (Thorfvé et al., 2012). Other work using cultures of rabbit articular chondrocytes that were initially fully differentiated showed that addition of Wnt5a-CM decreased type II collagen protein and RNA (Ryu and Chun, 2006). These effects were mediated by the JNK pathway similar to our results. Our work extends and expands these studies by following the cells post-differentiation. Furthermore, the embryonic chicken system may be a good system in which to recapitulate the early steps in cartilage degradation seen in osteoarthritis.

At the heart of osteoarthritis is the increased expression and activity of enzymes such as MMPs and Aggrecanases (Goldring, 2012; Troeberg and Nagase, 2012). Using embryonic

chicken mandibular mesenchyme we showed that Wnt5a is a potent inducer of *MMP1*, *MMP13* and *ADAMTS5* thus the molecular changes are similar to those seen in osteoarthritis.

2.4.3 The Wnt5a micromass phenotype is not due to precocious chondrocyte hypertrophy

An alternative interpretation for the loss of cartilage matrix is that Wnt5a has accelerated the process of hypertrophy and that changes in the matrix are secondary to this process. There are two markers for hypertrophy present in our system, type X collagen and *MMP13*. However the expression of these markers may be an artifact of the culture media. Work from others showed that ascorbic acid in the media induces type X collagen expression in mandibular micromass cultures (Ekanayake and Hall, 1994). It turns out that *MMP13* is also a marker for hypertrophic cartilage in limbs (Tuckermann et al., 2000). We noted that *MMP13* expression was significantly upregulated in control cultures as they matured even though there was no resulting matrix loss. We attribute the increase in expression of this gene to the ascorbic acid in the media. Although the Wnt5a-treated cultures expressed type X collagen and *MMP13* they did not possess the other hallmarks of hypertrophy including mineralization of the nodules which would be shown by increased staining with Picrosirius red. In sections of the cultures, the staining was similar in the fibroblasts between the nodules and in the nodules themselves. In addition, cultures that were stained for alkaline phosphatase activity showed a reduction in staining in the presence of Wnt5a and staining was restricted to the non-chondrogenic regions (S. Hosseini-Farahabadi, unpublished data). Apoptosis is also a hallmark of hypertrophic chondrocytes (Gibson et al., 1997) and we did not see increased TUNEL staining in Wnt5a cultures. Furthermore hypertrophy is a gradual process and here we saw a rapid progression from peak matrix secretion to almost complete loss in a period of 48h. The more likely explanation for the matrix loss in Wnt5a-treated cultures is the cumulative induction of several enzymes, especially *MMP1* which is

upregulated 1000 fold compared to controls, rather than precocious hypertrophy. An additional mechanism at play is the fact that aggrecan is itself a substrate for MMPs (Durigova et al., 2011; Fosang et al., 1996; Toriyama et al., 1998), therefore induction of MMPs would accelerate removal of the proteoglycans.

2.4.4 The signaling pathway used by Wnt5a to degrade matrix involves JNK

Using SuperTopflash reporter we found that Wnt5a inhibits canonical signalling; however, we ruled out Wnt5a antagonism of canonical Wnt pathway as the mechanism involved in matrix loss. Instead the rescue of chondrogenesis by the JNK antagonist suggests that the activation of the JNK signalling pathway is accelerating matrix degradation (Fig. 2.13B). Although we did not measure the level of *MMP1* in the JNK antagonist treated cultures, others have shown that *MMP1* is induced by JNK signaling in osteosarcoma cells (Kimura et al., 2011). Other in vitro studies also support our hypothesis that JNK signaling is required for induction of matrix degrading enzymes. Wnt5a acts via Ror2 to induce JNK signalling which then leads to direct activation of *Mmp13* transcription in osteosarcoma cells (Yamagata et al., 2012). However, these authors did not carry out functional experiments to examine whether Mmp13 is mediating a cellular phenotype. It should be noted that two receptors, *ROR2* (Stricker et al., 2006) and *FZD7* (Geetha-Loganathan et al., 2009) are expressed at high levels in chicken mandibular mesenchyme and could be mediating the effects of Wnt5a-CM on JNK activity in our system.

We conclude that WNT5A functions as a critical regulator of cartilage matrix homeostasis in development and disease and that it is important to study the mechanism in a defined system such as ours. In the future it will be possible to design new drugs targeting

WNT5A or other pathway components to protect against matrix loss in patients with debilitating diseases such as osteoarthritis.

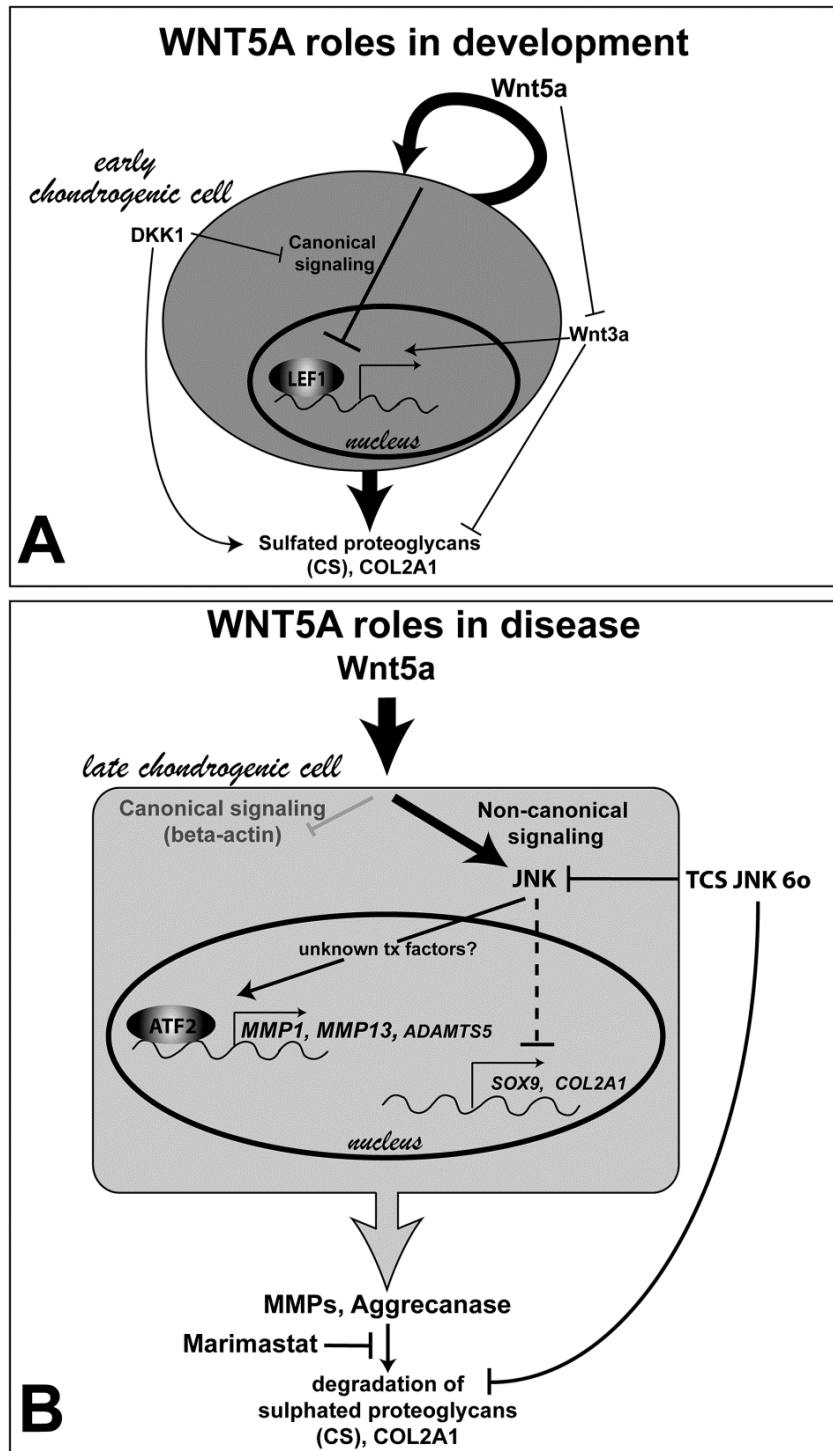


Figure 2.13 Summary of Wnt5a functions during cartilage development and disease.

A) During normal development, there is synthesis of WNT5A in the cartilage blastema and by the newly differentiated chondrocytes. The secreted WNT5A acts back on the same cells to inhibit canonical activity. The net result of reducing canonical activity is to promote chondrocyte differentiation and matrix secretion. The data in this paper supporting this model are the increase in chondrogenesis caused by DKK1, the inhibition of chondrogenesis by Wnt3a and the antagonism of canonical signaling by Wnt5a as shown in luciferase assays. **B)** During disease or where high levels of Wnt5a are present, chondrocytes are induced to degrade their own matrix which could be considered a disease phenotype. The pathways shown in this paper include the increase in JNK signaling measured in luciferase assays, the increased RNA expression for the three matrix degrading enzymes and the rescue of the cartilage with either Marimastat (works at the enzyme level) or TCS JNK 60 which works at the JNK phosphorylation level.

3. Role of WNT5A in mandibular morphogenesis

3.1 Introduction

Multipotent, migratory neural crest cells are the origin of face. Neural crest cells for the face originate from the dorsal margins of the neural tube and migrate to the ventral regions of the head to form the facial mesenchyme (Couly et al., 1993; Creuzet et al., 2005). Once neural crest cells have reached the presumptive face, local interactions with the surrounding tissues begin and the facial prominences begin to grow out. Three prominences come together to form the upper jaw - the frontonasal, maxillary and lateral nasal prominences. Each of the prominences contributes to a specific group of skeletal elements (Lee et al., 2004; MacDonald et al., 2004; Richman and Tickle, 1989). The lower jaw is made entirely by the mandibular prominence. During development, there are striking changes in morphology of facial structures. The facial prominences become narrower in the mediolateral axis (horizontal axis) and longer in the cranio-caudal axis (vertical axis) which may be due to convergent extension (Kamel et al., 2013). Convergent extension is defined as laterally positioned cells moving together and intercalating to form a narrow column which extends in length in a perpendicular axis (Wallingford et al., 2002). This facial narrowing is typical for mammals and in humans midline defects such as wide-set eyes (hypertelorism), a wide nasal bridge or a deficient midline (holoprosencephaly), might be due to a failure of convergent extension.

Cell activities such as cell migration and intercalation are important processes during morphogenesis. Others have studied cell movements using dye injection during jaw development (He et al., 2008; Lee et al., 2004; McGonnell et al., 1998). Using DiI labelling, Lee et al. showed that mandibular cells originate from first pharyngeal arch while post-optic mesenchyme is the major origin of maxillary cells (Lee et al., 2004). In normal mouse palatal shelves, posterior cells

migrate anteriorly and anterior cells move laterally (He et al., 2008). Particularly relevant to my studies are the findings of McGonnell et al. (1998). They injected DiI into stage 20 embryos and followed them for 48h until stage 28. The authors showed that during normal mandibular development lateral cells move towards the midline whereas medially-located cells have a tendency for cranio-caudal directional movements (McGonnell et al., 1998). The limitations of this study were that cells increased in number due to cell proliferation over 48h therefore the authors were careful to say that expansion of the dye spot was due to a combination of migration and proliferation. They also only used one type of dye which made it impossible to determine whether intercalation had taken place.

There are several signals such as BMPs (Ashique et al., 2002), FGFs (Szabo-Rogers et al., 2008), and WNTs operating during facial morphogenesis and some of these may direct the narrower shape of the prominences. Of these growth factors the most likely to be involved in cell rearrangements are the WNT growth factors. WNTs are secreted glycoproteins and are classified into two main groups of canonical and non-canonical (Logan and Nusse, 2004; Seidensticker and Behrens, 2000; Veeman et al., 2003). The canonical pathway is of importance during cell fate specification. The non-canonical signaling is involved in several developmental processes such as convergent extension. Non-canonical WNTs are particularly important for cytoskeletal changes and activate either calcium pathway (Kohn and Moon, 2005; Kuhl et al., 2000) or the JNK/planar cell polarity (PCP) pathway (Fanto and McNeill, 2004; Gray et al., 2011) both of which may affect directed cell migration, coordinated shape change in cells or intercalation of cells. PCP signalling is not only active in planar tissues such as epithelia but is also important for cell migration and organization of mesenchyme (Gray et al., 2011). Components of the PCP pathway include cell membrane proteins Frizzled, Dishevelled (Dvl, recruited to the receptor Fzd

upon ligand binding), Vangl, Celsr, Prickle and Inversin (Gray et al., 2011; Karner et al., 2006). Non-canonical WNTs can antagonize the canonical pathway in the presence of appropriate receptors (Maye et al., 2004; Mikels et al., 2009; Mikels and Nusse, 2006). For example, Ror2 is a Wnt5a alternative receptor and upon Wnt5a binding antagonizes canonical signaling (Mikels and Nusse, 2006; Rao and Kuhl, 2010). Mouse and human studies have shown links between Wnt5a signaling and facial morphogenesis. Defects in convergent extension are likely to be caused by Wnt5a loss-of-function since *Wnt5a* null mice show shortening of the central body axis, the jaws and limbs (Yamaguchi et al., 1999; Yang et al., 2003). The other possible mechanisms causing shortening phenotypes include decrease in cell proliferation or a perturbed differentiation.

Mutations in *WNT5A* or its receptor, *ROR2*, cause Robinow Syndrome in human (Person et al., 2010; Schwabe et al., 2004; Stricker et al., 2006). Robinow syndrome is a rare genetic disorder which is mainly characterized by short stature, limb shortening and distinctive facial abnormalities named as “fetal facies” (Patton and Afzal, 2002). Some facial features include hypertelorism, midfacial hypoplasia, micrognathia (small lower jaw) and dental irregularities and could be consistent with an earlier defect in cell organization within the facial prominences. There are two forms of Robinow Syndrome, the recessive form which is caused by loss-of-function mutations in *WNT5A* receptor, *ROR2* (van Bokhoven et al., 2000) and the dominant form (DRS). DRS is caused by amino acid substitutions of two cysteine residues, either C83S or C182R (Person et al., 2010). These mutations are on either side of the cysteine 104 that is palmitoylated (Kurayoshi et al., 2007). We are just now learning about the domain structures of WNT proteins. Progress has been impeded by difficulty in expressing the protein in its fully processed and translationally modified form so that it will bind to its receptors. *WNT5A* has yet

to be crystalized in this manner. So far only *Xenopus* WNT8 has been crystalized. Based on XWNT8 crystal structure (Bazan et al., 2012; Janda et al., 2012), computational modeling of 3D structures of human WNT1 in complex with FZD1 (Ain et al., 2013) and alignments of the XWnt8/hWNT5A proteins conducted by myself, it is likely that Cysteine 83 and 182 are in the N-terminal Frizzled binding domain of WNT5A. It is not known precisely where WNT5A binds to ROR2 however it is likely that binding is mediated by the cysteine rich domain (Mikels et al., 2009). Mutations in *WNT5A* may therefore affect ROR2 mediated signaling. It is also likely that the mutated forms of WNT5A are trapped within the cells and therefore are not secreted to the same levels as wtWNT5A.

Wnt5a is required for cell migration (Gros et al., 2010) and orientation of chondrocytes in the mouse (Gray et al., 2011). The only craniofacial data on Wnt5a effects on cell behavior was collected on the secondary palates of *Wnt5a*^{-/-} embryos (He et al., 2008). Injection of *GFP*-expressing cells into the anterior palatal shelf followed by culture in vitro for 24 and 48 hours showed that cell movements were blocked and these effects correlated with lack of extension of the palatal shelves. No previous studies have investigated the function of WNT5A in the mandibular prominence. Since there is strong expression of *WNT5A* in mandible (Geetha-Loganathan et al., 2009; Hosseini-Farahabadi et al., 2013), I hypothesize that the mandibular phenotype caused by *WNT5A* mutations originate from disturbed cell activities during early morphogenesis. Here, in this project, we have used the chicken embryo in order to examine these questions. We hypothesize that *WNT5A* mutations (C182R and C83S) lead to a partial loss-of-function, possibly acting in a dominant-negative manner on wtWNT5A. The effects could include a loss of oriented cell movements and failure of chondrocyte intercalation/organization both of which could impede convergent extension of mandibular mesenchyme in chicken. Using

retroviruses to misexpress the various forms of *WNT5A* in the mandible, we discovered a similar phenotype of micrognathia and reduction in limb outgrowth to that seen in human. The phenotypes were more frequent and more severe with the C83S mutation and imply a reduction in *WNT5A* function has occurred.

3.2 Materials and methods

3.2.1 Virus preparation and injection

pENTRY plasmid containing full length open reading frames for human *WNT5A* (NM-003392.3) was obtained from Life Technologies (Clone ID IOH39817). Primers were used to incorporate the mutations (Table 3.1) using restriction-free cloning (Bond and Naus, 2012). PCR products were sequenced to confirm mutations. Then pENTRY plasmids containing human *wtWNT5A*, *WNT5A^{C182R}* and *WNT5A^{83S}* inserts were recombined with avian retrovirus RCASBP-Y using Gateway cloning (Loftus et al., 2001). Virus was grown up and concentrated as described (Logan and Tabin, 1998). Aliquoted viral particles were then injected into the forelimb and mandibular regions of stage 15 embryos using a picospritzer microinjector. Embryos were incubated until stage 37 and 38 for limb and mandible, respectively and then were fixed in 100% Ethanol.

Table 3.1 Primers used to incorporate mutations into human *WNT5A*.

Mutation	Primer sequence
C182R (544-545CT→TC)	Fw: GGCGGTCGCGGCGACAAC
	Rev: GGCCTGCAAGTGCCATGGG
C83S (284G→C)	Fw: GACAGAAGAACTGTCCCCTTGTATC
	Rev: GTGGTGAACGCCATGAGC

3.2.2 Immunofluorescence antibody staining of virus protein

Following dewaxing and rehydration, slides were washed 3x in PBS, then sections were steamed in 1x Diva Decloaker in H₂O at 99°C for 15 minutes. Slides were rinsed in 1x PBS, then blocking serum was applied (blocking serum: 10% goat serum in PBS) and slides were incubated in a humidified chamber at room temperature for 30 minutes. Then the blocking serum was removed and primary antibody was applied. Mouse 3C2 monoclonal antibody (1:4 dilution of supernatant; Developmental Studies Hybridoma Bank) was used. The primary antibody was incubated in humidified chamber at 4°C overnight. Slides were rinsed 3x in PBS and secondary anti-mouse antibody was applied. Secondary antibody was tagged with Alexa fluor 488 (1:200, Invitrogen) and was incubated in humidified chamber at room temperature for 30min in the dark. The slides were rinsed in PBS and cover slipped with Prolong Gold with DAPI (Life Technologies, cat no. 36930). Sections were viewed under blue and green fluorescence illumination.

3.2.3 BrdU, TUNEL staining and analysis

Chicken embryos at stage 28-29 were labeled with BrdU by injecting 50 µl of 100 mM BrdU into the heart two hours prior to fixation. Embryos were removed from the egg, fixed in 4% PFA and then processed into wax. The BrdU antibody (GE Healthcare, cat no. RPN202) was used neat. Antigen retrieval was the same as section 3.2.2. TUNEL was carried out using the ApopTag Apoptosis Kit (Chemicon, S7101) and was detected using anti-digoxigenin tagged with fluorescein. Single slices at maximum intensity were collected using Leica DM 6000 CS Confocal microscope.

Quantification of cell proliferation and apoptosis was carried out using the particle counter Plugin for ImageJ. The region infected with virus was determined by overlapping anti-GAG fluorescent pictures and BrdU/TUNEL pictures and cells in the virally infected area were counted. Then BrdU or TUNEL-positive cells were counted in the green channel to obtain the number of labeled cells. The total cell number was determined by counting TO-PRO-3 iodide (Life technologies, cat no. T3605) stained nuclei. The proportion of BrdU or TUNEL positive cells to total cells was determined for the infected area.

3.2.4 Cell tracking

DF1 cells expressing *wtWNT5A*, *WNT5A^{C182R}* or *WNT5A^{C83S}* were collected, spun down and mixed with 2 µg/ml DiO (Invitrogen, D7778). Stage 24 heads were dissected and placed on 1% agarose gel in H₂O. Mandibular prominences were injected medially with DF1 cells+DiO (green) and lateral host mesenchyme was labelled with CellTracker CM-DiI (Red, Invitrogen, C7000). Then mandibles were dissected and cultured on membranes in organ culture plates for 24 hours. Photos were taken every 6 hours with green and red fluorescent channels, however only the 6 and 24-hour data were used since changes were incremental in between these time points. After 24 hours, cultured mandibles were fixed in 100% methanol briefly and then placed into 4% PFA overnight. Following rinsing off the fixative, organ cultures were embedded in 2% agarose, processed into paraffin and sectioned at 7µm thickness with microtome. Sections were put on slides, dewaxed and cover slipped using Prolong Gold with DAPI (Life Technologies, cat no. 36930) and photographed using Olympus BX61 fluorescence microscope.

3.2.5 Chondrocyte intercalation analysis

Embryos injected into right mandible at stage 15 with retrovirus were fixed in 4% PFA at stage 29-30. The heads were processed into wax and sectioned frontally. Sections were stained

with Picrosirius Red and Alcian Blue. The ferret diameters (the longest and shortest diameters of an ellipse on perpendicular axes) were measured using ImageJ for at least 50 random chondrocytes per technical replicate (3) and 3 biological replicates per virus. The average of ferret proportion from each biological replicate was used for statistical analysis.

3.3 Results

3.3.1 Human *WNT5A* mutations cause shortening of limb and mandible in chicken

To investigate the effects of *WNT5A* mutations on mandibular and limb development, we mutated wild type human *WNT5A* to contain the same missense mutations as in DRS (Table 3.1). These constructs were used to recombine with Gateway compatible avian retrovirus, RCASBPY. I checked DF1 cells for the presence of human *WNT5A* inserts by PCR using primers specifically for human *WNT5A* gene (Table 3.2) and found out that all transfected DF1 cells contain exogenous human *WNT5A* (Fig. 3.1). I infected mesenchymal cells destined for mandible or limb at HH15 with RCAS::*wtWNT5A*, RCAS::*WNT5A^{C182R}*, RCAS::*WNT5A^{C83S}* or RCAS::*GFP* as the control. The skeletal phenotypes resembled the ones in human patients with Robinow syndrome i.e. shortening of the limb and lower jaw (Person et al., 2010). There was a lack of proximo-distal extension of both mandible and limb on the injected side compared to controls (Fig. 3.2A-D' and Fig. 3.3A-D'). Interestingly, 100% of the embryos injected with RCAS::*WNT5A^{C83S}* had this phenotype (n=7/7 and 9/9 for mandible and limb, respectively and Table 3.3 and 3.4). The most affected mandibular elements included angular and surangular bones and Meckel's cartilage. Mandibular deviation was seen in 1/4, 3/7, 7/7 of the embryos injected with RCAS::*wtWNT5A*, RCAS::*WNT5A^{C182R}*, RCAS::*WNT5A^{C83S}*, respectively (Fig. 3.2B,C,D). Deviation is probably caused by unilateral shortening of the beak. In the limb, the stylopod and zeugopod were shorter (Fig. 3.3B',C',D' and Table 3.4). A number of treated embryos in our

study showed a delayed or absent ossification in the limb (1/6, 2/10, 9/9 of the embryos injected with RCAS::*wtWNT5A*, RCAS::*WNT5A^{C182R}*, RCAS::*WNT5A^{C83S}*, respectively; Fig. 3.3D'). In mandible, 1/4, 1/7 and 2/7 of embryos injected with RCAS::*wtWNT5A*, RCAS::*WNT5A^{C182R}*, RCAS::*WNT5A^{C83S}*, respectively, had a moth-eaten lesion in mandibular bones (insets in Fig. 3.2C'',D'').

There are at least three possible mechanisms within the focus of this study which can explain shortening of the injected mandible or limbs. They include: 1) decreased cell proliferation; 2) increased cell death; 3) impaired oriented cell activities.

Table 3.2 Primer sets used to check human *WNT5A* inserts in DF1 cells.

Primer set	Primer sequence
Primer set 1	Fw: GGGGATGGCTGGAAGTGC
	Rev: GATGCCTGTCTTCGCGCCT
Primer set 2	Fw: ATTCTTGGTGGTCGCTAGGT
	Rev: GCAGTTCCACCTTCGATGTC

Table 3.3 Biological replicates and detailed phenotype analysis of embryos injected with viruses into mandibular prominences.

Injected virus	Normal	Deviation	Splenial reduced	Dentary reduced	Angular reduced	Surangular reduced	Meckel's reduced	Moth-eaten bone
RCAS:: <i>GFP</i> (n=3)	3	0	0	0	0	0	0	0
RCAS:: <i>wtWNT5A</i> (n=4)	1	1	2	2	2	2	2	1
RCAS:: <i>WNT5A^{C182R}</i> (n=7)	3	3	2	2	4	4	4	1
RCAS:: <i>WNT5A^{C83S}</i> (n=7)	0	7	3	4	6	6	7	2

Table 3.4 Biological replicates and detailed phenotype analysis of embryos injected with viruses into prospective limb region.

Injected virus	Normal or minor shortening of one bone	Only stylopod abnormalities	Stylopod plus zeugopod abnormalities	Stylopod, zeugopod and autopod abnormalities	Delayed or absent ossification in any bone
RCAS:: <i>GFP</i> (n=4)	4	0	0	0	0
RCAS:: <i>wtWNT5A</i> (n=6)	3	0	0	2	1
RCAS:: <i>WNT5A^{C182R}</i> (n=10)	2	3	0	5	2
RCAS:: <i>WNT5A^{C83S}</i> (n=9)	0	0	3	6	9

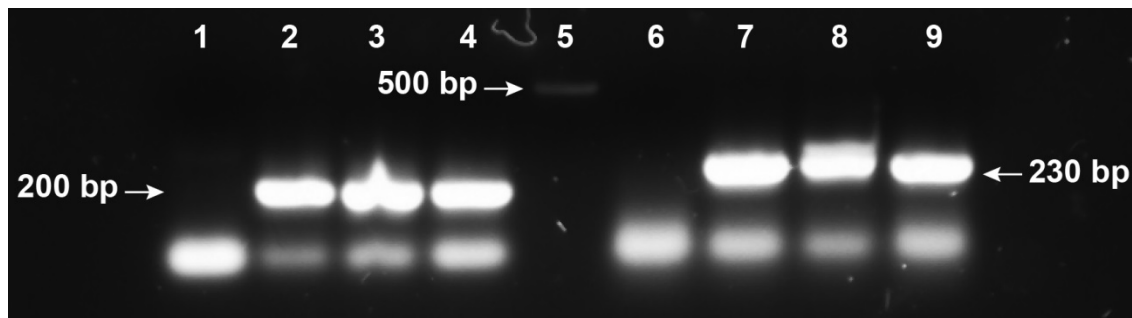


Figure 3.1 PCR analysis to confirm presence of h*WNT5A* in DF1 cells.

Lanes 1 and 6: empty DF1 cells; Lanes 2 and 7: DF1 cells expressing human *wtWNT5A*; Lanes 3 and 8: DF1 cells expressing *WNT5A^{C182R}*; Lanes 4 and 9: DF1 cells expressing *WNT5A^{C83S}*; Lane 5: 1 kb ladder. Lanes 1,2,3 and 4 are PCR products of primer set 1 (200 bp). Lanes 6,7,8 and 9 are PCR products of primer set 2 (230 bp). There is no difference in band sizes between mutant and *wt WNT5A* amplicons. The bottom bands are primer dimers.

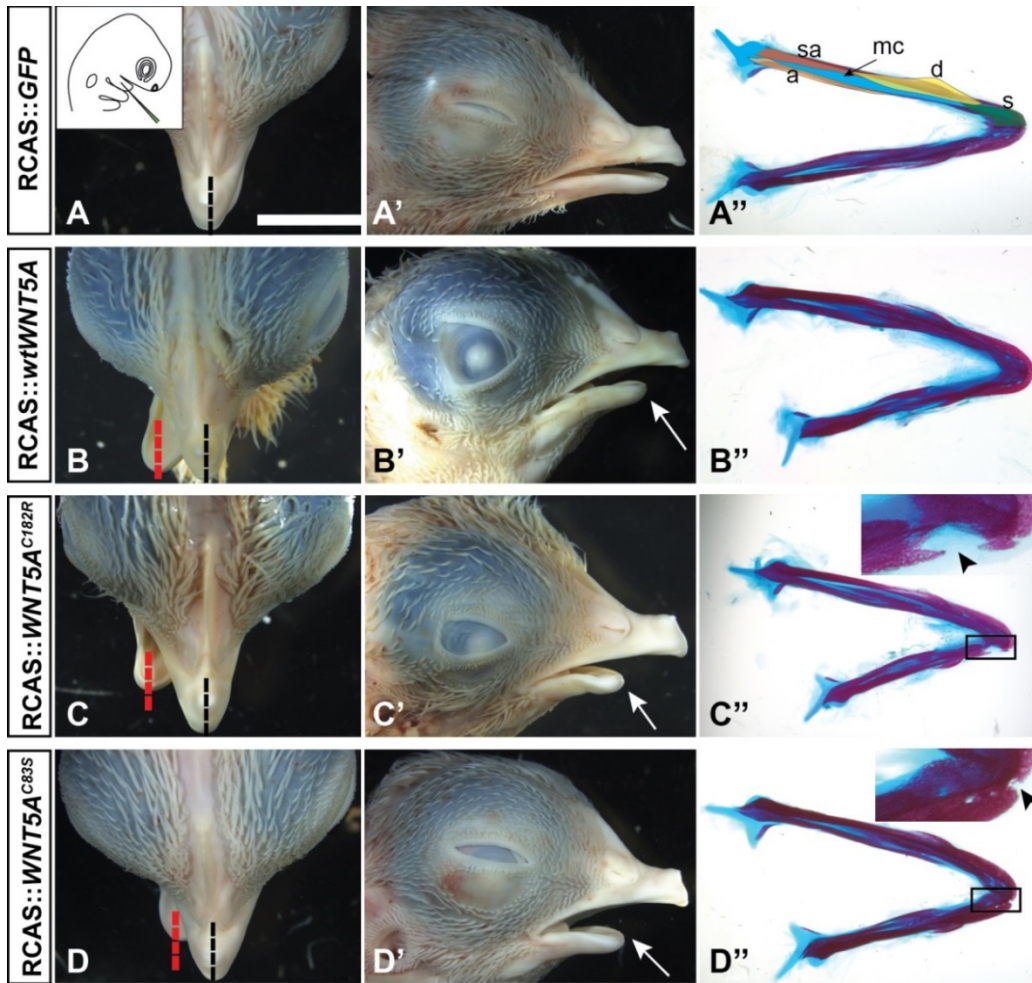


Figure 3.2 In vivo injection of RCAS::GFP, RCAS::wtWNT5A, RCAS::WNT5A^{C182R} and RCAS::WNT5A^{C83S} retroviruses into mandible.

Embryos injected with RCAS::GFP, RCAS::wtWNT5A, RCAS::WNT5A^{C182R} and RCAS::WNT5A^{C83S} into the mandibular arch at stage 15 (inset in A) and fixed 12 days post-injection at stage 38. **A,B,C,D)** The injected heads were collected and photographed from above. Red dashed lines show lower beak deviated from midline (black dashed lines). A) An embryo injected with RCAS::GFP has formed a normal beak. Beak deviation towards right is seen in embryos injected with RCAS::wtWNT5A (B), RCAS::WNT5A^{C182R} (C) and RCAS::WNT5A^{C83S} (D). **A',B',C',D')** Side view of the embryos injected with viruses. Arrows show shortening of lower beaks. A') An embryo injected with RCAS::GFP develops a normal beak. Shortening of right lower beak is seen in the embryos injected with RCAS::wtWNT5A (B'), RCAS::WNT5A^{C182R} (C') and RCAS::WNT5A^{C83S} (D'). The upper beak has formed normally showing accurate injection technique. **A'',B'',C'',D'')** The dorsal view of whole mount lower beaks stained with alizarin red and alcian blue reveals that many skeletal elements were affected in the treated embryos. A'') The whole mount stained lower beak from the same embryo as in A develops normal skeleton. B'') The whole mount stained lower beak from the same embryo as in B showed short mandibular bones and Meckel's cartilage. C'') The whole mount stained mandible from the same embryo as in C had shorter mandibular bones and Meckel's cartilage. This particular embryo also had a moth-eaten splenial bone (inset). D'') The whole mount stained lower beak from the same embryo as in D had short bones specially angular and surangular bones and Meckel's cartilage. This embryo also has a midline defect in splenial bone (inset). Scale bar for A-D'' = 5 mm. Key: a – angular bone, d – dentary bone, mc – Meckel's cartilage, sa – surangular bone, s – splenial bone.

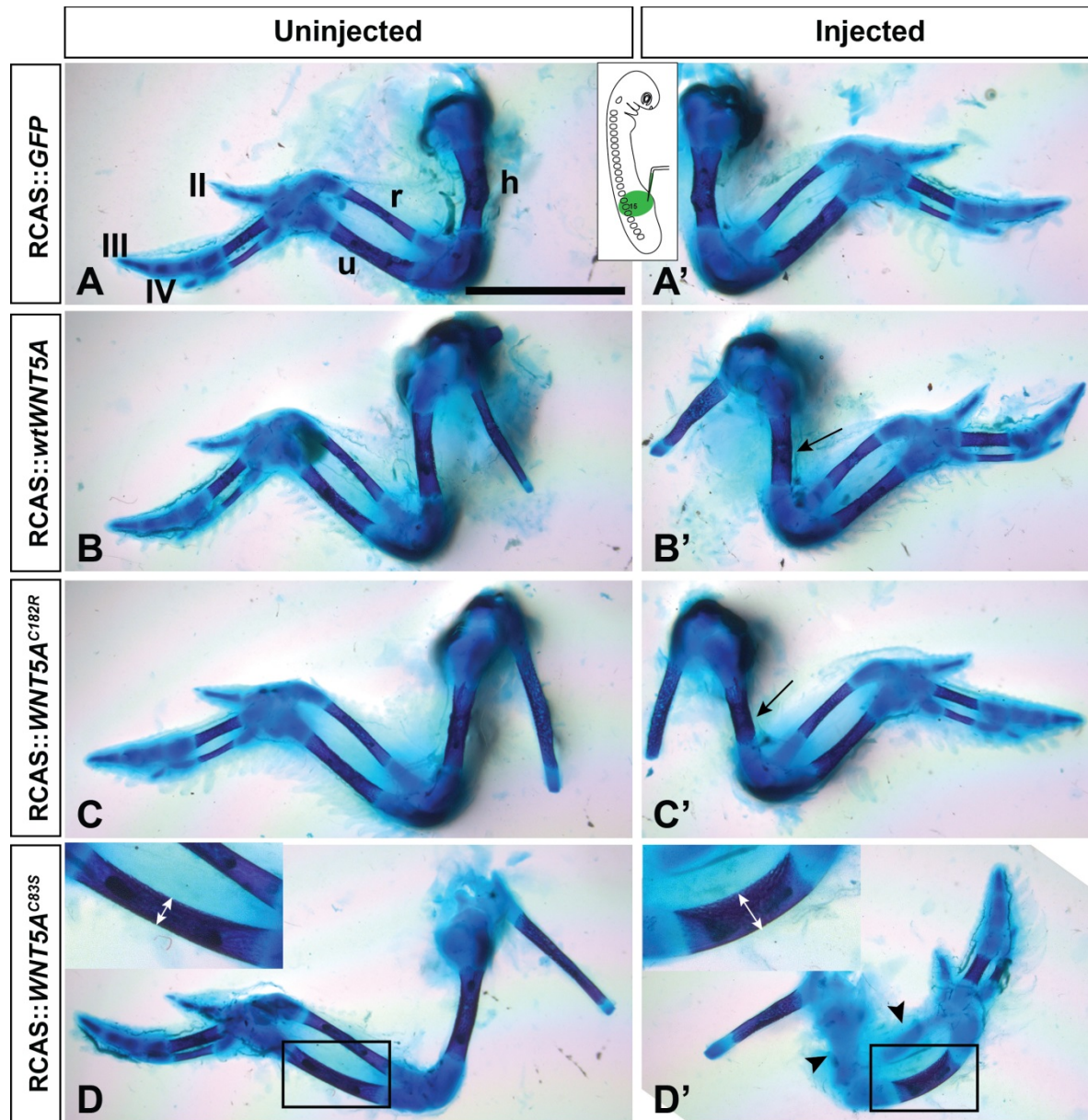


Figure 3.3 In vivo injection of RCAS::GFP, RCAS::wtWNT5A, RCAS::WNT5A^{C182R} and RCAS::WNT5A^{C83S} retroviruses into limb.

Whole mount limbs from stage 37 embryos stained with alizarin red and alcian blue reveals that some skeletal elements of the limb were affected in the treated embryos. The schematic inset at the top shows the site of virus injection in green. **A,B,C,D)** Left uninjected limbs form normal limb bones and cartilages. **A',B',C',D')** Right injected limbs were stained for bone and cartilage and cleared. **A')** The right stained limb from the same embryo as in **A** injected with RCAS::GFP develops normal limb skeleton. **B')** The right stained limb from the same embryo as in **B** injected with RCAS::wtWNT5A had a shorter humerus (arrow). **C')** The right stained limb from the same embryo as in **C** injected with RCAS::WNT5A^{C182R} showed a short humerus. **D')** The right stained limb from the same embryo as in **D** injected with RCAS::WNT5A^{C83S} showed severe phenotype. Humerus and radius bones did not form (arrowheads) and ulna was short (box). Also bone formation in digits was delayed. The whole limb is much shorter than control limb. The insets in **D** and **D'** are higher magnification of boxed regions in **D** and **D'** and show thickness (double ended arrows) of ulna in control (**D**) and injected (**D'**) limbs. Scale bar for **A-D'** = 5 mm. Key: h – humerus, r – radius, u – ulna.

3.3.2 WtWNT5A and WNT5A mutations reduce cell proliferation

It has previously been shown that both gain and loss of *WNT5A* function reduce cell proliferation in mice (Yamaguchi et al., 1999; Yang et al., 2003). To investigate whether cell death or proliferation was altered in embryos infected with *WNT5A* mutations, I used TUNEL and BrdU incorporation, respectively. Cell death was not changed (Fig. 3.4A'',B'',C'',D'',F) but there was a significant reduction in cell proliferation in the mandibles injected with RCAS::*wtWNT5A*, RCAS::*WNT5A^{C182R}* and RCAS::*WNT5A^{C83S}* when compared to control RCAS::*GFP* (p=0.04, 0.02, 0.03, respectively; Fig. 3.4A',B',C',D',E). I quantified cell proliferation in the areas infected with the virus shown by viral GAG expression (Fig. 3.4A,B,C,D). In this assay, BrdU positive cells were counted in at least three biological replicates and between 2-6 sections of every embryo. In controls, 50% of the cells had incorporated BrdU whereas only 31%, 29% and 27% of cells were BrdU positive in embryos infected with RCAS::*wtWNT5A*, RCAS::*WNT5A^{C182R}* and RCAS::*WNT5A^{C83S}*, respectively. In addition to these results, I noticed that the condensations for Meckel's cartilage had lower proliferation compared to the surrounding mesenchyme (compare Fig. 3.4C',D' to 3.4C'' and D'' and GFP data not shown). It is not immediately clear why the *wtWNT5A* has similar effects on proliferation to those of the mutant forms of *WNT5A*. We assume that there are different mechanisms leading to the same phenotype. Reduced cell proliferation within the viral infected domain suggests that mandibular shortening caused by *wtWNT5A* and the mutant forms of the virus may arise, at least in part, from decreased cell proliferation in the treated embryos.

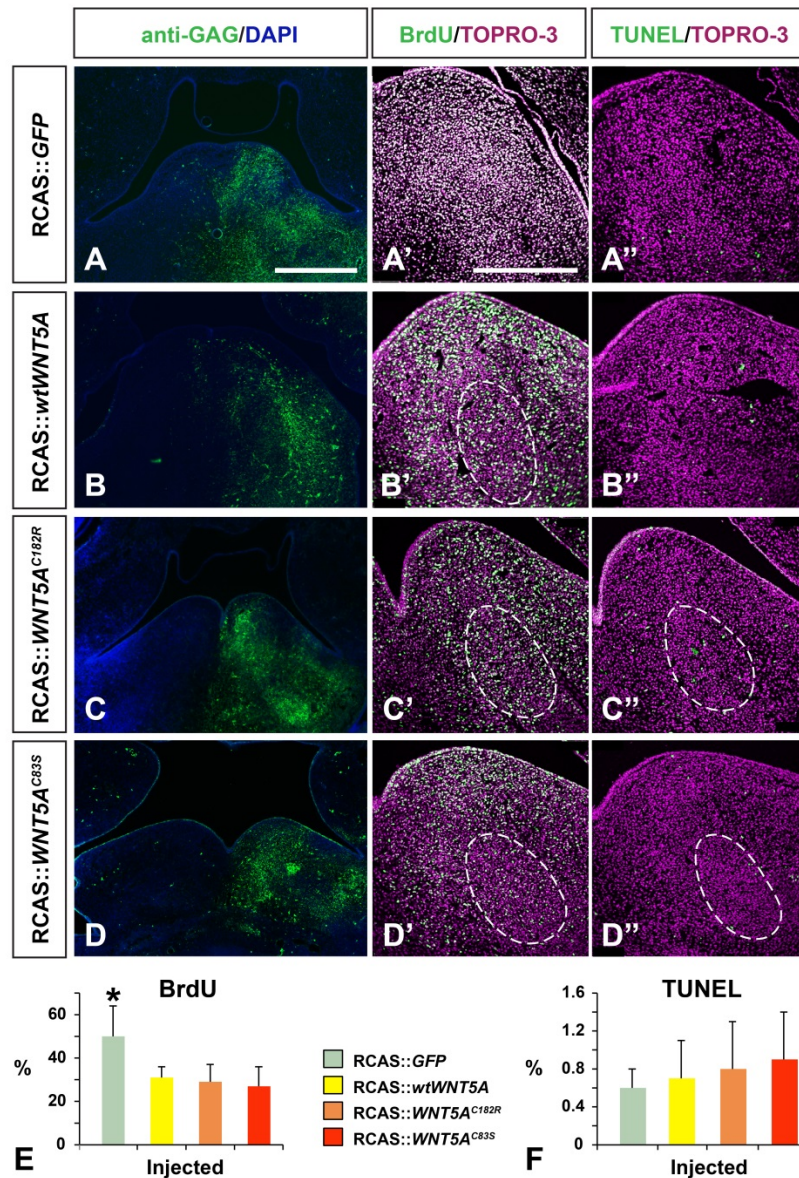


Figure 3.4 Effects of *WNT5A* and its mutations on cell proliferation and cell death.

A,B,C,D) Paraffin sections of injected embryos stained with antibody against viral GAG. Photographs have been taken on the green (Alexa 488 secondary antibody) and blue channels (Dapi). GAG expression is seen throughout right mandibular prominences. **A',B',C',D')** BrdU incorporation into mandibles injected with viruses. These are the adjacent sections from the same embryos as shown in left column. Fewer cells have uptake BrdU in the mandibles injected with RCAS::*wtWNT5A* (B'), RCAS::*WNT5A*^{C182R} (C') and RCAS::*WNT5A*^{C83S} (D'). **A'',B'',C'',D'')** TUNEL staining of the mandibles injected with RCAS::*GFP* (A''), RCAS::*wtWNT5A* (B''), RCAS::*WNT5A*^{C182R} (C'') and RCAS::*WNT5A*^{C83S} (D''). These are the near-adjacent sections from the same embryos as shown in left column. Dashed lines in B', C', C'', D' and D'' mark the edges of Meckel's cartilage. **E,F)** Graphs showing changes in BrdU and TUNEL staining. Bars are color-coded for each virus. **E)** There is a significant decrease in BrdU labeling in the embryos injected with RCAS::*wtWNT5A*, RCAS::*WNT5A*^{C182R} and RCAS::*WNT5A*^{C83S} compared to control RCAS::*GFP* ($p=0.04, 0.02, 0.03$, respectively). **F)** There are no significant changes in TUNEL staining between different viruses. Scale bar = 500 μ m for A-D, 300 μ m for A'-D''.

3.3.3 Oriented cell movement is impaired in the embryos injected with RCAS::WNT5A^{C83S}

Cell movements and rearrangements are crucial processes during facial development (McGonnell et al., 1998). It has previously been shown that Wnt5a regulates directional cell movements during limb and palate development in mouse (Gros et al., 2010; He et al., 2008) and in chicken embryos (Gao et al., 2011; Gros et al., 2010).

To investigate the effects of *WNT5A* or human *WNT5A* mutations on cell movements (Fig. 3.5), I injected the DiO-labeled DF1 cells (green) expressing human *wtWNT5A*, *WNT5A*^{C182S}, or *WNT5A*^{C83S} into the medial regions of the mandibular prominences at HH24. The mandibular host cells were labeled by DiI (red) injected at the lateral edge. The whole mandible was then cultured for 24 hours and pictures were taken 6 (Fig. 3.6A-D and Fig. 3.7A-D) and 24 hours (Fig. 3.6A'-D' and Fig. 3.7A'-D' and Table 3.5) post-injection. The cultures were then fixed, sectioned and stained with DAPI as the nuclear marker (Fig. 3.6A''-D'', A'''-D''' and Fig. 3.7A''-D''). The controls included mandibles injected with empty DF1 cells.

In the control cultures, the host cells had directional movement towards the midline and intercalated between medially-injected donor cells (Fig. 3.6A-A''' and Fig. 3.7A-A''). This medial movement is what normally happens during mandibular development (McGonnell et al., 1998). Movement of host cells toward *wtWNT5A*-expressing DF1 cells was similar to that of controls (n = 3/4; Fig. 3.6B-B''' and Fig. 3.7B-B''). Others showed that when cells expressing *wtWNT5A* virus were injected in chicken limb, the neighboring *GFP*-labeled cells were attracted and intermingled with donor cells (Gros et al., 2010). DF1 cells expressing *WNT5A*^{C182R} inhibited most cell movement since few host cells seem to move towards donor cells (Fig. 3.6C-C''' ; Fig. 3.7C-C'' ; arrowheads in C''). The results with *WNT5A*^{C83S} were much clearer. None of the DiI labeled cells overlapped the green donor cells (Fig. 3.6D-D''' and Fig. 3.7D-D''). It

seems that the original distance between donor and host cells does not affect the final result since even though in some cases such as Fig. 3.6D the green donor and the red host cells are closely injected at first place, no overlap is seen after 24h (Fig. 3.6D’).

Notably, it is hard to capture all injected donor and host cells in one 7 μ m section. The entire organ cultures were cut and all the sections were analyzed in order not to miss any sections with mixed DiO and DiI labeled cells. Sometimes few donor cells appeared to have moved laterally (Fig. 3.6C’’ and Fig. 3.7B’’). Taken together, the *wtWNT5A* does not interfere with normal cell movements whereas the *WNT5A* mutations particularly *WNT5A*^{C83S} disrupt the normal directional movement of cells towards midline.

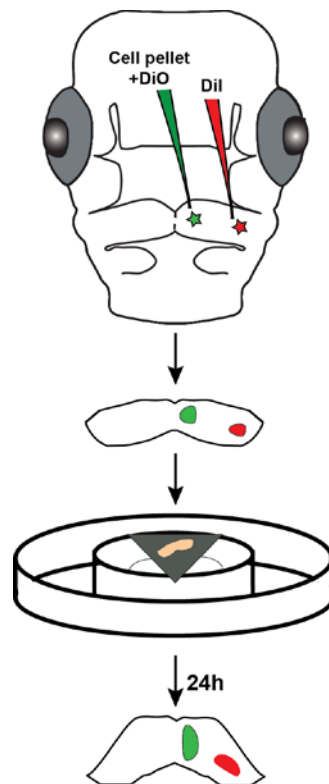


Figure 3.5 Procedures used for cell migration assay

Donor green cells were mixed with DiO (green) and injected into midline of mandibular mesenchyme of dissected heads. Host cells were labelled by DiI (red) injected to the lateral of mandibular prominences. Mandibles were then dissected and cultured for 24h on membranes in organ culture plates. Pictures were taken every 6 hours.

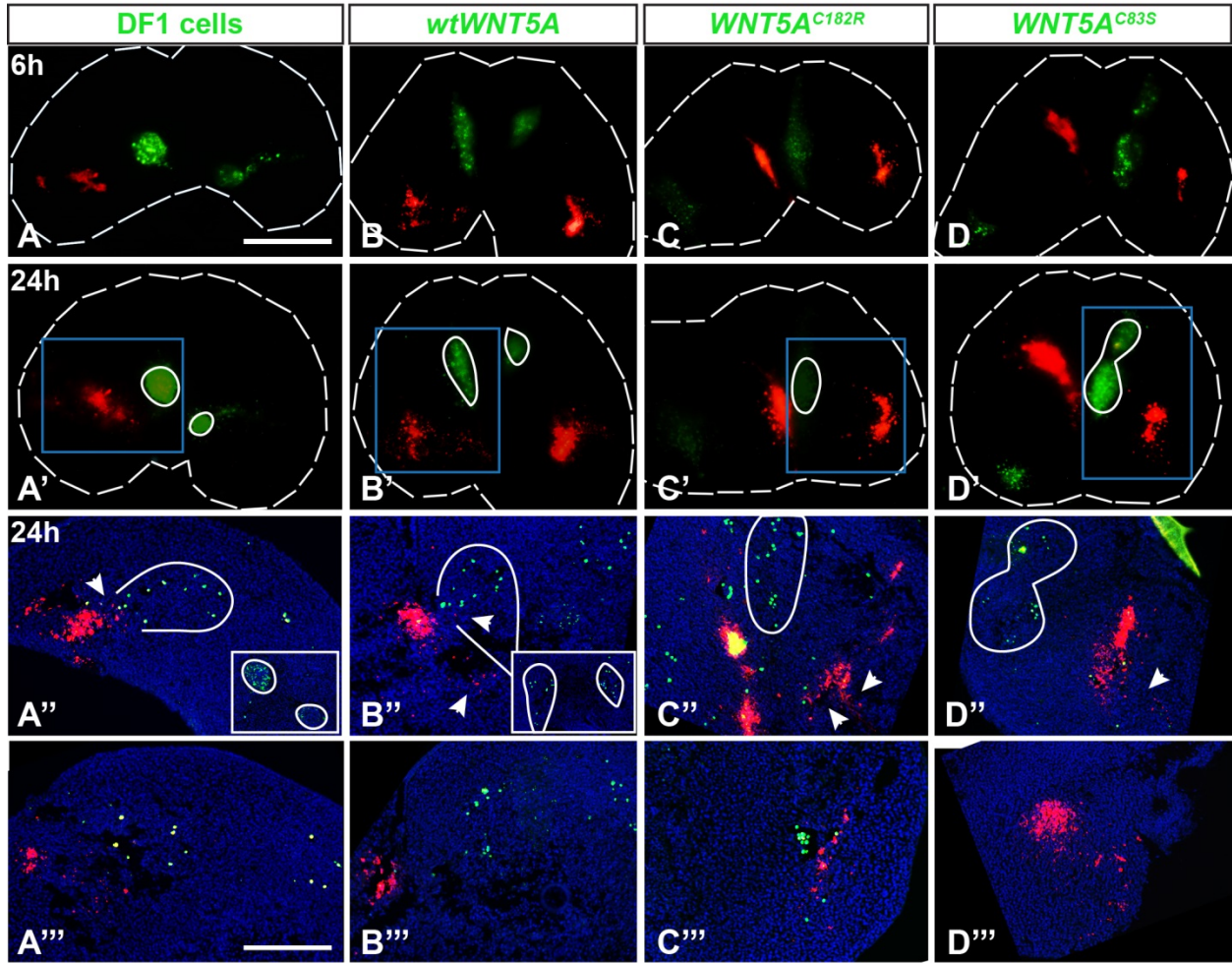


Figure 3.6 Cell movement studies in the embryos injected with RCAS::*GFP*, RCAS::*wtWNT5A*, RCAS::*WNT5A^{C182R}* and RCAS::*WNT5A^{C83S}*.

Mandibular organ cultures 6 and 24h post-injection. DiO-labeled donor cells (green) were injected medially. DiI (red) was injected laterally. **A-D**) Whole mount mandibular cultures 6h post-injection. **A'-D')** Whole mount mandibular cultures 24h post-injection. **A')** The control mandibles were injected with empty DF1 cells. The host cells had directional movement towards the green cells as the distance between red and green cells is less compared to **A**. **B')** The red host cells moved medially toward *wtWNT5A*-expressing DF1 cells as shown in the boxed area compared to **B**. **C')** Red cells spread out both medially towards green DF1 cells expressing *WNT5A^{C182R}* and laterally towards the edge when compared to **C**. **D')** Red host cells did not move towards green donor cells expressing *WNT5A^{C83S}*. **A''-D'')** The same mandibular cultures shown in **A'-D')** were fixed, sectioned and stained with DAPI as the nuclear marker. **A'')** DiI-labeled red cells overlapped DiO-labeled DF1 cells (arrowhead). **B'')** Red cells moved medially towards *wtWNT5A*-expressing DF1 cells (arrowheads). **C'')** Few red cells overlapped *WNT5A^{C182R}*-expressing DF1 cells (arrowheads). The yellow region is bleed through of DiO into red channel. **D'')** There is no overlap of green *WNT5A^{C83S}*-expressing DF1 cells and red DiI-labeled host cells (arrowhead). **A'''-D''')** Near-adjacent sections from the same whole mount cultures shown in **A'-D')**. Scale bar = 500 μ m for **A-D')**, 200 μ m for **A''-D''')**.

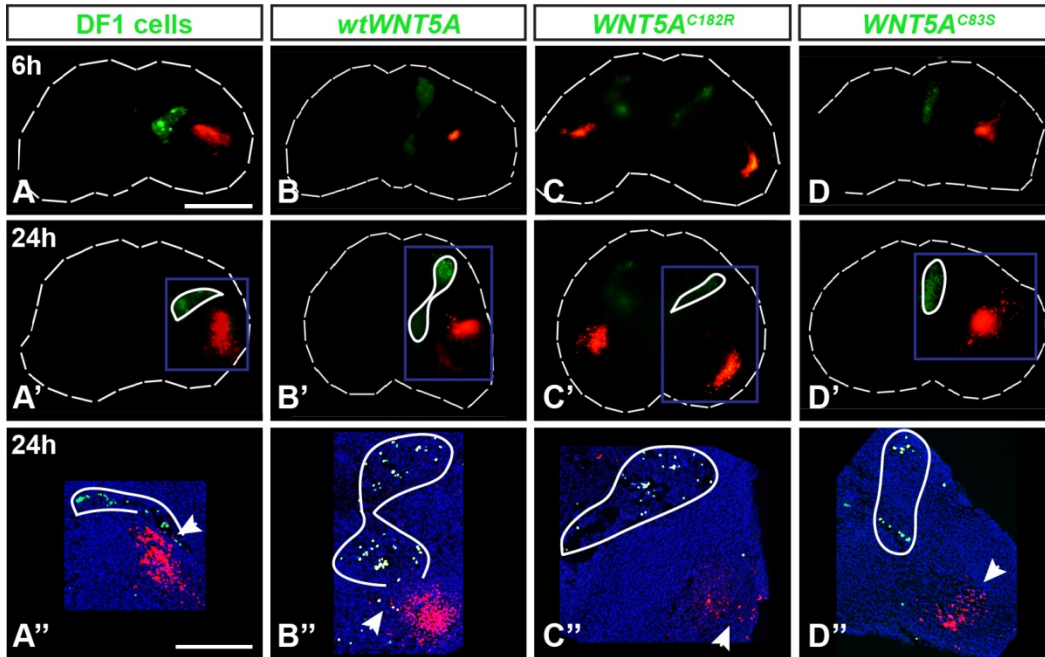


Figure 3.7 Cell movement studies in the embryos injected with RCAS::*GFP*, RCAS::*wtWNT5A*, RCAS::*WNT5A^{C182R}* and RCAS::*WNT5A^{C182R}*.

Mandibular organ cultures 6 and 24h post-injection. DiO-labeled donor cells (green) were injected medially. DiI (red) was injected laterally. **A-D**) Whole mount mandibular cultures 6h post-injection. **A'-D')** Whole mount mandibular cultures 24h post-injection. **A')** The control mandibles were injected with empty DF1 cells. The host cells had directional movement towards the green cells compared to **A**. **B')** The red host cells moved medially toward *wtWNT5A*-expressing DF1 cells as shown in the boxed area compared to **B**. **C')** Red cells did not move towards green DF1 cells expressing *WNT5A^{C182R}*. **D')** Red host cells did not move towards green donor cells expressing *WNT5A^{C83S}*. **A''-D'')** The same mandibular cultures shown in **A'-D')** were fixed, sectioned and stained with DAPI as the nuclear marker. **A'')** DiI-labeled red cells overlapped DiO-labeled DF1 cells (arrowhead). **B'')** Red cells moved medially towards and overlapped *wtWNT5A*-expressing DF1 cells (arrowhead). **C'')** There is no overlap of *WNT5A^{C182R}*-expressing DF1 cells and host cells (arrowhead). **D'')** There is no overlap of green *WNT5A^{C83S}*-expressing DF1 cells and red DiI-labeled host cells (arrowhead). Scale bar = 500 μ m for **A-D'**, 200 μ m for **A''-D''**.

Table 3.5 Biological replicates of cell tracking experiment.

Biological replicates and detailed analysis of mandibles injected with DiO-labeled empty DF1 cells or DF1 cells expressing *wtWNT5A*, *WNT5A^{C182R}* or *WNT5A^{C83S}*. Host cells were labeled with DiI. Mandibles were cultured for 24h, fixed, sectioned and photographed.

Type of donor cells	Phenotypes of DiI dispersion		
	Host cells expand towards donor cells	Host cells expand but not towards donor cells	Intercalation of DiI between donor cells
DF1 cells (n=3)	3	0	2
wtWNT5A (n=4)	3	1	2
WNT5A ^{C182R} (n=4)	2	2	0
WNT5A ^{C83S} (n=4)	0	4	0

3.3.4 Chondrocyte elongation and organization is lost in the embryos infected with RCAS::*wtWNT5A*, RCAS::*WNT5A^{C182R}* and RCAS::*WNT5A^{C83S}*

Since Meckel's cartilage directs the mediolateral and cranio-caudal growth of mandibular prominences (Bhaskar et al., 1953), I tested whether shortened lower beak in the embryos injected with mutated forms of *WNT5A* was due to disrupted PCP in Meckel's chondrocytes. It has previously been shown that PCP is required for an organized orientation of chondrocytes in the limb (Gao et al., 2011). In our control embryos injected with RCAS::*GFP* Meckel's chondrocytes were flattened and elongated along the mediolateral axis (Fig. 3.8A-B''). Such elongation and organization of chondrocytes was lost in the mandibles injected with RCAS::*wtWNT5A*, RCAS::*WNT5A^{C182R}* and RCAS::*WNT5A^{C83S}* (Fig. 3.8C-F'') and they showed a randomized organization (compare Fig. 3.8C'',D'',E'',F'' to the controls, A'' and B''). These chondrocytes had elongation defects and looked roundish (compare insets in Fig. 3.8C'',D'',E'',F'' to those in A'',B''). I measured the ferret diameters of each chondrocyte. I had 3 biological replicates per condition and did the measurements for at least 50 random chondrocytes per replicate. As shown in Figure 3.8G, the ferret diameter ratio was significantly

lower in the embryos injected with RCAS::*wtWNT5A*, RCAS::*WNT5A^{C182R}* and RCAS::*WNT5A^{C83S}* compared to controls (p=0.01 for all three viruses; Fig. 3.8G). Therefore, loss of proper intercalation, organization and elongation of chondrocytes within Meckel's cartilage potentially cause shortening of mandible.

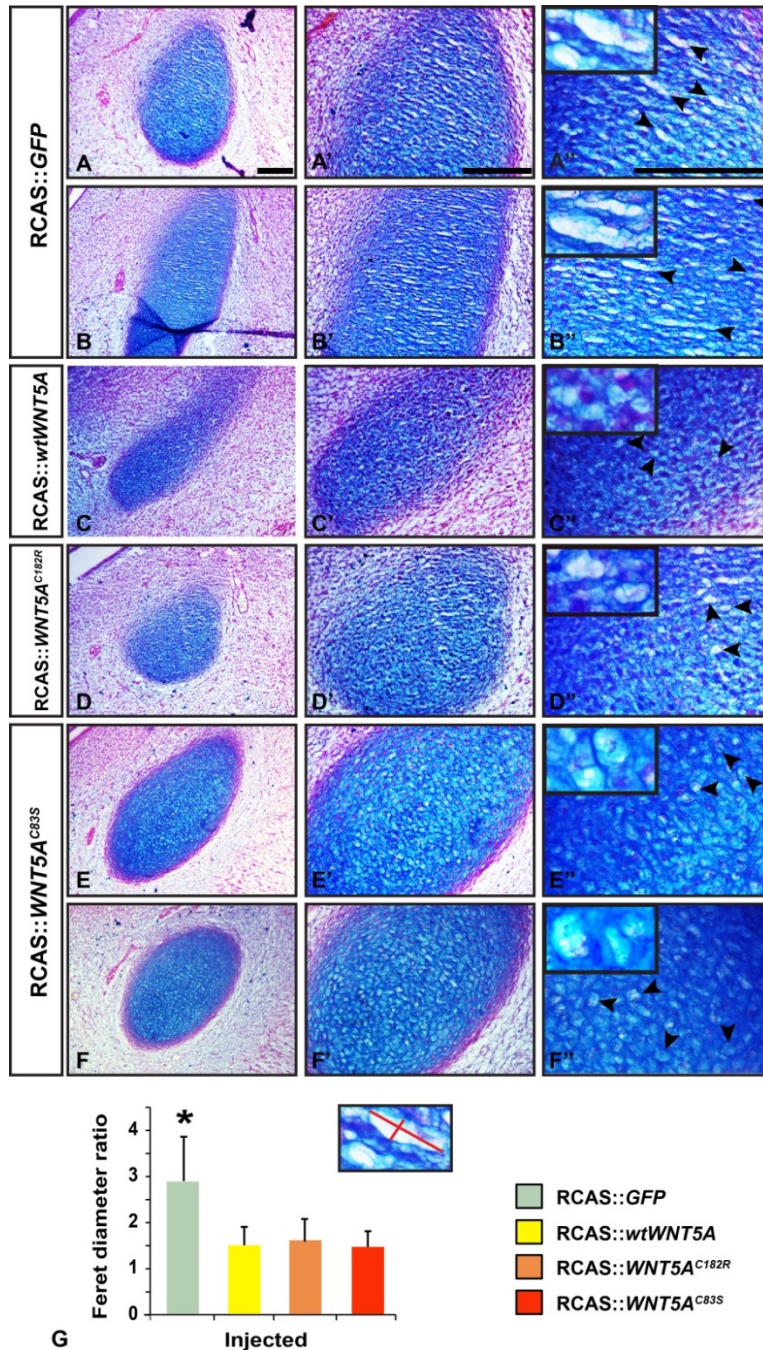


Figure 3.8 Chondrocyte intercalation and shape is affected in the embryos infected with RCAS::wtWNT5A, RCAS::WNT5A^{C182R} and RCAS::WNT5A^{C83S}.

A-F'') Mandibles injected with viral constructs were fixed at stage 29-30, sectioned frontally and stained with alcian blue. A-B'') Meckel's chondrocytes in control embryos injected with RCAS::GFP are flattened and very well organized (arrowheads). C-F'') Meckel's chondrocytes in the embryos injected with RCAS::wtWNT5A (C-C''), RCAS::WNT5A^{C182R} (D-D'') and RCAS::WNT5A^{C83S} (E-F'') are disorganized and roundish (arrowheads) compared to controls.. G) The graph compares average of ferret diameter ratio of Meckel's chondrocytes injected with different viruses. The bars are color coded. There is a significant reduction in ferret ratio in treated chondrocytes compared to controls. Red lines in the inset show an example of ferret diameter measurement. Scale bar = 100 μm for A-F'').

3.4 Discussion

In the case of gene mutations, the functional consequence of missense mutations is the most difficult to predict without experimental data. Here, we studied the effects of retrovirus containing human *wtWNT5A* or the *WNT5A* mutations on chicken mandibular morphogenesis. We used a combination of cellular experiments on proliferation and on cell migration as well as whole embryo morphogenesis. In all our experiments, we infected the whole mesenchyme but not the epithelium (as shown by 3C2 antibody staining). However, it is possible that there are indirect effects of *WNT5A* on the overlying epithelium which fed back on the mesenchyme to enhance the phenotype. We did not examine expression of epithelial target genes such as *FGF8* or *BMP4* in our study. It is possible that some aspects of the phenotype such as regulation of cell proliferation might have been attributed to altered epithelial signaling.

In all of our experiments, we expressed viral constructs in a background of normal gallus *WNT5A* expression. This is important for the interpretation of the *WNT5A* mutant data. Since the viral expression levels are much higher than those of the endogenous *WNT5A* the majority of receptors would therefore be occupied by the exogenous WNT. Some of our studies on other viruses have shown up to 60 fold higher expression of the exogenous viral RNA using qPCR. Although I have not measured levels of *hWNT5A* in my system, I did observe high levels of viral infection with the 3C2 antibody. Here we are learning the capabilities of *WNT5A* and mutant variations of the protein in a system where we push the signaling to a high level.

3.4.1 Human *wtWNT5A* and *WNT5A* mutations causing DRS negatively affect length of the limb which may result from a convergent extension defect

In our study, three main aspects of the skeletal phenotypes in the virus-infected limbs were assessed: 1) Regions of the limbs affected by the viruses; 2) Delayed ossification; 3) Widening of the skeletal elements.

In previous studies using *wtWNT5A* virus injection into chicken limb buds, the zeugopod was the most affected area of the limb followed by the stylopod (Hartmann and Tabin, 2000; Kawakami et al., 1999). Autopod defects were seen only when *WNT5A* was overexpressed in stage 21-23 limbs (Hartmann and Tabin, 2000). I noted that the C83S virus affects all three regions of the limb more frequently than the C182R mutation. In most embryos the *wtWNT5A* produced very mild phenotypes consisting of slight shortening of the stylopod. Therefore, there could be differences in the mechanism of action of increased *wtWNT5A* versus the mutant versions. Interestingly, my limb results are reminiscent of the human Robinow syndrome phenotypes. The most useful feature in sonographic prenatal diagnosis in human is shortening of the humerus and ulna/radius (Castro et al., 2013; Guven et al., 2006; Loverro et al., 1990; Percin et al., 2001).

I found a delay in ossification which was especially evident in the *WNT5A*^{C83S} mutated form of the virus. In the previous study on *WNT5A* effects on chicken, markers of chondrocyte hypertrophy were examined using radioactive in situ hybridization (Hartmann and Tabin, 2000) and they found that *COL10A1* and *PTHrPR* were reduced in *WNT5A* infected limbs. In my study, I allowed the embryos to develop to stage 37 and stained for bone and cartilage in wholemount. It was clear that there was delayed or absent bone formation in the treated limbs from the virus containing *WNT5A*^{C83S} (n = 9/9). Therefore the C83S mutant version of the virus

acts to inhibit bone formation whereas the wtWNT5A or the C182R do not affect differentiation as much.

The third main aspect of the skeletal phenotype in the limbs was the widening of humerus, radius and ulna, especially in embryos infected with RCAS::*WNT5A*^{C83S}. It is possible that all limbs infected with RCAS::*WNT5A*^{C83S} display some degree of skeletal widening which will need to be confirmed using morphometric analysis. The previous studies with g*WNT5A* commented briefly on the increased radial thickness of cartilage in infected limbs (Hartmann and Tabin, 2000). In my study both wt and mutated versions of *WNT5A* can give the same phenotype in the chicken limb. However, the C83S phenotypes are far more exaggerated compared to the wtWNT5A suggesting that the mechanisms may be distinct. The expanded cartilages in the C83S virus are suggestive of a convergent-extension defect that is due to differences in chondrocyte orientation or shape. The connection between *Wnt5a* and convergent extension has been studied in detail in the *Wnt5a* null mice. Gao et al. showed shorter and thicker humeri in *Wnt5a* null mice compared to controls (Gao et al., 2011). Interestingly, the expression of mutated versions of *ROR2* in chicken limbs also increases the thickness of cartilage elements (Stricker et al., 2006). However in this study the wild-type *ROR2* was not used due to the large size of the insert. It is therefore not possible to say whether there were differences between the mutant and wild-type versions of *ROR2*. Expressing mutated WNT5A ligand or mutated receptors may impair signal transduction leading to defects in convergent extension of limb cartilages.

3.4.2 Chondrocyte shape and organization in the mandible is affected by *WNT5A* imbalance

To the best of our knowledge, there is no information on chondrocyte shape in Meckel's cartilage in response to either gain or loss of *Wnt5a* function (Yamaguchi et al., 1999; Yang et al., 2003). We observed more rounded chondrocytes in Meckel's of injected mandibles with

RCAS::*wtWNT5A*, RCAS::*WNT5A^{C182R}* and RCAS::*WNT5A^{C83S}*. Chondrocyte shape in Meckel's cartilage is important for elongation of the cartilage as shown in the zebrafish mutant *knypek* (homolog of *Glypican* in mammals). *Knypek* plays an extracellular role in PCP signaling and other pathways, and in mutant fish, there was loss of elongation and intercalation in Meckel's chondrocytes (Topczewski et al., 2001).

During normal chondrogenesis in the limb, cells are oriented proximo-distally with the leading edge of the chondrocytes pointing distally as determined by Vangl2 antibody staining (Gao et al., 2011). In *Wnt5a* mutants, the chondrocytes of the growth plate were randomly oriented with Vangl2 antibody staining not localized to one end of the cell (Gao et al., 2011). Furthermore, in the same study when RCAS::*wtWNT5A* cells were injected into chicken limb, the cartilage condensations adjacent to the viral cell pellet had randomly oriented chondrocytes (Gao et al., 2011). This chicken limb result is directly relevant to our study and can explain the shorter, wider limb cartilages. It is interesting that both loss and gain of function induced randomized orientation in limb chondrocytes (Gao et al., 2011).

3.4.3 The role of WNT5A signaling is to regulate cell proliferation

Meckel's cartilage was shorter in our study showing that jaw shortening could be due to the cartilage not growing lengthwise. The main mechanism for reduction jaw length is the lack of outgrowth at an earlier stage in development. We showed that overexpression of *wt* and *WNT5A* mutations decrease cell proliferation. Interestingly, there were no increases in cell apoptosis supporting the idea that the viruses were not generally toxic to the embryo. There were no significant differences in the level of proliferation amongst the *wtWNT5A* and the two mutant forms. This result does not allow us to distinguish whether the viruses have caused a gain- or loss-of-function of WNT5A signaling. Insights into the role of *Wnt5a* in regulating cell

proliferation can be obtained from the work on mouse loss and gain-of-function mutants in the limb. Transgenic mice expressing *Wnt5a* in cartilage have reduced chondrocyte proliferation (Yang et al., 2003).

Curiously, the loss of *Wnt5a* function also led to decreased cell proliferation in the organs with distal outgrowth such as limbs and tail (Yamaguchi et al., 1999). Even more surprising is the data from the palate of the same strain of *Wnt5a* null mice. Here the authors measured an increase in cell proliferation in the anterior region whereas there was a reduced proliferation in the posterior (He et al., 2008). It is easy to reconcile the posterior decrease in proliferation in the absence of *Wnt5a* based on *Wnt5a* null mice data. It is however difficult to model how anterior proliferation would be increased in the *Wnt5a* mutants since this is where the gene is abundantly expressed. The authors have discussed multiple signaling pathways being involved in this effect of *Wnt5a* in anterior region. From the *Wnt5a*^{-/-} mice we know that *Wnt5a* is required to maintain cell proliferation. Also at high levels (as in our study) *WNT5A* does not act as a mitogen; instead cell proliferation is actively inhibited possibly by antagonizing the canonical pathway or some other signaling pathway such as FGF. The mutations in *WNT5A* that we studied here do not alter the ability of *WNT5A* to inhibit cell proliferation.

3.4.4 *WNT5A* mutations disrupt normal oriented cell movements in mandible

The general principles of cell movements and their role during morphogenesis can be derived from a detailed 3D study in the normal mouse limb. Time-lapse imaging showed that limb proximo-distal elongation is achieved by directional cell activities such as oriented cell division and migration rather than spatially-controlled cell proliferation (Boehm et al., 2010). Others showed that limb mesenchymal cells undergo oriented cell division and migration towards the AER (Gros et al., 2010; Li and Muneoka, 1999).

The roles of Wnt5a in oriented cell movements have also been investigated in limb (Gao et al., 2011; Gros et al., 2010). Limb bud cells did not follow the normal oriented cell migration in *Wnt5a* null mice (Gros et al., 2010). Some work on WNT5A effects on mesenchymal cell behaviour was also carried out in the chicken limb bud. To label the mesenchyme, a *GFP* plasmid was electroporated into the limb field at a nearly stage. Then an ectopic injection of WNT5A-expressing cells to the limb was performed. The *wtWNT5A* led to reorientation and intercalation of *GFP*-labelled cells between WNT5A-expressing cells (Gros et al., 2010). These studies imply that WNT5A is required and sufficient to direct oriented cell activities in the limb. We hypothesize that mandibular phenotype of WNT5A mutations can be partially explained by aberrant cell movement in mandible. During mandibular development the lateral cells normally move medially (McGonnell et al., 1998). Hypothetically, these oriented cell movements lead to mandibular shape changes i.e. forming a triangular narrow mandible or a pointed beak. We observed unchanged normal cell movements and intermingling in the mandibles injected with *wtWNT5A*-expressing cells. These cell activities were not seen following injection of WNT5A^{C83S}-expressing cells in any of the samples.

There are three alternative explanations for the mixing of WNT viral-expressing cells with the DiI cells that need to be considered: 1) Donor green cells actively migrated from medial to lateral; 2) green donor cells spread out due to pressure from the needle injection i.e. this was their original position and some happened to be close to the red host cells or 3) Red host cells moved medially towards green donor cells. The first explanatory mechanism, the medial to lateral cell movement idea, is contrary to in vivo fate-maps of mandibular mesenchyme published by others (McGonnell et al., 1998). The second explanation is less possible. Comparing the whole mount 6h and 24h cultured mandibles one can see that the green donor

cells are clustered at the original injection site. Therefore, the best explanatory mechanism is the third one, where medially directed movement of red host cells results in mixing with donor green cells. This pattern concurs with the fate maps showing medial expansion of laterally labeled mandibular mesenchyme (McGonnell et al., 1998).

This is of great importance to note that patterns of expansion are a combination of proliferation and movement. Others tracked the facial cells for 48h which is up to 6 rounds of cell division in chicken (Lee et al., 2004; McGonnell et al., 1998). After 48 hours of growth the majority of the expansion could be due to cell proliferation. I tracked the cells for 24h similar to other studies in mouse palate using dye injection (He et al., 2008). In addition I showed that wt*WNT5A* and the mutant viruses inhibited rather than promoted cell proliferation in mandibular mesenchyme. Thus it is likely that movement of host mesenchymal cells during the experimental period was due to migration rather than proliferation. The number of host cells migrated and the extent of migration may also depend on the amount of donor cells injected initially. This is a limitation and may be a good reason for why there were variations in the migration pattern between replicates. Discrepancies seen in cell migration pattern with *WNT5A*^{C182R}-expressing cells fits with the more frequent normal phenotypes observed with this virus injection. It is possible that the C83S mutation blocks cell movement but in order to prove this we would need to use live cell imaging. Taken together, changes in directional cell movements caused by *WNT5A* mutations and in particular the C83S mutation are contributing to the skeletal phenotypes.

3.4.5 The point mutations in *WNT5A* may act in a dominant-negative manner to reduce signaling

Does our study help us to determine whether human *WNT5A* mutations work as loss or gain of function mutations? In table 3.6 we provide some arguments to answer this question based on our current findings.

Table 3.6 Arguments discussing whether *WNT5A* mutations work as loss or gain of function.

Arguments for a loss-of-function caused by the point mutations
<ol style="list-style-type: none"> 1. More severe and frequent limb and beak phenotypes were seen in mutated versions of <i>WNT5A</i> in particular with C83S compared to wt<i>WNT5A</i>. 2. Inhibition of cell migration with C83S virus, to a lesser extent for C182R and no effect on migration caused by wt<i>WNT5A</i>. 3. Mouse <i>Wnt5a</i>^{-/-} limb phenotypes include increased width of cartilage elements similar to the limbs infected with mutated forms of <i>WNT5A</i> particularly with C83S.
Arguments for gain-of-function caused by the point mutations
<ol style="list-style-type: none"> 1. Proliferation effects are identical for over expression of wt <i>WNT5A</i> (gain-of-function) and the mutants. 2. Jaw and limb shortening is similar in wt and mutant viruses as well as <i>Wnt5a</i> transgene mice. 3. Chondrocyte shape in Meckel's is the same for all three viruses.
Arguments for C83S being a dominant-negative mutation
<ol style="list-style-type: none"> 1. More severe and more frequent limb phenotypes. 2. Cell migration is blocked more completely with this mutation as compared to C182R. 3. Disruption of cell migration is not seen in gain-of-function experiments.

We observed a similar shortening of the limbs and jaws following increased expression of the three *WNT* constructs as compared to the mouse with a complete loss-of-function of *Wnt5a* (Yamaguchi et al., 1999; Yang et al., 2003). These parallel phenotypes in the chicken and mouse loss-of-function would suggest that our chicken model has produced a loss-of-function. However, in that case we would expect to see distinct phenotypes in the wt*WNT5A* versus the mutated versions. One difference was that we observed thicker skeletal elements in a subset of

embryos injected with *WNT5A* mutations and not as much with *wtWNT5A*. The other difference was that *wtWNT5A* retrovirus caused less frequent mandibular deviations and did not appear to interfere with cell migration. The *wtWNT5A* and mutant viruses shared decreased proliferation and failure of intercalation of chondrocytes.

Other model organisms have been used to investigate the functional effects of C182R and C83S. Here the authors (Person et al., 2010) misexpressed mutant or *wtWnt5a* RNA in zebrafish or frog embryos. There was a failure of islet cells to organize in zebrafish and failure to inhibit activin-induced elongation of *Xenopus* animal caps. These studies imply that there is a loss-of-function. However, both are rather tangential and do not directly test the function of the protein in such processes as convergent extension or gastrulation. In the mouse model, biochemical studies have been carried out with the equivalent human *WNT5A* mutations put into the mouse *Wnt5a* gene (Gao et al., 2011). These mutant plasmids were unable to phosphorylate Vangl2 to the same extent as *wtWnt5a*. Lower phosphorylation of Vangl2 could interfere with signal transduction by Wnt5a and therefore lead to a loss-of-function. Moreover, cell migration assessment in our study indicated that *WNT5A* mutations disturbed normal oriented cell movements in mandible. More in depth analysis using cell orientation markers such as Vangl2 as well as measuring cell migration speed in time-lapse video microscopy might reveal additional differences between the wt and mutant versions of *WNT5A* in the chicken embryo.

It is possible that even though *wtWNT5A* has similar effects in many assays to those of the mutant forms, the mechanisms are different. For example, the high levels of *wtWNT5A* might antagonize the canonical pathway via ROR2 (Mikels et al., 2009) which could reduce proliferation. We have shown this antagonism to be operating in micromass cultures treated with Wnt5a-conditioned media (Hosseini-Farahabadi et al., 2013). Another possibility is that

wtWNT5A upregulates an antagonist of the pathway such as sFRP2 (Lescher et al., 1998). For now, we do not have an explanation for why the *wt* virus acts in a similar manner to the mutant versions however a similar result was obtained in the mouse where overexpression of *Wnt5a* in cartilage caused limb and jaw shortening (Yang et al., 2003). Moreover, the orientation of limb chondrocytes was randomized by either a loss of function or gain of function in *Wnt5a* (Gao et al., 2011). The congruence of mouse and chicken data suggest that levels of *Wnt5a* must be maintained within a narrow range in order to promote normal development.

Taken together, our results showed that human *WNT5A* mutations that cause Robinow syndrome in human, lead to shortening of mandible in chicken which is resulted by a collection of decreased cell proliferation, loss of directional mesenchymal cell movements and impaired chondrocyte intercalation (Fig. 3.9). Our findings when supplemented with more detailed studies in mouse can shed light on the cellular and molecular basis for Robinow syndrome. The *Wnt5a* mouse studies did not look at the jaw phenotype in as much detail as the limb. In particular, facial assessments of the crosses of *Vangl2* and *Wnt5a* mice need to be done.

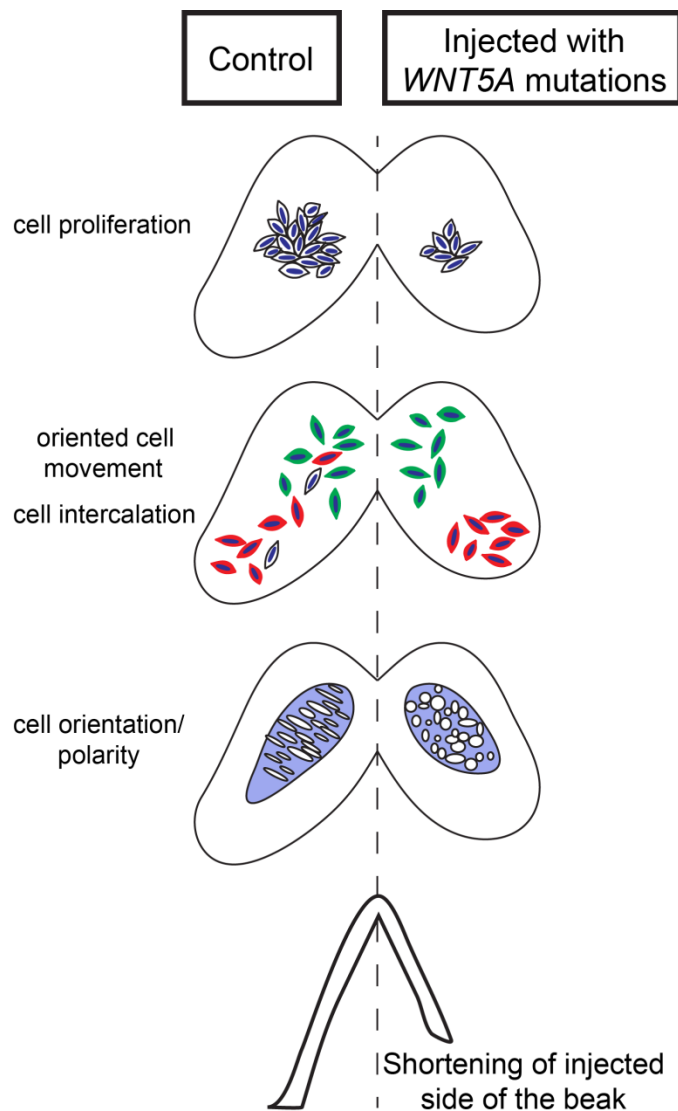


Figure 3.9 Summary of effects of *WNT5A* mutations on mandibular morphogenesis.

Left side shows processes during normal mandibular morphogenesis including cell proliferation, directional cell movements and cell intercalation/polarity. These processes are disturbed by *WNT5A* mutations leading to short mandible. Chondrocyte stacking may be affected leading to shortening of Meckel's cartilage.

4. Discussion

In the development arena, knowledge of a signaling pathway could be helpful in efficient analysis of defects, diagnosis of diseases and perhaps therapy. Little is known about the functions of the non-canonical WNT signaling especially in the face. WNT5A is a non-canonical WNT with proven roles during development. In this dissertation, I advanced understanding of WNT5A functions during cartilage development and the morphological defects caused by human *WNT5A* mutations in vitro and in vivo using chicken-based models.

4.1 Concluding remarks

4.1.1 In vivo versus in vitro differences in the phenotypes caused by WNT5A suggest context dependent signaling is taking place

There are quite a few differences in the results obtained in vivo as compared to in vitro. In vivo, the entire mandible was shortened and there was a general inhibition of bone and cartilage development. This was due to a significant decrease in proliferation. However in vitro, there was no difference in proliferation observed. In vivo we saw no evidence for cartilage resorption after it was formed, whereas in vitro the main effect of Wnt5a-CM was to cause enzymatic cartilage resorption. It is difficult to reconcile the differences in cellular responses but we can provide two possible explanations. One is that there is a stage difference between the time of treatment in the two systems and the other is that the tissue context is preserved with the in vivo experiments whereas in vitro, cells are removed from their normal context. The early onset of the virus is prior to cell commitment to a chondrogenic lineage and affects all cells in the mandible. In the in vitro culture system, cells are more mature and already programmed to become cartilage by the time they are placed into culture. Another difference between the in vivo and in vitro systems is that with the in vivo injections the epithelium is present but in micromass

cultures epithelium is removed. We cannot rule out that the viral effects are mediated by the epithelium in an indirect manner. Another difference in the context of in vivo versus in vitro experiments is that in tissue inhibitors of MMPs may be present in vivo that protect the cartilage from resorption.

4.1.2 Spatially and temporally-controlled WNT antagonists may participate in mandibular patterning and cartilage differentiation

WNT5A is abundantly expressed in early mesenchyme of face and limb (Dealy et al., 1993; Gavin et al., 1990; Geetha-Loganathan et al., 2009; Kawakami et al., 1999). One of the most exciting findings of our study was the observation that *WNT5A* has a highly dynamic expression during mandibular cartilage outgrowth, differentiation and maturation. *WNT5A* expression is spatially and temporally controlled to enable formation of a functional lower jaw in human and lower beak in chicken. It is also of interest how little variations in *Wnt5a* signaling can disturb normal mandibular development. These all make *wnt5a* as an intriguing hot topic to study.

In the 2nd chapter, we showed the importance of *Wnt5a* in mandibular cartilage development. When cartilage begins to differentiate, abundant *WNT5A* within Meckel's regulates cartilage initiation and differentiation indirectly by repressing canonical WNT signaling. Later on, in mature differentiated Meckel's, cartilage completely lacks *WNT5A* expression preserving cartilage matrix. This restricted expression of *WNT5A* within cartilage may be regulated by WNT antagonists. For example in the mouse limb expression domains of *Wnt5a* and Wnt antagonist, *Frzb*, overlap in distal mesenchyme during pre-differentiation stages; however, at differentiation stages *Wnt5a* is restricted to the perichondrium (Gavin et al., 1990) whereas *Frzb* is excluded from the perichondrium and the expression overlaps with *Col2* expression domains in differentiating humerus (Hoang et al., 1998). In chicken mandible *WNT5A* and *FRZB* have

complementary expression patterns at pre-differentiation stages of cartilage development (Ladher et al., 2000). There is however no study describing the detailed expression of *FRZB* in differentiated Meckel's cartilage but we speculate that *FRZB* pattern of expression helps maintain the described spatially/temporally-controlled expression of *WNT5A* within the mandible. There are other WNT antagonists (mentioned in section 1.4.5.3) which may also define boundaries for *WNT5A* expression. The complementary pattern of expression of *WNT5A* and antagonist(s) may help in the formation of a WNT gradient required for proper morphogenesis of an organ such as the mandible. During early mandibular development, *WNT5A* is strongly expressed in the midline where there is the highest outgrowth of the developing beak. This may indicate importance of *WNT5A* in cell proliferation and directionality of lower beak in that region. We showed changes in cell proliferation and oriented cell activities by perturbing *WNT5A* signaling. Our findings from chapters 2 and 3 suggest the roles of *WNT5A* in cartilage development as to be the maintenance of mature cartilage matrix and regulation of chondrocyte intercalation.

4.1.3 PCP signaling pathway regulated by *WNT5A* mediates cartilage development and mandibular morphogenesis

Using an in vitro culture system in chapter 2 we showed that *WNT5A* regulates cartilage development by both repression of canonical signaling and activation of JNK pathway using luciferase assays and phenotype assessments. In chapter 3, we showed that the *WNT5A* mutations cause phenotypes similar to those of perturbed PCP pathway. We did not however look for any molecular changes in PCP signaling. Based on our data from chapter 2, *WNT5A* could both antagonise canonical signaling and activate PCP/JNK pathways in the mandible. The effect on Meckel's cartilage initiation and differentiation is mediated through inhibitory actions of *WNT5A* on canonical signaling whereas the effect on mature cartilage matrix is through

activation of JNK pathway. The question here is which mechanism was affected by *WNT5A* mutations leading to mandibular phenotypes, repression of canonical or activation of non-canonical signaling? Based on our comprehensive discussion in chapter 3 section 3.4.5, *WNT5A* mutations are loss-of-function mutations. Therefore, if inhibitory effects of canonical signaling were responsible for the observed phenotypes, then by removing these effects by *WNT5A* mutations one would expect to see canonical WNT activation and changes in cell fate. We observed delayed or absent ossification in both mandible and limb which cannot be explained by loss of PCP. Interestingly, when canonical pathway components are mutated, phenotypes similar to loss of PCP signaling were observed. For example, null *Tcf;Lef* mice have hypertelorism and open eyelids (Brugmann et al., 2007), symptoms of loss of PCP. Furthermore, *Lrp6* knock-out mice show cleft palate (Pinson et al., 2000; Zhou et al., 2010), another defect caused by defective PCP. These all show strong links between canonical and non-canonical pathways. Collectively, this suggests that *WNT5A* impacts both repression of canonical signaling and activation of PCP/JNK functions in our system and that these combinatory effects were disrupted by exogenous human *WNT5A* mutations.

4.1.4 MMPs and cell migration: a mechanism at play?

In the 2nd chapter we showed induction of *MMP1*, *MMP13* and *ADAMTS5* genes by Wnt5a. Several studies have shown important roles of MMPs during cell migration and mostly in tumorigenesis. MMPs provide changes in the cell microenvironment required for cell migration (Kessenbrock et al., 2010; Nabeshima et al., 2002). *MMP1*, *MMP13* and *ADAMTS5* are involved in cell invasion and metastasis (Held-Feindt et al., 2006; Kessenbrock et al., 2010; Liu et al., 2012; Nabeshima et al., 2002; Wang et al., 2013a). It is possible the induction of MMPs by Wnt5a-CM in mandibular cultures in chapter 2 may have also occurred in the viral-infected

tissues in chapter 3. In this case we would have predicted that at least the wt*WNT5A* virus would have increased cell migration, perhaps even having chemoattractive effects on host mesenchyme cells. Such behavior was reported in response to chicken fibroblasts expressing RCAS::g*WNT5A* implanted into the limb bud (Gros et al., 2010). The lack of measureable change in cell migration may be a result of inadequate imaging techniques. It is also possible that the induced levels of *MMPs* may not have reached high enough levels to increase cell movements. In the case of the mutant forms of *WNT5A*, the presence of the abnormally functioning *WNT5A* inhibited rather than promoted the migration of cells in the mandible. Perhaps these mutant *WNTs* decreased the amount of *MMPs* in the tissue thereby making the matrix less conducive to cell migration.

4.1.5 Face and limb with unique embryonic origins and functions share developmental mechanisms

As mentioned earlier, we focused our studies on neural crest-derived mesenchyme of mandible. This is different from mesodermally-derived limbs which have been the focus of many studies. Throughout our study, we kept comparing and validating our face data with that of limbs. We found that the general mechanisms involved in face and limb development are similar except for little differences. For example, the level of *MMP13* expression increased steadily over time in the face but not in the limb. The other difference was that endochondral bones of the limb were more sensitive to *WNT5A* mutations than the intramembranous bones of the lower jaw.

Looking back to our hypotheses, the first hypothesis was accepted that *WNT5A* is sufficient to regulate Meckel's cartilage initiation and differentiation in vivo and in vitro. We showed that highly expressed *WNT5A* in Meckel's cartilage promotes cartilage initiation and differentiation by suppressing canonical *Wnts* but later on in mature differentiated cartilage, *WNT5A* signal is downregulated in order for cartilage matrix to be maintained. We also accept 2nd hypothesis that mesenchymal *WNT5A* functions via non-canonical *WNT* pathway using

ATF2 luciferase assay; however, in our in vitro system WNT5A did not affect cartilage differentiation; instead, we showed that WNT5A is important for the maintenance of fully-differentiated mature cartilage matrix. We accept the 3rd hypothesis that we could create phenotypes reminiscent of Robinow syndrome by expressing human *WNT5A* mutations in developing chicken; however, the wt*WNT5A* virus also produced similar phenotypes. We partially accept hypothesis 4 in terms of *WNT5A* mutations affecting cell activities. We accept the hypothesis in terms of the mutant forms of the protein inhibiting cell migration in the cell tracking assay. We reject the hypothesis in relation to cell proliferation and chondrocyte shape since the mutant and wt*WNT5A* had similar effects. Figure 4.1 summarizes my findings and proposes a model whereby changes in WNT5A signaling can cause defective development.

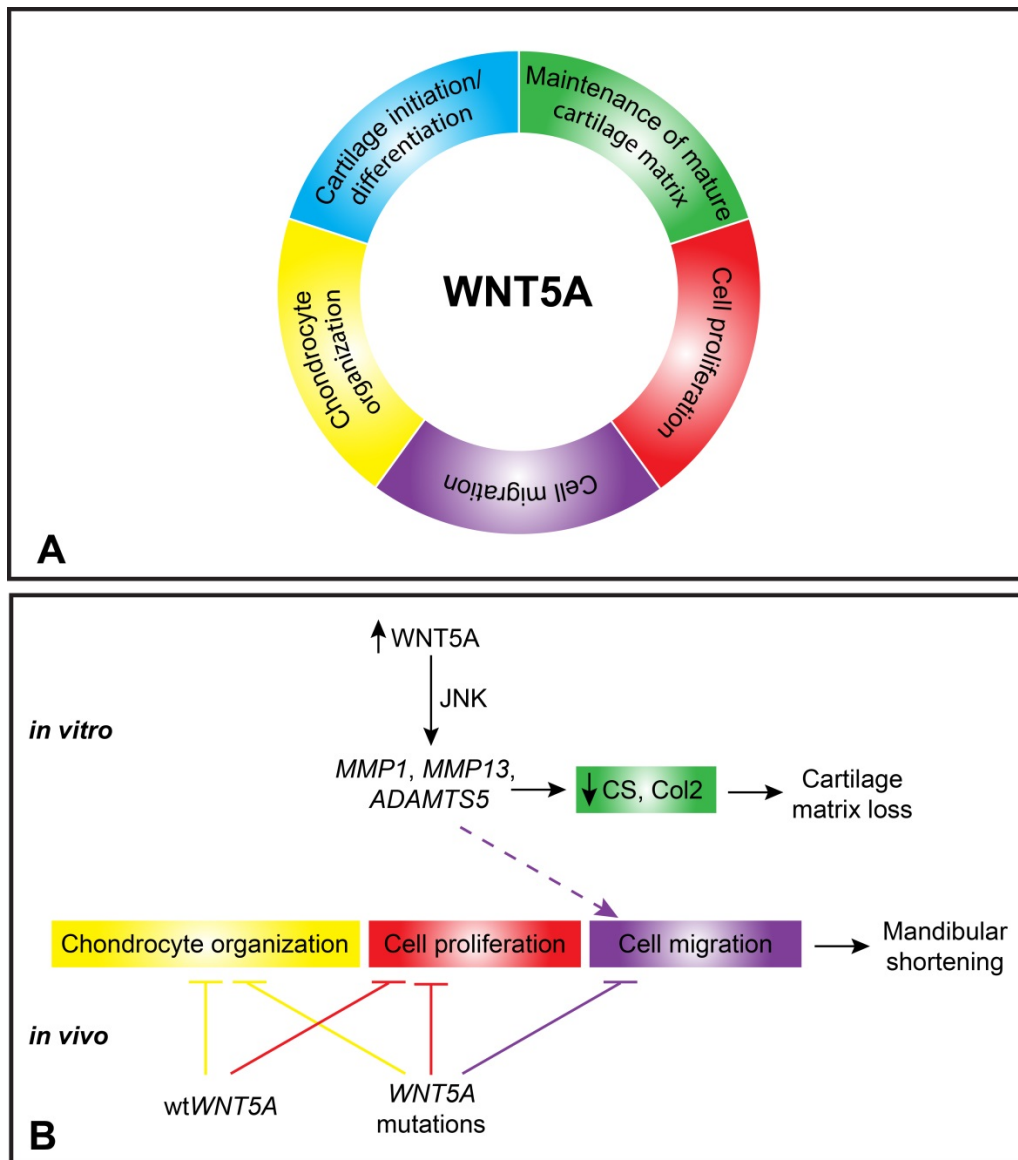


Figure 4.1 Summary of WNT5A functions during facial normal and defective development.

A) During normal development, WNT5A has regulatory effects on cartilage initiation/differentiation, maintenance of mature cartilage matrix, cell proliferation, cell migration and chondrocyte organization. **B)** Using in vitro culture system we showed that during abnormal conditions, high levels of WNT5A by induction of MMPs cause cartilage matrix loss seen in diseases such as osteoarthritis. Using in vivo system we also showed that *WNT5A* mutations decrease cell proliferation and inhibit normal cell activities including chondrocyte organization and cell migration. These all lead to mandibular shortening seen in diseases such as Robinow syndrome. Human *wtWNT5A* also inhibits chondrocyte intercalation and cell proliferation but not cell migration. Dashed arrow shows others finding that MMPs increase cell migration (Kessenbrock et al., 2010).

4.2 Overall significance

The non-canonical WNT pathway is at the root of many embryonic defects such as the ones affecting axis elongation and neural tube closure; however the role of this pathway in craniofacial development has not been explored. Through the approaches outlined in this dissertation we elucidated the functions of non-canonical WNT5A in facial development so that we can better understand the causes of abnormalities such as micrognathia and osteoarthritis. Our findings define importance of WNT5A in facial development. Understanding the pathways mediating WNT functions (canonical vs. non-canonical) can be used to better target therapies for a variety of WNT-related diseases including cancer.

4.3 Future directions

The other non-canonical pathway, calcium pathway, may also be a mechanism involved in our system. To elucidate the role of this signaling in mandibular development, we had few options. We could use an antagonist of calcium pathway such as CAMKII antagonist, KN93, or dominant negative CAMKII (Ishitani et al., 2003). If the phenotype was mediated by calcium pathway then we would expect to rescue phenotypes by using these inhibitors. Micromass culture would definitely be a perfect system to try these experiments. To directly show involvement of calcium pathway we could also use an NFAT luciferase reporter to measure the activity of this pathway in our system (Bradley and Drissi, 2010). Nuclear factor of activated T-cells (NFAT) is a family of transcription factors activated by calcium signaling (Crabtree and Olson, 2002). We did not study calcium pathway but we think it is worthwhile studying this pathway during facial development. This can help better understand the mechanisms of WNT5A function in facial mesenchyme and can be a good option for rescue experiments and maybe for therapeutic purposes if the involvement is proven.

I can infect mandibles with wt*WNT5A* or the mutant viruses in vivo and make cultures of the mesenchyme. This may show up differences in chondrogenesis between mutants and wt*WNT5A*. We could also expand this work and study the effects of the mutations of *WNT5A* on phosphorylation of JNK using western blots or with luciferase assays using ATF2, the JNK pathway reporter (as we have used before in chapter 2).

There is also need for more quantitative approaches to examine cell behavior in the presence of wt and mutated forms of *WNT5A* protein. The static images presented here, although intriguing were only showing part of the picture. I would like to measure the differential effects of *WNT5A* mutations on oriented cell division, cell velocity and directed cell movement since the loss of *Wnt5a* has been shown to affect these processes in the limb (Gros et al., 2010). Finally, I would like to compare my data to cells in which *WNT5A* has been knocked down with either siRNA or morpholinos. The similarities and differences would help to strengthen my preliminary conclusion that the *WNT5A* mutations are causing a loss of function by interfering with the wt*WNT5A*.

Other degrading enzymes with proven roles in collagen catabolism are cathepsins with cathepsins K, S and L being able to cleave collagen II and aggrecan (Bromme and Wilson, 2011). Therefore, it is worthwhile to investigate the involvement of these enzymes in mediating *Wnt5a* cartilage phenotype in micromass cultures. We can examine this possibility by using anti-cathepsin antibodies or quantitative PCR.

Finally, I did not look at downstream mediators of *WNT5A* signaling. This can be done with candidate gene and/or transcriptome profiling approaches. Examples of candidate genes with roles during mandibular development are *DLX5* (Distal-less homeobox), *OTX2* (Orthodenticle homeobox) and *PITX1* (Pituitary homeobox). Mouse mutants of these

transcription factors show lower jaw shortening (Depew et al., 1999; Lanctot et al., 1999; Matsuo et al., 1995; Mina, 2001). Micromass cultures treated with Wnt5a-conditioned media would be an ideal system to profile the expression of these genes. I can also use in vivo injection of constructs containing *GFP*, wt*WNT5A* and mutated forms of *WNT5A* and then profile gene expression in order to identify the genes mediating WNT5A effects on cell behavior. We can also assay expression of many genes including other transcription factors, PCP pathway components and secreted proteins by microarray analysis or RNAseq. These expression profiling experiments would go a long way to understanding the cross talk with other pathways.

Bibliography

Abzhanov, A., Protas, M., Grant, B.R., Grant, P.R., Tabin, C.J., 2004. Bmp4 and morphological variation of beaks in Darwin's finches. *Science* 305, 1462-1465.

Abzhanov, A., Rodda, S.J., McMahon, A.P., Tabin, C.J., 2007. Regulation of skeletogenic differentiation in cranial dermal bone. *Development (Cambridge, England)* 134, 3133-3144.

Abzhanov, A., Tabin, C.J., 2004. Shh and Fgf8 act synergistically to drive cartilage outgrowth during cranial development. *Developmental biology* 273, 134-148.

Ain, Q.U., Seemab, U., Rashid, S., Nawaz, M.S., Kamal, M.A., 2013. Prediction of structure of human WNT-CRD (FZD) complex for computational drug repurposing. *PloS one* 8, e54630.

Akiyama, H., Lyons, J.P., Mori-Akiyama, Y., Yang, X., Zhang, R., Zhang, Z., Deng, J.M., Taketo, M.M., Nakamura, T., Behringer, R.R., McCrea, P.D., de Crombrughe, B., 2004. Interactions between Sox9 and beta-catenin control chondrocyte differentiation. *Genes & development* 18, 1072-1087.

Angers, S., Moon, R.T., 2009. Proximal events in Wnt signal transduction. *Nature reviews* 10, 468-477.

Ashique, A.M., Fu, K., Richman, J.M., 2002. Endogenous bone morphogenetic proteins regulate outgrowth and epithelial survival during avian lip fusion. *Development (Cambridge, England)* 129, 4647-4660.

Barlow, A.J., Francis-West, P.H., 1997. Ectopic application of recombinant BMP-2 and BMP-4 can change patterning of developing chick facial primordia. *Development (Cambridge, England)* 124, 391-398.

Bazan, J.F., Janda, C.Y., Garcia, K.C., 2012. Structural architecture and functional evolution of Wnts. *Developmental cell* 23, 227-232.

Benouaiche, L., Gitton, Y., Vincent, C., Couly, G., Levi, G., 2008. Sonic hedgehog signalling from foregut endoderm patterns the avian nasal capsule. *Development (Cambridge, England)* 135, 2221-2225.

Bhaskar, S.N., Weinmann, J.P., Schour, I., 1953. Role of Meckel's cartilage in the development and growth of the rat mandible. *Journal of dental research* 32, 398-410.

Boehm, B., Westerberg, H., Lesnicar-Pucko, G., Raja, S., Rautschka, M., Cotterell, J., Swoger, J., Sharpe, J., 2010. The role of spatially controlled cell proliferation in limb bud morphogenesis. *PLoS biology* 8, e1000420.

Bond, S.R., Naus, C.C., 2012. RF-Cloning.org: an online tool for the design of restriction-free cloning projects. *Nucleic acids research* 40, W209-213.

Bradley, E.W., Drissi, M.H., 2010. WNT5A Regulates Chondrocyte Differentiation through Differential Use of the CaN/NFAT and IKK/NF- κ B Pathways. *Molecular endocrinology* (Baltimore, Md).

Brault, V., Moore, R., Kutsch, S., Ishibashi, M., Rowitch, D.H., McMahon, A.P., Sommer, L., Boussadia, O., Kemler, R., 2001. Inactivation of the beta-catenin gene by Wnt1-Cre-mediated deletion results in dramatic brain malformation and failure of craniofacial development. *Development* (Cambridge, England) 128, 1253-1264.

Brito, J.M., Teillet, M.A., Le Douarin, N.M., 2006. An early role for sonic hedgehog from foregut endoderm in jaw development: ensuring neural crest cell survival. *Proceedings of the National Academy of Sciences of the United States of America* 103, 11607-11612.

Bromme, D., Wilson, S., 2011. *Extracellular Matrix Degradation*. Springer-Verlag Berlin Heidelberg.

Brugmann, S.A., Goodnough, L.H., Gregorieff, A., Leucht, P., ten Berge, D., Fuerer, C., Clevers, H., Nusse, R., Helms, J.A., 2007. Wnt signaling mediates regional specification in the vertebrate face. *Development* (Cambridge, England) 134, 3283-3295.

Bryja, V., Andersson, E.R., Schambony, A., Esner, M., Bryjova, L., Biris, K.K., Hall, A.C., Kraft, B., Cajanek, L., Yamaguchi, T.P., Buckingham, M., Arenas, E., 2009. The extracellular domain of Lrp5/6 inhibits noncanonical Wnt signaling in vivo. *Molecular biology of the cell* 20, 924-936.

Buchert, M., Athineos, D., Abud, H.E., Burke, Z.D., Faux, M.C., Samuel, M.S., Jarnicki, A.G., Winbanks, C.E., Newton, I.P., Meniel, V.S., Suzuki, H., Stacker, S.A., Nathke, I.S., Tosh, D., Huelsken, J., Clarke, A.R., Heath, J.K., Sansom, O.J., Ernst, M., 2010. Genetic dissection of differential signaling threshold requirements for the Wnt/beta-catenin pathway in vivo. *PLoS genetics* 6, e1000816.

Carroll, T.J., Park, J.S., Hayashi, S., Majumdar, A., McMahon, A.P., 2005. Wnt9b plays a central role in the regulation of mesenchymal to epithelial transitions underlying organogenesis of the mammalian urogenital system. *Developmental cell* 9, 283-292.

Castro, S., Peraza, E., Barraza, A., Zapata, M., 2013. Prenatal diagnosis of robinow syndrome: A case report. *Journal of clinical ultrasound : JCU*.

Caterson, B., Flannery, C.R., Hughes, C.E., Little, C.B., 2000. Mechanisms involved in cartilage proteoglycan catabolism. *Matrix biology : journal of the International Society for Matrix Biology* 19, 333-344.

Church, V., Nohno, T., Linker, C., Marcelle, C., Francis-West, P., 2002. Wnt regulation of chondrocyte differentiation. *Journal of cell science* 115, 4809-4818.

Cordero, D., Marcucio, R., Hu, D., Gaffield, W., Tapadia, M., Helms, J.A., 2004. Temporal perturbations in sonic hedgehog signaling elicit the spectrum of holoprosencephaly phenotypes. *The Journal of clinical investigation* 114, 485-494.

- Couly, G., Creuzet, S., Bennaceur, S., Vincent, C., Le Douarin, N.M., 2002. Interactions between Hox-negative cephalic neural crest cells and the foregut endoderm in patterning the facial skeleton in the vertebrate head. *Development (Cambridge, England)* 129, 1061-1073.
- Couly, G.F., Coltey, P.M., Le Douarin, N.M., 1993. The triple origin of skull in higher vertebrates: a study in quail-chick chimeras. *Development (Cambridge, England)* 117, 409-429.
- Crabtree, G.R., Olson, E.N., 2002. NFAT signaling: choreographing the social lives of cells. *Cell* 109 Suppl, S67-79.
- Creuzet, S., Couly, G., Le Douarin, N.M., 2005. Patterning the neural crest derivatives during development of the vertebrate head: insights from avian studies. *Journal of anatomy* 207, 447-459.
- Curtin, J.A., Quint, E., Tsipouri, V., Arkell, R.M., Cattnach, B., Copp, A.J., Henderson, D.J., Spurr, N., Stanier, P., Fisher, E.M., Nolan, P.M., Steel, K.P., Brown, S.D., Gray, I.C., Murdoch, J.N., 2003. Mutation of *Celsr1* disrupts planar polarity of inner ear hair cells and causes severe neural tube defects in the mouse. *Curr Biol* 13, 1129-1133.
- Danielian, P.S., McMahon, A.P., 1996. Engrailed-1 as a target of the Wnt-1 signalling pathway in vertebrate midbrain development. *Nature* 383, 332-334.
- Daumer, K.M., Tufan, A.C., Tuan, R.S., 2004. Long-term in vitro analysis of limb cartilage development: involvement of Wnt signaling. *Journal of cellular biochemistry* 93, 526-541.
- Davis, E.K., Zou, Y., Ghosh, A., 2008. Wnts acting through canonical and noncanonical signaling pathways exert opposite effects on hippocampal synapse formation. *Neural development* 3, 32.
- Day, T.F., Guo, X., Garrett-Beal, L., Yang, Y., 2005. Wnt/beta-catenin signaling in mesenchymal progenitors controls osteoblast and chondrocyte differentiation during vertebrate skeletogenesis. *Developmental cell* 8, 739-750.
- Dealy, C.N., Roth, A., Ferrari, D., Brown, A.M., Kosher, R.A., 1993. Wnt-5a and Wnt-7a are expressed in the developing chick limb bud in a manner suggesting roles in pattern formation along the proximodistal and dorsoventral axes. *Mechanisms of development* 43, 175-186.
- DeChiara, T.M., Kimble, R.B., Poueymirou, W.T., Rojas, J., Masiakowski, P., Valenzuela, D.M., Yancopoulos, G.D., 2000. *Ror2*, encoding a receptor-like tyrosine kinase, is required for cartilage and growth plate development. *Nature genetics* 24, 271-274.
- Depew, M.J., Liu, J.K., Long, J.E., Presley, R., Meneses, J.J., Pedersen, R.A., Rubenstein, J.L., 1999. *Dlx5* regulates regional development of the branchial arches and sensory capsules. *Development (Cambridge, England)* 126, 3831-3846.
- Dixon, M.J., 1996. Treacher Collins syndrome. *Human molecular genetics* 5 Spec No, 1391-1396.

Dixon, M.J., Marazita, M.L., Beaty, T.H., Murray, J.C., 2011. Cleft lip and palate: understanding genetic and environmental influences. *Nature reviews. Genetics* 12, 167-178.

Ducy, P., Zhang, R., Geoffroy, V., Ridall, A.L., Karsenty, G., 1997. *Osf2/Cbfa1*: a transcriptional activator of osteoblast differentiation. *Cell* 89, 747-754.

Durigova, M., Nagase, H., Mort, J.S., Roughley, P.J., 2011. MMPs are less efficient than ADAMTS5 in cleaving aggrecan core protein. *Matrix biology : journal of the International Society for Matrix Biology* 30, 145-153.

Eames, B.F., de la Fuente, L., Helms, J.A., 2003. Molecular ontogeny of the skeleton. *Birth defects research. Part C, Embryo today : reviews* 69, 93-101.

Eames, B.F., Helms, J.A., 2004. Conserved molecular program regulating cranial and appendicular skeletogenesis. *Dev Dyn* 231, 4-13.

Eames, B.F., Schneider, R.A., 2008. The genesis of cartilage size and shape during development and evolution. *Development (Cambridge, England)* 135, 3947-3958.

Eames, B.F., Sharpe, P.T., Helms, J.A., 2004. Hierarchy revealed in the specification of three skeletal fates by *Sox9* and *Runx2*. *Developmental biology* 274, 188-200.

Ekanayake, S., Hall, B.K., 1994. Hypertrophy is not a prerequisite for type X collagen expression or mineralization of chondrocytes derived from cultured chick mandibular ectomesenchyme. *The International journal of developmental biology* 38, 683-694.

Fanto, M., McNeill, H., 2004. Planar polarity from flies to vertebrates. *Journal of cell science* 117, 527-533.

Fokina, V.M., Frolova, E.I., 2006. Expression patterns of Wnt genes during development of an anterior part of the chicken eye. *Dev Dyn* 235, 496-505.

Fosang, A.J., Last, K., Knauper, V., Murphy, G., Neame, P.J., 1996. Degradation of cartilage aggrecan by collagenase-3 (MMP-13). *FEBS letters* 380, 17-20.

Gao, B., 2012. Wnt regulation of planar cell polarity (PCP). *Current topics in developmental biology* 101, 263-295.

Gao, B., Song, H., Bishop, K., Elliot, G., Garrett, L., English, M.A., Andre, P., Robinson, J., Sood, R., Minami, Y., Economides, A.N., Yang, Y., 2011. Wnt signaling gradients establish planar cell polarity by inducing *Vangl2* phosphorylation through *Ror2*. *Developmental cell* 20, 163-176.

Gavin, B.J., McMahon, J.A., McMahon, A.P., 1990. Expression of multiple novel *Wnt-1/int-1*-related genes during fetal and adult mouse development. *Genes & development* 4, 2319-2332.

- Geetha-Loganathan, P., Nimmagadda, S., Antoni, L., Fu, K., Whiting, C.J., Francis-West, P., Richman, J.M., 2009. Expression of WNT signalling pathway genes during chicken craniofacial development. *Dev Dyn* 238, 1150-1165.
- Geetha-Loganathan, P., Nimmagadda, S., Hafez, I., Fu, K., Cullis, P.R., Richman, J.M., 2011. Development of high-concentration lipoplexes for in vivo gene function studies in vertebrate embryos. *Dev Dyn* 240, 2108-2119.
- Geetha-Loganathan, P., Nimmagadda, S., Huang, R., Christ, B., Scaal, M., 2006. Regulation of ectodermal Wnt6 expression by the neural tube is transduced by dermomyotomal Wnt11: a mechanism of dermomyotomal lip sustainment. *Development (Cambridge, England)* 133, 2897-2904.
- Gibson, G., Lin, D.L., Roque, M., 1997. Apoptosis of terminally differentiated chondrocytes in culture. *Experimental cell research* 233, 372-382.
- Glass, D.A., 2nd, Karsenty, G., 2007. In vivo analysis of Wnt signaling in bone. *Endocrinology* 148, 2630-2634.
- Goldring, M.B., 2012. Chondrogenesis, chondrocyte differentiation, and articular cartilage metabolism in health and osteoarthritis. *Therapeutic advances in musculoskeletal disease* 4, 269-285.
- Gordon, M.D., Nusse, R., 2006. Wnt signaling: multiple pathways, multiple receptors, and multiple transcription factors. *The Journal of biological chemistry* 281, 22429-22433.
- Graham, A., 2003. Development of the pharyngeal arches. *American journal of medical genetics* 119A, 251-256.
- Gray, R.S., Abitua, P.B., Wlodarczyk, B.J., Szabo-Rogers, H.L., Blanchard, O., Lee, I., Weiss, G.S., Liu, K.J., Marcotte, E.M., Wallingford, J.B., Finnell, R.H., 2009a. The planar cell polarity effector Fuz is essential for targeted membrane trafficking, ciliogenesis and mouse embryonic development. *Nature cell biology* 11, 1225-1232.
- Gray, R.S., Bayly, R.D., Green, S.A., Agarwala, S., Lowe, C.J., Wallingford, J.B., 2009b. Diversification of the expression patterns and developmental functions of the dishevelled gene family during chordate evolution. *Dev Dyn* 238, 2044-2057.
- Gray, R.S., Roszko, I., Solnica-Krezel, L., 2011. Planar cell polarity: coordinating morphogenetic cell behaviors with embryonic polarity. *Developmental cell* 21, 120-133.
- Grenier, J., Teillet, M.A., Grifone, R., Kelly, R.G., Duprez, D., 2009. Relationship between neural crest cells and cranial mesoderm during head muscle development. *PloS one* 4, e4381.
- Gress, C.J., Jacenko, O., 2000. Growth plate compressions and altered hematopoiesis in collagen X null mice. *The Journal of cell biology* 149, 983-993.

Gros, J., Hu, J.K., Vinegoni, C., Feruglio, P.F., Weissleder, R., Tabin, C.J., 2010. WNT5A/JNK and FGF/MAPK pathways regulate the cellular events shaping the vertebrate limb bud. *Curr Biol* 20, 1993-2002.

Gross, J.B., Hanken, J., 2008. Review of fate-mapping studies of osteogenic cranial neural crest in vertebrates. *Developmental biology* 317, 389-400.

Guo, N., Hawkins, C., Nathans, J., 2004. Frizzled6 controls hair patterning in mice. *Proceedings of the National Academy of Sciences of the United States of America* 101, 9277-9281.

Güven, M.A., Batukan, C., Ceylaner, S., Uzel, M., Özbek, A., Demirpolat, G., 2006. Prenatal and postnatal findings in a case with the autosomal recessive type of Robinow syndrome. *Fetal diagnosis and therapy* 21, 386-389.

Hamblet, N.S., Lijam, N., Ruiz-Lozano, P., Wang, J., Yang, Y., Luo, Z., Mei, L., Chien, K.R., Sussman, D.J., Wynshaw-Boris, A., 2002. Dishevelled 2 is essential for cardiac outflow tract development, somite segmentation and neural tube closure. *Development (Cambridge, England)* 129, 5827-5838.

Hamburger, V., Hamilton, H., 1951. A series of normal stages in the development of the chick embryo. *Journal of morphology* 88, 49-92.

Hardingham, T.E., Fosang, A.J., 1992. Proteoglycans: many forms and many functions. *Faseb J* 6, 861-870.

Hartmann, C., Tabin, C.J., 2000. Dual roles of Wnt signaling during chondrogenesis in the chicken limb. *Development (Cambridge, England)* 127, 3141-3159.

He, F., Popkie, A.P., Xiong, W., Li, L., Wang, Y., Phiel, C.J., Chen, Y., 2010. Gsk3beta is required in the epithelium for palatal elevation in mice. *Dev Dyn* 239, 3235-3246.

He, F., Xiong, W., Yu, X., Espinoza-Lewis, R., Liu, C., Gu, S., Nishita, M., Suzuki, K., Yamada, G., Minami, Y., Chen, Y., 2008. Wnt5a regulates directional cell migration and cell proliferation via Ror2-mediated noncanonical pathway in mammalian palate development. *Development (Cambridge, England)* 135, 3871-3879.

He, X., Semenov, M., Tamai, K., Zeng, X., 2004. LDL receptor-related proteins 5 and 6 in Wnt/beta-catenin signaling: arrows point the way. *Development (Cambridge, England)* 131, 1663-1677.

Held-Feindt, J., Paredes, E.B., Blomer, U., Seidenbecher, C., Stark, A.M., Mehdorn, H.M., Mentlein, R., 2006. Matrix-degrading proteases ADAMTS4 and ADAMTS5 (disintegrins and metalloproteinases with thrombospondin motifs 4 and 5) are expressed in human glioblastomas. *International journal of cancer. Journal international du cancer* 118, 55-61.

Helms, J.A., Cordero, D., Tapadia, M.D., 2005. New insights into craniofacial morphogenesis. *Development (Cambridge, England)* 132, 851-861.

- Heydeck, W., Liu, A., 2011. PCP effector proteins inturnd and fuzzy play nonredundant roles in the patterning but not convergent extension of mammalian neural tube. *Dev Dyn* 240, 1938-1948.
- Ho, H.Y., Susman, M.W., Bikoff, J.B., Ryu, Y.K., Jonas, A.M., Hu, L., Kuruvilla, R., Greenberg, M.E., 2012. Wnt5a-Ror-Dishevelled signaling constitutes a core developmental pathway that controls tissue morphogenesis. *Proceedings of the National Academy of Sciences of the United States of America* 109, 4044-4051.
- Hoang, B.H., Thomas, J.T., Abdul-Karim, F.W., Correia, K.M., Conlon, R.A., Luyten, F.P., Ballock, R.T., 1998. Expression pattern of two Frizzled-related genes, Frzb-1 and Sfrp-1, during mouse embryogenesis suggests a role for modulating action of Wnt family members. *Dev Dyn* 212, 364-372.
- Hosseini-Farahabadi, S., Geetha-Loganathan, P., Fu, K., Nimmagadda, S., Yang, H.J., Richman, J.M., 2013. Dual functions for WNT5A during cartilage development and in disease. *Matrix biology : journal of the International Society for Matrix Biology* 32, 252-264.
- Hsieh, J.C., Kodjabachian, L., Rebbert, M.L., Rattner, A., Smallwood, P.M., Samos, C.H., Nusse, R., Dawid, I.B., Nathans, J., 1999. A new secreted protein that binds to Wnt proteins and inhibits their activities. *Nature* 398, 431-436.
- Hu, D., Colnot, C., Marcucio, R.S., 2008. Effect of bone morphogenetic protein signaling on development of the jaw skeleton. *Dev Dyn* 237, 3727-3737.
- Hu, D., Marcucio, R.S., Helms, J.A., 2003. A zone of frontonasal ectoderm regulates patterning and growth in the face. *Development (Cambridge, England)* 130, 1749-1758.
- Hwang, S.G., Yu, S.S., Lee, S.W., Chun, J.S., 2005. Wnt-3a regulates chondrocyte differentiation via c-Jun/AP-1 pathway. *FEBS letters* 579, 4837-4842.
- Ishitani, T., Kishida, S., Hyodo-Miura, J., Ueno, N., Yasuda, J., Waterman, M., Shibuya, H., Moon, R.T., Ninomiya-Tsuji, J., Matsumoto, K., 2003. The TAK1-NLK mitogen-activated protein kinase cascade functions in the Wnt-5a/Ca(2+) pathway to antagonize Wnt/beta-catenin signaling. *Molecular and cellular biology* 23, 131-139.
- James, C.G., Appleton, C.T., Ulici, V., Underhill, T.M., Beier, F., 2005. Microarray analyses of gene expression during chondrocyte differentiation identifies novel regulators of hypertrophy. *Molecular biology of the cell* 16, 5316-5333.
- Janda, C.Y., Waghray, D., Levin, A.M., Thomas, C., Garcia, K.C., 2012. Structural basis of Wnt recognition by Frizzled. *Science (New York, N.Y)* 337, 59-64.
- Jiang, X., Iseki, S., Maxson, R.E., Sucov, H.M., Morriss-Kay, G.M., 2002. Tissue origins and interactions in the mammalian skull vault. *Developmental biology* 241, 106-116.

- Joeng, K.S., Schumacher, C.A., Zylstra-Diegel, C.R., Long, F., Williams, B.O., 2011. Lrp5 and Lrp6 redundantly control skeletal development in the mouse embryo. *Developmental biology* 359, 222-229.
- Juriloff, D.M., Harris, M.J., Dewell, S.L., 2004. A digenic cause of cleft lip in A-strain mice and definition of candidate genes for the two loci. *Birth defects research. Part A, Clinical and molecular teratology* 70, 509-518.
- Kamel, G., Hoyos, T., Rochard, L., Dougherty, M., Kong, Y., Tse, W., Shubinets, V., Grimaldi, M., Liao, E.C., 2013. Requirement for *frzb* and *fzd7a* in cranial neural crest convergence and extension mechanisms during zebrafish palate and jaw morphogenesis. *Developmental biology* 381, 423-433.
- Karner, C., Wharton, K.A., Jr., Carroll, T.J., 2006. Planar cell polarity and vertebrate organogenesis. *Seminars in cell & developmental biology* 17, 194-203.
- Kato, M., Patel, M.S., Levasseur, R., Lobov, I., Chang, B.H., Glass, D.A., 2nd, Hartmann, C., Li, L., Hwang, T.H., Brayton, C.F., Lang, R.A., Karsenty, G., Chan, L., 2002. *Cbfa1*-independent decrease in osteoblast proliferation, osteopenia, and persistent embryonic eye vascularization in mice deficient in *Lrp5*, a Wnt coreceptor. *The Journal of cell biology* 157, 303-314.
- Kauskot, A., Adam, F., Mazharian, A., Ajzenberg, N., Berrou, E., Bonnefoy, A., Rosa, J.P., Hoylaerts, M.F., Bryckaert, M., 2007. Involvement of the mitogen-activated protein kinase c-Jun NH2-terminal kinase 1 in thrombus formation. *The Journal of biological chemistry* 282, 31990-31999.
- Kawakami, Y., Capdevila, J., Buscher, D., Itoh, T., Rodriguez Esteban, C., Izpisua Belmonte, J.C., 2001. WNT signals control FGF-dependent limb initiation and AER induction in the chick embryo. *Cell* 104, 891-900.
- Kawakami, Y., Wada, N., Nishimatsu, S.I., Ishikawa, T., Noji, S., Nohno, T., 1999. Involvement of Wnt-5a in chondrogenic pattern formation in the chick limb bud. *Development, growth & differentiation* 41, 29-40.
- Kawano, Y., Kypta, R., 2003. Secreted antagonists of the Wnt signalling pathway. *Journal of cell science* 116, 2627-2634.
- Kern, B., Shen, J., Starbuck, M., Karsenty, G., 2001. *Cbfa1* contributes to the osteoblast-specific expression of type I collagen genes. *The Journal of biological chemistry* 276, 7101-7107.
- Kessenbrock, K., Plaks, V., Werb, Z., 2010. Matrix metalloproteinases: regulators of the tumor microenvironment. *Cell* 141, 52-67.
- Kikuchi, A., Yamamoto, H., Sato, A., Matsumoto, S., 2012. Wnt5a: its signalling, functions and implication in diseases. *Acta physiologica* 204, 17-33.

- Kimura, R., Ishikawa, C., Rokkaku, T., Janknecht, R., Mori, N., 2011. Phosphorylated c-Jun and Fra-1 induce matrix metalloproteinase-1 and thereby regulate invasion activity of 143B osteosarcoma cells. *Biochimica et biophysica acta* 1813, 1543-1553.
- Koay, M.A., Brown, M.A., 2005. Genetic disorders of the LRP5-Wnt signalling pathway affecting the skeleton. *Trends in molecular medicine* 11, 129-137.
- Kohn, A.D., Moon, R.T., 2005. Wnt and calcium signaling: beta-catenin-independent pathways. *Cell calcium* 38, 439-446.
- Komiya, Y., Habas, R., 2008. Wnt signal transduction pathways. *Organogenesis* 4, 68-75.
- Kontges, G., Lumsden, A., 1996. Rhombencephalic neural crest segmentation is preserved throughout craniofacial ontogeny. *Development (Cambridge, England)* 122, 3229-3242.
- Kosaki, R., Fujimaru, R., Samejima, H., Yamada, H., Izumi, K., Iijima, K., Kosaki, K., 2007. Wide phenotypic variations within a family with SALL1 mutations: Isolated external ear abnormalities to Goldenhar syndrome. *American journal of medical genetics* 143A, 1087-1090.
- Kuhl, M., Sheldahl, L.C., Park, M., Miller, J.R., Moon, R.T., 2000. The Wnt/Ca²⁺ pathway: a new vertebrate Wnt signaling pathway takes shape. *Trends Genet* 16, 279-283.
- Kurayoshi, M., Yamamoto, H., Izumi, S., Kikuchi, A., 2007. Post-translational palmitoylation and glycosylation of Wnt-5a are necessary for its signalling. *The Biochemical journal* 402, 515-523.
- Kurihara, Y., Kurihara, H., Suzuki, H., Kodama, T., Maemura, K., Nagai, R., Oda, H., Kuwaki, T., Cao, W.H., Kamada, N., et al., 1994. Elevated blood pressure and craniofacial abnormalities in mice deficient in endothelin-1. *Nature* 368, 703-710.
- Ladher, R.K., Church, V.L., Allen, S., Robson, L., Abdelfattah, A., Brown, N.A., Hattersley, G., Rosen, V., Luyten, F.P., Dale, L., Francis-West, P.H., 2000. Cloning and expression of the Wnt antagonists Sfrp-2 and Frzb during chick development. *Developmental biology* 218, 183-198.
- Lammi, L., Arte, S., Somer, M., Jarvinen, H., Lahermo, P., Thesleff, I., Pirinen, S., Nieminen, P., 2004. Mutations in AXIN2 cause familial tooth agenesis and predispose to colorectal cancer. *American journal of human genetics* 74, 1043-1050.
- Lan, Y., Ryan, R.C., Zhang, Z., Bullard, S.A., Bush, J.O., Maltby, K.M., Lidral, A.C., Jiang, R., 2006. Expression of Wnt9b and activation of canonical Wnt signaling during midfacial morphogenesis in mice. *Dev Dyn* 235, 1448-1454.
- Lanctot, C., Moreau, A., Chamberland, M., Tremblay, M.L., Drouin, J., 1999. Hindlimb patterning and mandible development require the Ptx1 gene. *Development (Cambridge, England)* 126, 1805-1810.
- Langille, R.M., 1994. In vitro analysis of the spatial organization of chondrogenic regions of avian mandibular mesenchyme. *Dev Dyn* 201, 55-62.

- Le Douarin, N.M., Creuzet, S., Couly, G., Dupin, E., 2004. Neural crest cell plasticity and its limits. *Development (Cambridge, England)* 131, 4637-4650.
- Lee, S.H., Bedard, O., Buchtova, M., Fu, K., Richman, J.M., 2004. A new origin for the maxillary jaw. *Developmental biology* 276, 207-224.
- Lee, S.H., Fu, K.K., Hui, J.N., Richman, J.M., 2001. Noggin and retinoic acid transform the identity of avian facial prominences. *Nature* 414, 909-912.
- Lefebvre, V., Huang, W., Harley, V.R., Goodfellow, P.N., de Crombrughe, B., 1997. SOX9 is a potent activator of the chondrocyte-specific enhancer of the pro alpha1(II) collagen gene. *Molecular and cellular biology* 17, 2336-2346.
- Lefebvre, V., Li, P., de Crombrughe, B., 1998. A new long form of Sox5 (L-Sox5), Sox6 and Sox9 are coexpressed in chondrogenesis and cooperatively activate the type II collagen gene. *The EMBO journal* 17, 5718-5733.
- Lescher, B., Haenig, B., Kispert, A., 1998. sFRP-2 is a target of the Wnt-4 signaling pathway in the developing metanephric kidney. *Dev Dyn* 213, 440-451.
- Li, S., Muneoka, K., 1999. Cell migration and chick limb development: chemotactic action of FGF-4 and the AER. *Developmental biology* 211, 335-347.
- Linker, C., Lesbros, C., Gros, J., Burrus, L.W., Rawls, A., Marcelle, C., 2005. beta-Catenin-dependent Wnt signalling controls the epithelial organisation of somites through the activation of paraxis. *Development (Cambridge, England)* 132, 3895-3905.
- Liu, H., Kato, Y., Erzinger, S.A., Kiriakova, G.M., Qian, Y., Palmieri, D., Steeg, P.S., Price, J.E., 2012. The role of MMP-1 in breast cancer growth and metastasis to the brain in a xenograft model. *BMC cancer* 12, 583.
- Liu, K.J., Arron, J.R., Stankunas, K., Crabtree, G.R., Longaker, M.T., 2007. Chemical rescue of cleft palate and midline defects in conditional GSK-3beta mice. *Nature* 446, 79-82.
- Liu, W., Dong, X., Mai, M., Seelan, R.S., Taniguchi, K., Krishnadath, K.K., Halling, K.C., Cunningham, J.M., Boardman, L.A., Qian, C., Christensen, E., Schmidt, S.S., Roche, P.C., Smith, D.I., Thibodeau, S.N., 2000. Mutations in AXIN2 cause colorectal cancer with defective mismatch repair by activating beta-catenin/TCF signalling. *Nature genetics* 26, 146-147.
- Livak, K.J., Schmittgen, T.D., 2001. Analysis of relative gene expression data using real-time quantitative PCR and the 2(-Delta Delta C(T)) Method. *Methods* 25, 402-408.
- Loftus, S.K., Larson, D.M., Watkins-Chow, D., Church, D.M., Pavan, W.J., 2001. Generation of RCAS vectors useful for functional genomic analyses. *DNA Res* 8, 221-226.
- Logan, C.Y., Nusse, R., 2004. The Wnt signaling pathway in development and disease. *Annual review of cell and developmental biology* 20, 781-810.

- Logan, M., Tabin, C., 1998. Targeted gene misexpression in chick limb buds using avian replication-competent retroviruses. *Methods* 14, 407-420.
- Loverro, G., Guanti, G., Caruso, G., Selvaggi, L., 1990. Robinow's syndrome: prenatal diagnosis. *Prenatal diagnosis* 10, 121-126.
- Lyons, J.P., Mueller, U.W., Ji, H., Everett, C., Fang, X., Hsieh, J.C., Barth, A.M., McCrea, P.D., 2004. Wnt-4 activates the canonical beta-catenin-mediated Wnt pathway and binds Frizzled-6 CRD: functional implications of Wnt/beta-catenin activity in kidney epithelial cells. *Experimental cell research* 298, 369-387.
- MacDonald, B.T., Tamai, K., He, X., 2009. Wnt/beta-catenin signaling: components, mechanisms, and diseases. *Developmental cell* 17, 9-26.
- MacDonald, M.E., Abbott, U.K., Richman, J.M., 2004. Upper beak truncation in chicken embryos with the cleft primary palate mutation is due to an epithelial defect in the frontonasal mass. *Dev Dyn* 230, 335-349.
- Marcucio, R.S., Cordero, D.R., Hu, D., Helms, J.A., 2005. Molecular interactions coordinating the development of the forebrain and face. *Developmental biology* 284, 48-61.
- Matsuo, I., Kuratani, S., Kimura, C., Takeda, N., Aizawa, S., 1995. Mouse Otx2 functions in the formation and patterning of rostral head. *Genes & development* 9, 2646-2658.
- Maye, P., Zheng, J., Li, L., Wu, D., 2004. Multiple mechanisms for Wnt11-mediated repression of the canonical Wnt signaling pathway. *The Journal of biological chemistry* 279, 24659-24665.
- McBratney-Owen, B., Iseki, S., Bamforth, S.D., Olsen, B.R., Morriss-Kay, G.M., 2008. Development and tissue origins of the mammalian cranial base. *Developmental biology* 322, 121-132.
- McGonnell, I.M., Clarke, J.D., Tickle, C., 1998. Fate map of the developing chick face: analysis of expansion of facial primordia and establishment of the primary palate. *Dev Dyn* 212, 102-118.
- McMahon, A.P., Bradley, A., 1990. The Wnt-1 (int-1) proto-oncogene is required for development of a large region of the mouse brain. *Cell* 62, 1073-1085.
- Merrill, A.E., Eames, B.F., Weston, S.J., Heath, T., Schneider, R.A., 2008. Mesenchyme-dependent BMP signaling directs the timing of mandibular osteogenesis. *Development (Cambridge, England)* 135, 1223-1234.
- Mikels, A., Minami, Y., Nusse, R., 2009. Ror2 receptor requires tyrosine kinase activity to mediate Wnt5A signaling. *The Journal of biological chemistry* 284, 30167-30176.
- Mikels, A.J., Nusse, R., 2006. Purified Wnt5a protein activates or inhibits beta-catenin-TCF signaling depending on receptor context. *PLoS biology* 4, e115.

- Mina, M., 2001. Regulation of mandibular growth and morphogenesis. *Critical reviews in oral biology and medicine* : an official publication of the American Association of Oral Biologists 12, 276-300.
- Mina, M., Wang, Y.H., Ivanisevic, A.M., Upholt, W.B., Rodgers, B., 2002. Region- and stage-specific effects of FGFs and BMPs in chick mandibular morphogenesis. *Dev Dyn* 223, 333-352.
- Minami, Y., Oishi, I., Endo, M., Nishita, M., 2010. Ror-family receptor tyrosine kinases in noncanonical Wnt signaling: their implications in developmental morphogenesis and human diseases. *Dev Dyn* 239, 1-15.
- Mori-Akiyama, Y., Akiyama, H., Rowitch, D.H., de Crombrughe, B., 2003. Sox9 is required for determination of the chondrogenic cell lineage in the cranial neural crest. *Proceedings of the National Academy of Sciences of the United States of America* 100, 9360-9365.
- Morishima, M., Yasui, H., Nakazawa, M., Ando, M., Ishibashi, M., Takao, A., 1998. Situs variation and cardiovascular anomalies in the transgenic mouse insertional mutation, *inv*. *Teratology* 57, 302-309.
- Mukhopadhyay, M., Shtrom, S., Rodriguez-Esteban, C., Chen, L., Tsukui, T., Gomer, L., Dorward, D.W., Glinka, A., Grinberg, A., Huang, S.P., Niehrs, C., Izpisua Belmonte, J.C., Westphal, H., 2001. Dickkopf1 is required for embryonic head induction and limb morphogenesis in the mouse. *Developmental cell* 1, 423-434.
- Murray, P.D.F., 1963. Adventitious (secondary) cartilage in the chick embryo, and the development of certain bones and articulation in the chick skull. *Aust J Zool* 11, 368-430.
- Nabeshima, K., Inoue, T., Shimao, Y., Sameshima, T., 2002. Matrix metalloproteinases in tumor invasion: role for cell migration. *Pathology international* 52, 255-264.
- Niemann, S., Zhao, C., Pascu, F., Stahl, U., Aulepp, U., Niswander, L., Weber, J.L., Muller, U., 2004. Homozygous WNT3 mutation causes tetra-amelia in a large consanguineous family. *American journal of human genetics* 74, 558-563.
- Noden, D.M., 1982. Patterns and organization of craniofacial skeletogenic and myogenic mesenchyme: a perspective. *Progress in clinical and biological research* 101, 167-203.
- Noden, D.M., Trainor, P.A., 2005. Relations and interactions between cranial mesoderm and neural crest populations. *Journal of anatomy* 207, 575-601.
- Nusse, R., Brown, A., Papkoff, J., Scambler, P., Shackleford, G., McMahon, A., Moon, R., Varmus, H., 1991. A new nomenclature for int-1 and related genes: the Wnt gene family. *Cell* 64, 231.
- Ohkawara, B., Niehrs, C., 2011. An ATF2-based luciferase reporter to monitor non-canonical Wnt signaling in *Xenopus* embryos. *Dev Dyn* 240, 188-194.

- Otto, F., Thornell, A.P., Crompton, T., Denzel, A., Gilmour, K.C., Rosewell, I.R., Stamp, G.W., Beddington, R.S., Mundlos, S., Olsen, B.R., Selby, P.B., Owen, M.J., 1997. *Cbfa1*, a candidate gene for cleidocranial dysplasia syndrome, is essential for osteoblast differentiation and bone development. *Cell* 89, 765-771.
- Parr, B.A., Shea, M.J., Vassileva, G., McMahon, A.P., 1993. Mouse Wnt genes exhibit discrete domains of expression in the early embryonic CNS and limb buds. *Development (Cambridge, England)* 119, 247-261.
- Patton, M.A., Afzal, A.R., 2002. Robinow syndrome. *Journal of medical genetics* 39, 305-310.
- Percin, E.F., Guvenal, T., Cetin, A., Percin, S., Goze, F., Arici, S., 2001. First-trimester diagnosis of Robinow syndrome. *Fetal diagnosis and therapy* 16, 308-311.
- Perrimon, N., Mahowald, A.P., 1987. Multiple functions of segment polarity genes in *Drosophila*. *Developmental biology* 119, 587-600.
- Person, A.D., Beiraghi, S., Sieben, C.M., Hermanson, S., Neumann, A.N., Robu, M.E., Schleiffarth, J.R., Billington, C.J., Jr., van Bokhoven, H., Hooigeboom, J.M., Mazzeu, J.F., Petryk, A., Schimmenti, L.A., Brunner, H.G., Ekker, S.C., Lohr, J.L., 2010. WNT5A mutations in patients with autosomal dominant Robinow syndrome. *Dev Dyn* 239, 327-337.
- Pinson, K.I., Brennan, J., Monkley, S., Avery, B.J., Skarnes, W.C., 2000. An LDL-receptor-related protein mediates Wnt signalling in mice. *Nature* 407, 535-538.
- Plant, M.R., MacDonald, M.E., Grad, L.I., Ritchie, S.J., Richman, J.M., 2000. Locally released retinoic acid repatterns the first branchial arch cartilages in vivo. *Developmental biology* 222, 12-26.
- Ralphs, J.R., 1992. Chondrogenesis and myogenesis in micromass cultures of mesenchyme from mouse facial primordia. *In vitro cellular & developmental biology : journal of the Tissue Culture Association* 28A, 369-372.
- Rao, T.P., Kuhl, M., 2010. An updated overview on Wnt signaling pathways: a prelude for more. *Circulation research* 106, 1798-1806.
- Ravni, A., Qu, Y., Goffinet, A.M., Tissir, F., 2009. Planar cell polarity cadherin *Celsr1* regulates skin hair patterning in the mouse. *The Journal of investigative dermatology* 129, 2507-2509.
- Reid, B.S., Yang, H., Melvin, V.S., Taketo, M.M., Williams, T., 2011. Ectodermal Wnt/beta-catenin signaling shapes the mouse face. *Developmental biology* 349, 261-269.
- Richman, J.M., Buchtova, M., Boughner, J.C., 2006. Comparative ontogeny and phylogeny of the upper jaw skeleton in amniotes. *Dev Dyn* 235, 1230-1243.
- Richman, J.M., Crosby, Z., 1990. Differential growth of facial primordia in chick embryos: responses of facial mesenchyme to basic fibroblast growth factor (bFGF) and serum in micromass culture. *Development (Cambridge, England)* 109, 341-348.

- Richman, J.M., Lee, S.H., 2003. About face: signals and genes controlling jaw patterning and identity in vertebrates. *Bioessays* 25, 554-568.
- Richman, J.M., Tickle, C., 1989. Epithelia are interchangeable between facial primordia of chick embryos and morphogenesis is controlled by the mesenchyme. *Developmental biology* 136, 201-210.
- Richman, J.M., Tickle, C., 1992. Epithelial-mesenchymal interactions in the outgrowth of limb buds and facial primordia in chick embryos. *Developmental biology* 154, 299-308.
- Rodda, S.J., McMahon, A.P., 2006. Distinct roles for Hedgehog and canonical Wnt signaling in specification, differentiation and maintenance of osteoblast progenitors. *Development (Cambridge, England)* 133, 3231-3244.
- Ruest, L.B., Xiang, X., Lim, K.C., Levi, G., Clouthier, D.E., 2004. Endothelin-A receptor-dependent and -independent signaling pathways in establishing mandibular identity. *Development (Cambridge, England)* 131, 4413-4423.
- Ryu, J.H., Chun, J.S., 2006. Opposing roles of WNT-5A and WNT-11 in interleukin-1beta regulation of type II collagen expression in articular chondrocytes. *The Journal of biological chemistry* 281, 22039-22047.
- Sato, T., Kurihara, Y., Asai, R., Kawamura, Y., Tonami, K., Uchijima, Y., Heude, E., Ekker, M., Levi, G., Kurihara, H., 2008. An endothelin-1 switch specifies maxillomandibular identity. *Proceedings of the National Academy of Sciences of the United States of America* 105, 18806-18811.
- Satoh, W., Gotoh, T., Tsunematsu, Y., Aizawa, S., Shimono, A., 2006. Sfrp1 and Sfrp2 regulate anteroposterior axis elongation and somite segmentation during mouse embryogenesis. *Development (Cambridge, England)* 133, 989-999.
- Schiffirin, E.L., 2005. Vascular endothelin in hypertension. *Vascular pharmacology* 43, 19-29.
- Schmidt, C., McGonnell, I.M., Allen, S., Otto, A., Patel, K., 2007. Wnt6 controls amniote neural crest induction through the non-canonical signaling pathway. *Dev Dyn* 236, 2502-2511.
- Schneider, R.A., Helms, J.A., 2003. The cellular and molecular origins of beak morphology. *Science (New York, N.Y)* 299, 565-568.
- Schwabe, G.C., Trepczik, B., Suring, K., Brieske, N., Tucker, A.S., Sharpe, P.T., Minami, Y., Mundlos, S., 2004. Ror2 knockout mouse as a model for the developmental pathology of autosomal recessive Robinow syndrome. *Dev Dyn* 229, 400-410.
- Segreti, W.O., Maumanee, P., 1977. Familial occurrence of Pierre Robin anomalad. *Med. Coll. Va. Quart.* 13, 192-193.
- Seidensticker, M.J., Behrens, J., 2000. Biochemical interactions in the wnt pathway. *Biochimica et biophysica acta* 1495, 168-182.

Semenov, M., Tamai, K., He, X., 2005. SOST is a ligand for LRP5/LRP6 and a Wnt signaling inhibitor. *The Journal of biological chemistry* 280, 26770-26775.

Shimizu, H., Julius, M.A., Giarre, M., Zheng, Z., Brown, A.M., Kitajewski, J., 1997. Transformation by Wnt family proteins correlates with regulation of beta-catenin. *Cell growth & differentiation : the molecular biology journal of the American Association for Cancer Research* 8, 1349-1358.

Sokol, S., Christian, J.L., Moon, R.T., Melton, D.A., 1991. Injected Wnt RNA induces a complete body axis in *Xenopus* embryos. *Cell* 67, 741-752.

Song, H., Hu, J., Chen, W., Elliott, G., Andre, P., Gao, B., Yang, Y., 2010. Planar cell polarity breaks bilateral symmetry by controlling ciliary positioning. *Nature* 466, 378-382.

Spater, D., Hill, T.P., O'Sullivan R, J., Gruber, M., Conner, D.A., Hartmann, C., 2006. Wnt9a signaling is required for joint integrity and regulation of Ihh during chondrogenesis. *Development (Cambridge, England)* 133, 3039-3049.

St-Jacques, B., Hammerschmidt, M., McMahon, A.P., 1999. Indian hedgehog signaling regulates proliferation and differentiation of chondrocytes and is essential for bone formation. *Genes & development* 13, 2072-2086.

Stricker, S., Verhey van Wijk, N., Witte, F., Brieske, N., Seidel, K., Mundlos, S., 2006. Cloning and expression pattern of chicken Ror2 and functional characterization of truncating mutations in Brachydactyly type B and Robinow syndrome. *Dev Dyn* 235, 3456-3465.

Summerhurst, K., Stark, M., Sharpe, J., Davidson, D., Murphy, P., 2008. 3D representation of Wnt and Frizzled gene expression patterns in the mouse embryo at embryonic day 11.5 (Ts19). *Gene expression patterns : GEP* 8, 331-348.

Surmann-Schmitt, C., Widmann, N., Dietz, U., Saeger, B., Eitzinger, N., Nakamura, Y., Rattel, M., Latham, R., Hartmann, C., von der Mark, H., Schett, G., von der Mark, K., Stock, M., 2009. Wif-1 is expressed at cartilage-mesenchyme interfaces and impedes Wnt3a-mediated inhibition of chondrogenesis. *Journal of cell science* 122, 3627-3637.

Swalla, B.J., Owens, E.M., Linsenmayer, T.F., Solursh, M., 1983. Two distinct classes of prechondrogenic cell types in the embryonic limb bud. *Developmental biology* 97, 59-69.

Szabo-Rogers, H.L., Geetha-Loganathan, P., Nimmagadda, S., Fu, K.K., Richman, J.M., 2008. FGF signals from the nasal pit are necessary for normal facial morphogenesis. *Developmental biology* 318, 289-302.

Szabo-Rogers, H.L., Smithers, L.E., Yakob, W., Liu, K.J., 2010. New directions in craniofacial morphogenesis. *Developmental biology* 341, 84-94.

Tago, K., Nakamura, T., Nishita, M., Hyodo, J., Nagai, S., Murata, Y., Adachi, S., Ohwada, S., Morishita, Y., Shibuya, H., Akiyama, T., 2000. Inhibition of Wnt signaling by ICAT, a novel beta-catenin-interacting protein. *Genes & development* 14, 1741-1749.

- Takemaru, K., Yamaguchi, S., Lee, Y.S., Zhang, Y., Carthew, R.W., Moon, R.T., 2003. Chibby, a nuclear beta-catenin-associated antagonist of the Wnt/Wingless pathway. *Nature* 422, 905-909.
- Tanigawa, S., Wang, H., Yang, Y., Sharma, N., Tarasova, N., Ajima, R., Yamaguchi, T.P., Rodriguez, L.G., Perantoni, A.O., 2011. Wnt4 induces nephronic tubules in metanephric mesenchyme by a non-canonical mechanism. *Developmental biology* 352, 58-69.
- Thorfve, A., Dehne, T., Lindahl, A., Brittberg, M., Pruss, A., Ringe, J., Sittering, M., Karlsson, C., 2012. Characteristic Markers of the WNT Signaling Pathways Are Differentially Expressed in Osteoarthritic Cartilage. *Cartilage* 3, 43-57.
- Thrasivoulou, C., Millar, M., Ahmed, A., 2013. Activation of intracellular calcium by multiple Wnt ligands and translocation of beta-catenin into the nucleus: a convergent model of Wnt/Ca²⁺ and Wnt/beta-catenin pathways. *The Journal of biological chemistry*.
- Topczewski, J., Sepich, D.S., Myers, D.C., Walker, C., Amores, A., Lele, Z., Hammerschmidt, M., Postlethwait, J., Solnica-Krezel, L., 2001. The zebrafish glypican knypek controls cell polarity during gastrulation movements of convergent extension. *Developmental cell* 1, 251-264.
- Toriyama, M., Rosenberg, A.E., Mankin, H.J., Fondren, T., Treadwell, B.V., Towle, C.A., 1998. Matrix metalloproteinase digestion of aggrecan in human cartilage tumours. *European journal of cancer* 34, 1969-1973.
- Tortorella, M.D., Tomasselli, A.G., Mathis, K.J., Schnute, M.E., Woodard, S.S., Munie, G., Williams, J.M., Caspers, N., Wittwer, A.J., Malfait, A.M., Shieh, H.S., 2009. Structural and inhibition analysis reveals the mechanism of selectivity of a series of aggrecanase inhibitors. *The Journal of biological chemistry* 284, 24185-24191.
- Troeberg, L., Nagase, H., 2012. Proteases involved in cartilage matrix degradation in osteoarthritis. *Biochimica et biophysica acta* 1824, 133-145.
- Tu, X., Joeng, K.S., Nakayama, K.I., Nakayama, K., Rajagopal, J., Carroll, T.J., McMahon, A.P., Long, F., 2007. Noncanonical Wnt signaling through G protein-linked PKCdelta activation promotes bone formation. *Developmental cell* 12, 113-127.
- Tucker, A.S., Lumsden, A., 2004. Neural crest cells provide species-specific patterning information in the developing branchial skeleton. *Evolution & development* 6, 32-40.
- Tuckermann, J.P., Pittois, K., Partridge, N.C., Merregaert, J., Angel, P., 2000. Collagenase-3 (MMP-13) and integral membrane protein 2a (Itm2a) are marker genes of chondrogenic/osteoblastic cells in bone formation: sequential temporal, and spatial expression of Itm2a, alkaline phosphatase, MMP-13, and osteocalcin in the mouse. *Journal of bone and mineral research : the official journal of the American Society for Bone and Mineral Research* 15, 1257-1265.
- Tufan, A.C., Tuan, R.S., 2001. Wnt regulation of limb mesenchymal chondrogenesis is accompanied by altered N-cadherin-related functions. *Faseb J* 15, 1436-1438.

- van Amerongen, R., Fuerer, C., Mizutani, M., Nusse, R., 2012. Wnt5a can both activate and repress Wnt/beta-catenin signaling during mouse embryonic development. *Developmental biology* 369, 101-114.
- van Amerongen, R., Nusse, R., 2009. Towards an integrated view of Wnt signaling in development. *Development (Cambridge, England)* 136, 3205-3214.
- van Bokhoven, H., Celli, J., Kayserili, H., van Beusekom, E., Balci, S., Brussel, W., Skovby, F., Kerr, B., Percin, E.F., Akarsu, N., Brunner, H.G., 2000. Mutation of the gene encoding the ROR2 tyrosine kinase causes autosomal recessive Robinow syndrome. *Nature genetics* 25, 423-426.
- Veeman, M.T., Axelrod, J.D., Moon, R.T., 2003. A second canon. Functions and mechanisms of beta-catenin-independent Wnt signaling. *Developmental cell* 5, 367-377.
- Vlad, A., Rohrs, S., Klein-Hitpass, L., Muller, O., 2008. The first five years of the Wnt targetome. *Cellular signalling* 20, 795-802.
- Wallingford, J.B., Fraser, S.E., Harland, R.M., 2002. Convergent extension: the molecular control of polarized cell movement during embryonic development. *Developmental cell* 2, 695-706.
- Wang, B., Sinha, T., Jiao, K., Serra, R., Wang, J., 2011. Disruption of PCP signaling causes limb morphogenesis and skeletal defects and may underlie Robinow syndrome and brachydactyly type B. *Human molecular genetics* 20, 271-285.
- Wang, J.R., Li, X.H., Gao, X.J., An, S.C., Liu, H., Liang, J., Zhang, K., Liu, Z., Wang, J., Chen, Z., Sun, W., 2013a. Expression of MMP-13 is associated with invasion and metastasis of papillary thyroid carcinoma. *European review for medical and pharmacological sciences* 17, 427-435.
- Wang, Y., Thekdi, N., Smallwood, P.M., Macke, J.P., Nathans, J., 2002. Frizzled-3 is required for the development of major fiber tracts in the rostral CNS. *The Journal of neuroscience : the official journal of the Society for Neuroscience* 22, 8563-8573.
- Wang, Y., Zheng, Y., Chen, D., Chen, Y., 2013b. Enhanced BMP signaling prevents degeneration and leads to endochondral ossification of Meckel's cartilage in mice. *Developmental biology* 381, 301-311.
- Wang, Z., Shu, W., Lu, M.M., Morrisey, E.E., 2005. Wnt7b activates canonical signaling in epithelial and vascular smooth muscle cells through interactions with Fzd1, Fzd10, and LRP5. *Molecular and cellular biology* 25, 5022-5030.
- Watanabe, H., Kimata, K., Line, S., Strong, D., Gao, L.Y., Kozak, C.A., Yamada, Y., 1994. Mouse cartilage matrix deficiency (cmd) caused by a 7 bp deletion in the aggrecan gene. *Nature genetics* 7, 154-157.

- Wedden, S.E., 1987. Epithelial-mesenchymal interactions in the development of chick facial primordia and the target of retinoid action. *Development (Cambridge, England)* 99, 341-351.
- Weston, A.D., Rosen, V., Chandraratna, R.A., Underhill, T.M., 2000. Regulation of skeletal progenitor differentiation by the BMP and retinoid signaling pathways. *The Journal of cell biology* 148, 679-690.
- Whittaker, M., Floyd, C.D., Brown, P., Gearing, A.J., 1999. Design and therapeutic application of matrix metalloproteinase inhibitors. *Chemical reviews* 99, 2735-2776.
- Will, L.A., Meller, S.M., 1981. Primary palatal development in the chick. *Journal of morphology* 169, 185-190.
- Wu, P., Jiang, T.X., Shen, J.Y., Widelitz, R.B., Chuong, C.M., 2006. Morphoregulation of avian beaks: comparative mapping of growth zone activities and morphological evolution. *Dev Dyn* 235, 1400-1412.
- Wu, P., Jiang, T.X., Suksaweang, S., Widelitz, R.B., Chuong, C.M., 2004. Molecular shaping of the beak. *Science (New York, N.Y)* 305, 1465-1466.
- Wu, X., Tu, X., Joeng, K.S., Hilton, M.J., Williams, D.A., Long, F., 2008. Rac1 activation controls nuclear localization of beta-catenin during canonical Wnt signaling. *Cell* 133, 340-353.
- Yamagata, K., Li, X., Ikegaki, S., Oneyama, C., Okada, M., Nishita, M., Minami, Y., 2012. Dissection of Wnt5a-Ror2 signaling leading to matrix metalloproteinase (MMP-13) expression. *The Journal of biological chemistry* 287, 1588-1599.
- Yamaguchi, T.P., Bradley, A., McMahon, A.P., Jones, S., 1999. A Wnt5a pathway underlies outgrowth of multiple structures in the vertebrate embryo. *Development (Cambridge, England)* 126, 1211-1223.
- Yang, T., Bassuk, A.G., Fritsch, B., 2013. Prickle1 stunts limb growth through alteration of cell polarity and gene expression. *Dev Dyn* 242, 1293-1306.
- Yang, Y., Topol, L., Lee, H., Wu, J., 2003. Wnt5a and Wnt5b exhibit distinct activities in coordinating chondrocyte proliferation and differentiation. *Development (Cambridge, England)* 130, 1003-1015.
- Yin, H., Copley, C.O., Goodrich, L.V., Deans, M.R., 2012. Comparison of phenotypes between different vangl2 mutants demonstrates dominant effects of the Looptail mutation during hair cell development. *PloS one* 7, e31988.
- Yoshida, M., Assimacopoulos, S., Jones, K.R., Grove, E.A., 2006. Massive loss of Cajal-Retzius cells does not disrupt neocortical layer order. *Development (Cambridge, England)* 133, 537-545.
- Yu, H., Smallwood, P.M., Wang, Y., Vidaltamayo, R., Reed, R., Nathans, J., 2010. Frizzled 1 and frizzled 2 genes function in palate, ventricular septum and neural tube closure: general implications for tissue fusion processes. *Development (Cambridge, England)* 137, 3707-3717.

Yu, H., Ye, X., Guo, N., Nathans, J., 2012. Frizzled 2 and frizzled 7 function redundantly in convergent extension and closure of the ventricular septum and palate: evidence for a network of interacting genes. *Development (Cambridge, England)* 139, 4383-4394.

Yu, H.M., Jerchow, B., Sheu, T.J., Liu, B., Costantini, F., Puzas, J.E., Birchmeier, W., Hsu, W., 2005. The role of Axin2 in calvarial morphogenesis and craniosynostosis. *Development (Cambridge, England)* 132, 1995-2005.

Yu, J., Jheon, A.H., Ealba, E.L., Frank Eames, B., Butcher, K.D., Mak, S.S., Ladher, R., Alliston, T., Schneider, R.A., 2013. Evolution of a developmental mechanism: Species-specific regulation of the cell cycle and the timing of events during craniofacial osteogenesis. *Developmental biology*.

Yuasa, T., Otani, T., Koike, T., Iwamoto, M., Enomoto-Iwamoto, M., 2008. Wnt/beta-catenin signaling stimulates matrix catabolic genes and activity in articular chondrocytes: its possible role in joint degeneration. *Laboratory investigation; a journal of technical methods and pathology* 88, 264-274.

Zheng, D., Decker, K.F., Zhou, T., Chen, J., Qi, Z., Jacobs, K., Weilbaecher, K.N., Corey, E., Long, F., Jia, L., 2013. Role of WNT7B-induced noncanonical pathway in advanced prostate cancer. *Molecular cancer research : MCR* 11, 482-493.

Zhou, C.J., Wang, Y.Z., Yamagami, T., Zhao, T., Song, L., Wang, K., 2010. Generation of Lrp6 conditional gene-targeting mouse line for modeling and dissecting multiple birth defects/congenital anomalies. *Dev Dyn* 239, 318-326.

Zhu, X., Zhu, H., Zhang, L., Huang, S., Cao, J., Ma, G., Feng, G., He, L., Yang, Y., Guo, X., 2012. Wls-mediated Wnts differentially regulate distal limb patterning and tissue morphogenesis. *Developmental biology* 365, 328-338.